# Optimised antennas for small form-factor devices

-Development of quarter-wave antennas for small ground plane-

P7 report

Aalborg University
Electronics and IT

**Electronics and IT**
Aalborg University
http://www.aau.dk

**AALBORG UNIVERSITY**
STUDENT REPORT

**Title:**
Optimised antennas for small form-factor devices

**Theme:**
Optimisation and development of antennas in small devices

**Project Period:**
Fall Semester 2023

**Project Group:**
Group 715

**Participant(s):**
Oliver Falkenberg Damborg

**Supervisor(s):**
Igor Aleksandrovich Syrytsin

**Copies:** 1

**Page Numbers:** 100

**Date of Completion:**
January 4, 2024

**Abstract:**

With the widespread adoption of electronics, there is an increasing demand for wireless alternatives for various products. This increase is evident in smaller devices like headsets, prompting the need for antenna development specific to such compact designs. This project focuses on designing an antenna specifically for a small wireless headset, leveraging the mechanical specifications of the RTX A/S RTX8950 model. Prototypes are designed, simulated and measured to assess the correlation between simulation and measurement to improve on the simulation model and optimise the antennas. The antennas were utilised for the development of the double antenna PCBs. The selected prototypes demonstrated high gain upon measurement, yet it still requires slight matching adjustments to fully meet the return loss requirement. While the double antenna PCBs were not measured, simulations indicate promising results. However, there is a need to reduce the coupling between the antennas, given the power of the s12 in the simulations.

# Preface

This project was developed on seventh semester by Oliver Falkenberg Damborg with assistance from the supervisor Igor Aleksandrovich Syrytsin. The project has been drawn up on the basis of a proposal provided by RTX A/S regarding "Optimised Antenna Design for Compact Devices". The report is written on the basis that the knowledge within the subjects broached in this report are on the level of a seventh semester student in EIT.

Sources are indicated using the Modern Language Association's (MLA) reference system. When referring to a source, numbers are used to symbolise the position of the source in the source list. Figures, tables, and other attachments are also indicated in the text with a number. Appendix is indicated in the text in the form "X", where X is a modifying letter. All references in the report are click-able, with a click taking you to the reference itself.

Aalborg Universitet, January 4, 2024

Oliver Falkenberg Damborg

# Contents

# Introduction 1

With the widespread use of electronics, optimisation and minimisation of electronics have become more prevalent. Wireless options for products like earbuds and headsets have become a common and desirable quality for products. Wireless communication modules are a fundamental link in IoT devices that are widely applied in; vehicle monitoring, telemetry, small wireless networks, wireless meter reading, access control systems, industrial data collection systems, wireless tagging, identification, contact-less RF smart cards, fire safety systems, bio-signal acquisition, hydro-meteorological monitoring, robot control, digital audio, digital image trees, etc [1]. As a key module for the sending and receiving of data, the antenna performance directly impacts the quality of the communication network. With the constant development of IoT devices and minimisation of consumer electronics, integrated antennas are expected to be the direction the market will move towards, with printed PCB antennas frequently picked due to low cost, small size and high gain [1].

The common ground for IoT devices and consumer electronics is the requirement for compact communication modules and compact PCBs. With the reduction in size of the PCB and ground plane, the resonance frequency and impedance of the antenna is expected to be affected possibly making it harder to design an antenna.

This project is developed in cooperation with RTX A/S with a focus on DECT4.1 and antenna performance in headsets. The antenna performance will be researched in regards to finding a better antenna, with the focus being on the ground plan, and optimal use-age of the available ground while constrained inside the mechanics. This project will utilise the mechanic supplied from RTX for their RTX8950 headset with the physical constraints that this provides for the shape and size of the PCB.

## 1.1 Project structure

A brief description of the contents of each chapter is given below giving an overview on where to find relevant information.

**Chapter 2**

Chapter 2 contains the problem formulation obtained from RTX A/S together with a short description of the company.

**Chapter 3**

In Chapter 3 the requirements for the developed antenna are formulated and collected into a table.

**Chapter 4**

In Chapter 4 the problem formulation is analysed. The DECT protocol is described and the RTX8950 is shown. The general antenna parameters are described after which the term Electrically small is analysed, with an analysis of the relation between ground plane and antenna performance. The effect of user on antenna performance is then analysed for its effect on a prototype.

**Chapter 5**

Chapter 5 is where prototypes are developed along with a measurement and simulation of the RTX8950 antennas. Extension of ground plane is researched to determine its overall effect on the prototypes.

**Chapter 6**

Chapter 6 contains the measurements and testing of the prototype antennas. The prototypes are measured, optimised, compared and a choice of prototype is made.

**Chapter 7**

Chapter 7 contains the conclusion of the project. The chapters and results are summed up before concluding on the project and determining the fulfilment of requirements.

**Chapter 8**

Chapter 8 is where reflections across the project are accounted for in regards to the models, assumptions and sources of errors throughout the project.

**Appendices**

Appendices are where the test journals of the prototypes are placed. Appendix A contains simulations of ground plane relation with performance for different types of antennas. Appendix B contains the simulated and measured result test journals for the prototypes.

# Problem formulation 2

Established in 1993 in Nørresundby, Denmark, RTX A/S is a hub of innovation in wireless short-range systems. With its deep-rooted expertise, RTX A/S excels in designing and producing embedded devices, ranging from intercoms to headsets with a large part of the product portfolio focused on the DECT protocol. Tackling wireless challenges head-on, RTX integrates cutting-edge audio signal processing to ensure top-notch audio performance.

This project proposal delves into the optimization of antenna design for compact devices, emphasizing the learning aspects of antenna theory, DECT understanding, and electromagnetic simulations.

Compact devices are consistently impeded by

- Spatial constraints affecting antenna performance.
- Interference caused by body blocking.
- Alterations in the radiation pattern due to proximity to the human body.

From this we get the following project objective:
*To explore, conceptualize, and test an optimized antenna design for compact devices, focusing on RTX's DECT headset as a learning case, while strengthening participants' understanding of core electromagnetic principles.*

This project will focus on the RTX8950 headset in which follows mechanical constraints and requirements for the antenna performance.

# Requirements 3

With the project focusing on optimisation of an antenna in the RTX8950 headset, a series of requirement for the headset are obtained by using the aforementioned headset. The specific antenna under examination in the RTX8950 headset is designed for handling DECT communication and its performance is part of the communication link budget. With better performance comes more leniency in the link budget for products containing the antenna which is preferred. Utilising the specific headset, mechanical constraint requirements have been formulated. The specific requirements for the Antenna along with its mechanical constraints are available in Table 3.1.

| ID | Description | Condition | Requirement | Ref. |
|---|---|---|---|---|
| T.1 | PCB Size diameter | Circular | 3,1 cm | RTX8950 |
| T.2 | Antenna clearance | From antenna to mechanic | 1 mm | RTX8950 |
| T.3 | Spatial Volume allowed for antenna | Width x Height(PCB thickness included) x Length (Circular) | 4mm x3,5mm x 40 mm (across a 90° angle sweep) | RTX8950 |
| T.4 | Frequency band | Global DECT band (except Korea) Returnloss ≤ -10 dB[2] | 1880-1930 MHz | [3] |
| T.5 | Antenna Efficiency | Minimum | 35% (-4,6 dB) | Project Proposal |

**Table 3.1:** Technical requirements for the Antenna and PCB.

The current antenna setup in the RTX8950 headset utilises two antennas which is normally the standard in DECT or systems supporting fast antenna diversity. The antennas are often rotated in different polarities to ensure a consistently good signal. This is facilitated through the use of Fast Antenna Diversity.

# Analysis 4

The project's shape and content have been outlined based on the project formulation provided by RTX A/S and Aalborg University (AAU). With the problem statement focusing on optimising an antenna with spatial constraints constrained to the RTX headset product RTX8950, this project aims to enhance the antenna performance within the mechanic of the RTX8950.

Throughout this chapter the project formulation will be analysed with a focus on the important aspects for the project. This encompasses a description of the physical layer of the DECT protocol along with the associated requirements. Having described DECT the RTX8950 headset from RTX A/S is described in regards to its mechanic and spatial constraints for the antennas. Having covered the requirement specific subjects, a description of the criteria for the antenna to be electrically small is provided. Subsequently, the chapter will delve into the correlation between ground plane size and antenna performance, followed by an analysis of the impact of body blocking at different ranges.

Towards the conclusion of this chapter, a direction for the optimisation of antenna performance will be determined, with initial emphasis on integrating a single antenna.

## 4.1 DECT

The supplied mechanic for the project is the RTX8950 headset. The headset is designed towards utilising DECT communication, containing two antennas for the purpose. Through this section the specifics of the DECT protocol and applications of it. Towards the end of the section, the requirement for the DECT protocol are described in regards to for example headsets like the RTX8950.

### 4.1.1 About DECT

Digital enhanced cordless telecommunication (DECT) is a communication standard primarily used for deployment of cordless telephone systems such as intercom systems. As DECT was developed for telephone systems it focuses on ensuring consistent audio, meaning that re-transmission of packages is not included. This is due to the requirement for

latency being stricter for DECT than for Bluetooth or WiFi. DECT is defined in the ETSI document EN300 175 [3].

DECT is a communication technology based on telephone systems between devices and base-stations. Common names for devices and base-stations are "Portable Unit" and "Base-station" or for devices; "Portable part"(PP) and for base-stations; "Fixed part"(FP). A DECT FP/PP system consists of one or several PP's being connected to one or several FPs. Through this connection, the PP's can communicate with each others. For setups requiring more base-stations or requiring a long range, it is possible to connect base-stations through for example daisy-chain or using repeaters to increase the range.

To communicate between several devices at the same time, DECT utilises FDMA and TDMA on the physical layer of the protocol. FDMA(Frequency-division multiple access) is used to divide the available frequency band for the specific country-mode into channels with a width of 1,728 MHz. For EU DECT this would divide the band into 10 channels.

TDMA(Time-division multiple access) splits each channel into different *slots* which allows several units to communicate on the same channel. The DECT protocol separates the channel into 2x 12 full-slots with 12 slots for upstream and 12 slots for downstream of data. Sub categories exists which are called long slot and double slot. Long slot uses 1,5 full-slots per slot while double slot utilises 2 full-slots[3]. A connection between 2 DECT units will use a slot-pair such as slot 1 and slot 13 for the communication. On Figure 4.1, the structural frame for the DECT protocol is shown where the structure of each DECT packet is shown.

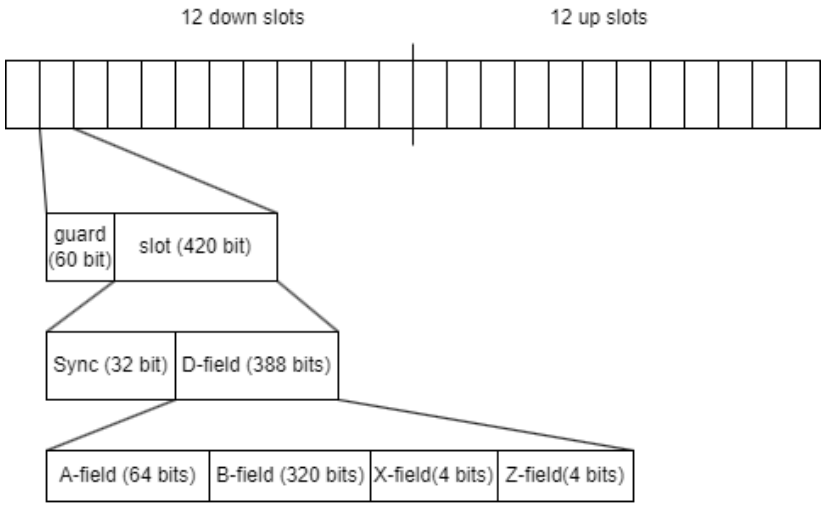


**Figure 4.1:** The DECT protocols Frame structure simplified. It shows a summary of which fields a DECT package contains and the bit-size of each field. Respect to [4] for use of Figure.

On Figure 4.1 the DECT Frame structure is visualised with the DECT packet frame being split into the different elements it consists of. Each frame has a length of 10 ms. 10 ms of audio is collected between each transmission, compressed and transmitted. The audio is collected from before the previous package is sent in order to include time for the codec to process the data. The audio is then sent and the next package will be sent. The delay between each transmission is 10 ms with audio having a slightly higher latency caused by the codec.

To delve into the DECT Packet Frame, we focus on the specific elements of the packet inside a slot shown on Figure 4.1. Looking at the information in the slot, it consists of a Sync field and a D-field containing the audio data. The 32 bit Sync field is responsible for synchronising the communication channel to avoid misinterpretations caused by bad sync. The D-field consists of an A-field, a B-field, a X-field and a Z-field. The A-field is the header for the payload which contains control-data and signal information. The A-field has a 16-bit CRC to check the data integrity, and in case the CRC fails, then the rest of the package will be dropped. The B-field serves as the carrier for the audio data payload, utilising the entirety of the B-field. To check the integrity of the B-field, the X-field is a 4-bit CRC which checks the integrity of the B-field. The Z-field is a copy of the X-field data which is used for collision-checking between two systems as DECT systems are not synchronised. The Z-field is optional and is therefore not required.

In cases where bit-errors occurs in a package the entire packet is dropped. The DECT protocol do not support re-transmission of lost packages due to the focus on audio transmission. With the low latency of 10 ms between each audio-package, a loss of one or two packages in a row will not disturb the audio to a noticeable degree for the human ear. In case of strong interference or loss of packages, the protocol will perform a handover. A handover is a change in utilised channel for the communication that occurs if the FP measures strong interference with the PP following to the new channel and thereby continuing the communication. By utilising both TDMA and FDMA, DECT is capable of dynamically changing the communication channel between FP and PP. This ensures that the DECT connection is with minimal disturbance and disturbance in case a source of powerful noise or lots of traffic is in the vicinity.

The DECT protocol is capable of utilising ten combinations of modulation schemes[3]. These ten combinations are a combination of GFSK, 16-QAM, 64-QAM and different variants of differential PSK such as $\pi/2$-DBPSK, $\pi/4$-DQPSK and $\pi/8$-D8PSK[3]. QAM will not be mentioned in this section. The two primary modulation-types available for DECT is Gaussian frequency-shift keying(GFSK) and different iterations of differential binary phase-shift keying (BPSK). GFSK is a Frequency-shift keying modulation-type that includes a Gaussian filter that the signal goes through before being decoded. Through the filtering of the signal, the side-lobes of the signal in the frequency domain are reduced outside the specified channel for the communication. For the DECT-protocol, the frequency

shift from the center frequency is 288 kHz. An increase in frequency is interpreted as binary 1 and reduction in frequency by 288 kHz is interpreted as binary 0.

The other protocol that can be used for DECT is differential PSK modulation like $\pi/2$-DBPSK, $\pi/4$-DQPSK and $\pi/8$-D8PSK[5]. DBPSK is a differential binary phase shift keying, which is a modulation scheme that defines a 180° shift in phase as binary 1 and no shift as a binary 0. $\pi/2$-DBPSK is a differential PSK where a shift in 90° is considered a binary 1. $\pi/4$-DQPSK consists of a quadrature PSK with two QPSK constallations. The construction is similar to normal QPSK but it has a lower maximum phase shift[6]. This modulation time has higher resistance to phase errors. $\pi/8$-D8PSK is similar to the DQPSK, but with 8 phase changes per symbol and a shift of 22,5°[6].

DECT is a standard that was originally developed in Europe but it has since then spread all across the world with a few differences depending on the country. The frequency band for DECT in EU is at 1880-1900 MHz that when split with FDMA gives EU DECT 10 channels. Other countries have available DECT channels in different frequency bands and with different amount of channels. The following is a short list of common DECT country modes, their frequency band and their amount of channels.

- Europa: 1880-1900 MHz, 10 channels
- Korea: 1786-1792 MHz, 3 channels
- Taiwan: 1880-1895 MHz, 8 channels
- Japan: 1893-1903 MHz, 6 channels
- Brazil: 1910-1919 MHz, 5 channels
- Latin America: 1910-1930 MHz, 10 channels
- USA and Canada: 1920-1930, 5 channels

In the different DECT country modes, there are different requirements for antenna gain and conducted power. USA has its own DECT standard which is dubbed as DECT 6.0, with the requirements for DECT in USA, that includes a maximum conducted power of 21 dBm and a maximum antenna gain of 3 dBi while specifying the frequency-band for DECT 6.0. For EU and several of the other country frequencies, there is a requirement of 24 dBm conducted and an antenna gain of 12 dBi.

In order to accommodate all the specified DECT modes within one hardware setup, the limit on the antenna gain is set to 3 dBi and for this project the conducted power is irrelevant. This gives the requirements for the antenna to be maximum 3 dBi with a 1880-1930 MHz frequency band.

## 4.2 RTX8950 headset mechanic description

The RTX8950 headset is one of the products developed by RTX A/S. The headset consists of a headband and the mechanical casing containing the headset electronics. The headband is of little consequence for the headset and can be changed between different types. The specific device utilised in this project is the RTX8950 device. The RTX8950 device consists of a cylinder-shaped casing with a diameter of 3,7 cm and a 2,9 cm quadrilateral protrusion from the cylinder casing. The quadrilateral protruding arm is the microphone arm in the headset. With the compact size of the mechanic, the spatial constraints for the PCB are strict for both the PCB and the antennas. The PCB has a size of 3,1 cm in diameter while being encased in closely fit mechanic. The closely fit mechanic encasing is from now on defined as capsule. The PCB and encasing can be seen on Figure 4.2(a) with Figure 4.2(b) showing the other side of the PCB where the antennas are attached.

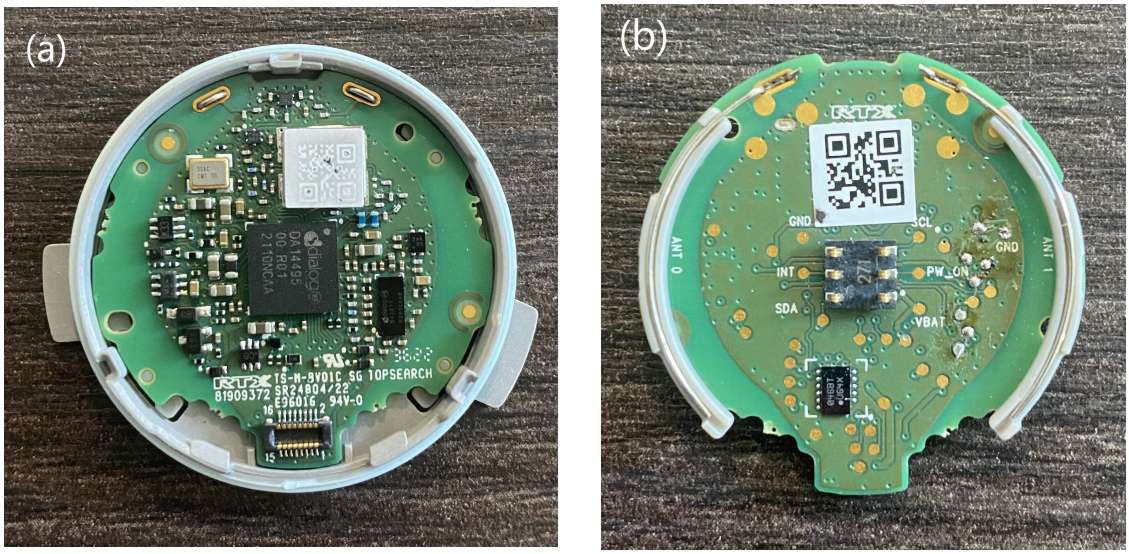


**Figure 4.2:** The PCB and capsule. (a) shows the front-side of the PCB being placed in the spatial constraints. Th capsule closely fit to the PCB when the lid is applied to ensure no PCB-movement. (b) shows the backside of PCB showcasing the positioning of the two antennas on the PCB. The antennas are wire antennas protruding slightly while being supported by plastic. With the protruding antennas, the capsule has indentations to fit the antennas.

From the mechanical constraints on PCB and antenna on Figure 4.2(a) and 4.2(b), the requirements in Table 3.1 were determined. The mechanical view from above can be seen in Figure 4.3.

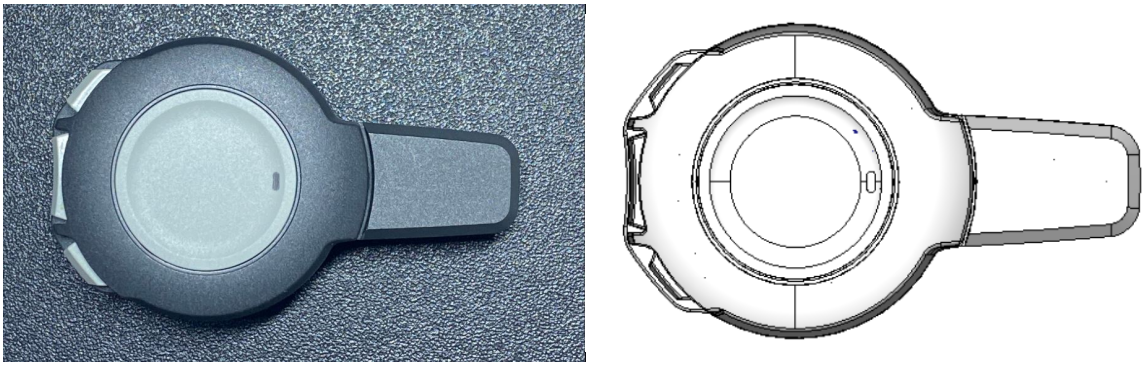

**Figure 4.3:** Mechanic top view for the RTX8950 used for the project.

The mechanic is the one that the antennas will be simulated and measured inside.

## 4.3 Antenna parameters

To determine and compare antennas a thorough understanding of the different parameters for the antenna is required. The parameters for an antenna are interconnected and several of the parameters are needed to determine an antennas performance.

### 4.3.1 Reflection

A starting point to understand the connection of the parameters to the antennas, is the requirement for bandwidth and frequency. By defining the frequency and bandwidth the other parameters can be defined. To determine the other parameters the bandwidth and frequency is needed and from it a requirement for the return loss can be found for the antenna. The bandwidth is defined as the frequency spectrum where the reflection in the antenna is -10 dB, which equals a reflection of ≈31,5% of the transmitted signal. ≈ 68,5% of the energy will therefore either be radiated or turned into heat in the antenna. The reflection of -10 dB is an appropriate rule of thumb[7] as a minimum for the bandwidth in order to avoid any significant disturbance caused by the reflection. Measurements of the reflection are commonly called S11-measurements from the way that a network analyser transmits and measures from the same port[8].

When a signal is transmitted from the radio to the antenna, it travels through a copper wire which is matched to have an impedance of 50 Ω. When the signal travels to the antenna, the antenna is likely to not have a similar impedance. With a different impedance in the desired frequency band, a reflection between the two impedance areas will occur, which in turn creates a reflected wave that will interfere with the transmitted signal. That interference will become a loss of power that the antenna wont be able to radiate[7]. In order to

avoid a reflection of the conducted power, the antenna is therefore designed and matched to be equal or close to 50Ω.

### 4.3.2 Efficiency

The efficiency of the antenna is an important parameter for the performance of the antenna. The efficiency of an antenna is defined as how much of the input power can be radiated out into the far-field. When matching an antenna, the impedance and reflection is measured by doing a s11 measurement. To determine the impedance matching efficiency we minus the return loss from the total signal. With a return loss of -10 dB we get:

$$\eta_m = 1 - 10^{\frac{-10}{10}} = 0{,}9 = 90\% \approx -0{,}46 \text{ dB} \tag{4.1}$$

with $\eta_m$ being the impedance matching efficiency, 1 being the total signal and $-10$ being the s11 return loss. The impedance matching efficiency is a part of the total efficiency of an antenna. Another part of the total efficiency is the radiated efficiency of the antenna. The radiated efficiency is defined as the ratio between radiated power and the input power that enter the antenna after the return loss[9].

$$\eta_r = \frac{P_{Radiated}}{P_{input}} [.]$$

Being a ratio, the value is between 0 and 1 which is a radiation between 0% and 100%, often described in dB with 10% being -10 dB and 50% as -3 dB.

In order to find the total efficiency of the antenna, both the impedance matching efficiency and the radiated efficiency are included. To find the total efficiency of the antenna, the impedance matching efficiency and radiated efficiency are multiplied as in equation (4.2)[9]. With body-blocking in proximity we include $\eta_B$ as the blocking that will occur due to near-presence of bio-tissue or other objects in close proximity,

$$\begin{aligned} \eta_T &= \eta_m \cdot \eta_r \cdot \eta_B \quad [.] \\ \eta_T &= \eta_m + \eta_r + \eta_B \quad [\text{dB}] \end{aligned} \tag{4.2}$$

From this, the total efficiency for the system can be found. During simulations in CST, the total efficiency is obtained as a result. During measurements, it would be needed to know the s11 return loss, radiated power and conducted power, but the gain of the antenna is often more important than the efficiency for measured antennas. Utilising the Stargate at AAU, it is possible to determine the efficiency for measurements.

### 4.3.3 Radiation pattern and directivity

Another important antenna parameter is the radiation pattern and the parameters that come from the radiation pattern. These antenna parameters are the gain and the directivity of the antenna. Both gain and directivity are connected to each others through Equation

(4.3).

$$G_g(\theta,\varphi) = \eta_T \cdot D_g(\theta,\varphi)$$
$$G_0 = \eta_T \cdot D_0 \tag{4.3}$$

where $G_g(\theta,\varphi)$ is the gain at a specific 3-dimensional angle, $\eta_T$ is the total antenna efficiency, $D_g(\theta,\varphi)$ is the directive gain, $G_0$ is the peak gain and $D_0$ is the directivity. The directivity is found from the maximum radiation intensity and the radiation power density. The directive gain is the gain in the antenna at a specific direction described by the angle $\theta$ and $\varphi$.

The directivity and gain of an antenna are both found from the radiation pattern of the antenna. The radiation pattern is a mathematical or graphical representation of the radiation properties of an antenna. These properties can consist of the amplitude, phase and the polarisation of the antenna[10]. The radiation pattern can be described as either Isotropic, Omni-directional, Semi-directional or directional.

An isotropic radiation pattern is the pattern a theoretical isotropic radiator creates with equal radiation power in all directions. This radiator is purely theoretical, but is used as a comparator to real antennas.

### Omni-directional radiation pattern

The most similar to the theoretical isotropic radiator is the omni-directional radiation pattern. An omni-directional pattern will radiate power in all directions to some extent. Examples of this is the monopole, dipole and L-antennas. A common pattern for a monopole is a torus surrounding the antenna. The radiation pattern for a monopole can be seen on Figure 4.4.

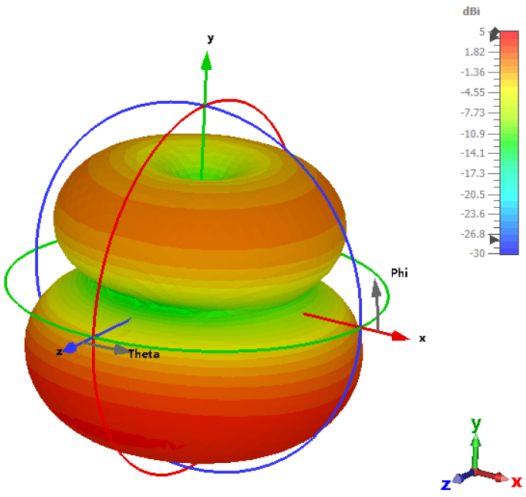


**Figure 4.4:** Monopole simulated in appendix A showing the effect of a large ground on the radiation pattern for a monopole. The large ground shows as the lower torus with the top torus being the pattern for the antenna.

On the figure, the characteristic torus is visible in the upper part of the figure which is the location of the monopole antenna. The torus in the lower part of the figure is the radiation caused by current affecting the ground plane of the antenna causing it to radiate.

### Semi-directional radiation pattern

Semi-directional radiation patterns are caused by antennas such as the Patch or the Yagi-Uda[11]. A semi-directional antenna is a type of antenna which is directive but with a wider half power Bandwidth (HPBW) than a directive antenna. This means that while a directive antenna, it radiates in a larger angle with the primary lobe radiating up to 180°. While the radiating area is smaller than the omni-directional, the gain in the antenna is increased. One of the semi-directive antennas is the Patch antenna known for radiating in approximately 180°, with a peak gain between 6 and 9 dB[12]. The radiation pattern for a Patch antenna can be seen on Figure 4.5.

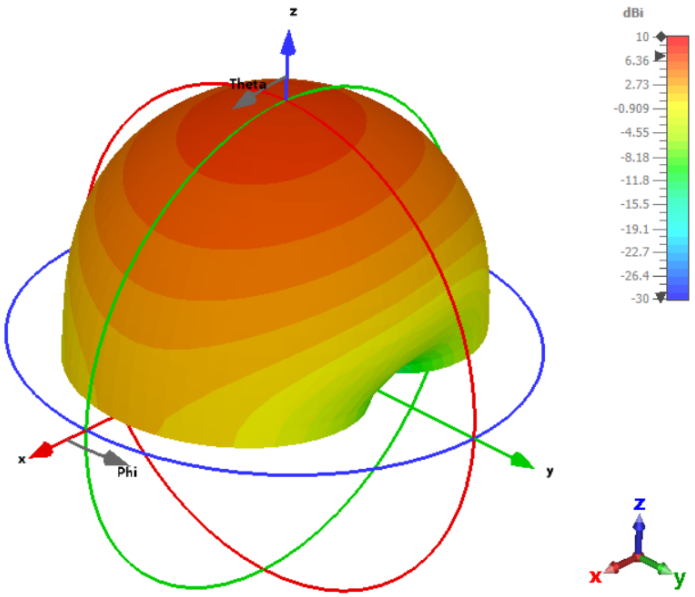


**Figure 4.5:** Radiation pattern of a patch antenna. The semi-directional pattern shows the pattern for an antenna only being fully directional in one direction which is common for patch antennas.

Semi-directional radiation patterns and the antennas that create them are often utilised in for example creating a network bridge between two buildings. Another utility is mounting it high up on a wall where it has a longer indoor range due to antenna gain being higher than for an omni-directional. Semi-directional antennas are for these reasons commonly used in indoor environments to reach places where the omni-directional antenna could not.

**Directional radiation pattern.**

The directional radiation pattern is a radiation pattern with a small HPBW with most power being transmitted in one direction. The type of antennas that utilise this radiation pattern typically has higher gain than the other radiation patterns and as a consequence, a longer range. Antennas in this category are used for long distance communication with types such as the Horn antenna being commonly used. Other types of directional Antennas are the Grid and Dish antenna commonly known from parabolic television. By narrowing the radiation pattern, the area of the radiation pattern is decreased with all the power concentrated in a small area which gives rise to the directional radiation pattern. For a horn antenna, the gain obtained is within the spectrum of 10 to 25 dB[13]. The radiation pattern for a horn antenna can be seen on Figure 4.6.

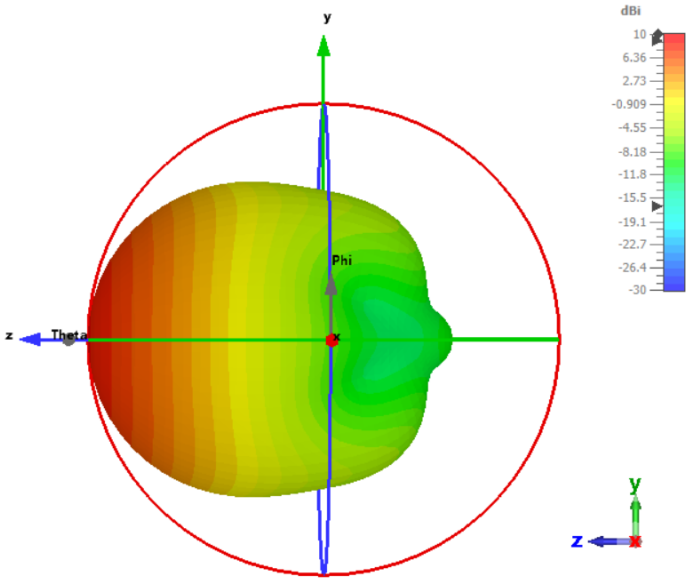


**Figure 4.6:** The directional pattern of a horn antenna. The scale for this pattern is increased compared to Figure 4.5 and 4.4 due to the high directivity of a horn antenna. The semi-directional antenna is radiating in one direction but the horn antenna has a more narrow radiation area.

**Summary**

Through the previous sections the radiation patterns were described and visualised. The optimal radiation pattern for the RTX8950 headset is a radiation pattern that radiates in as many directions as possible with a gain while reducing the amount of power deposited in the head of the user. This requirements directly declines the directional antenna type. In regards to avoiding deposit of power and a high directivity, the semi-directional antenna is the optimal choice. The semi-directional antenna like the patch only radiates in one direction and the directivity is generally high, but the lack of many directions is unwanted due to the product losing its functionality as soon as the head turns away with the antenna.

The omni-directional radiation pattern is chosen due to this. This pattern radiates in all directions around the PCB. One detrimental effect of this is deposits of power in the head. This lessens the efficiency, but will still make it possible for the antenna to receive signal from all directions.

## 4.4 Electrically small antennas

When small electronic devices are communicating wirelessly, both the antenna and the ground-plane are affected by the size. If either the antenna or the ground-plane is considerably small, the device is called an electrically small device. An antenna or ground-plane is defined as electrically small if the largest dimension is smaller than a tenth of the wavelength or if the wavenumber multiplied by the length is less than a half[14]. Shown as equations it is,

$$\begin{aligned} a &< \frac{\lambda}{10} \\ k \cdot\ a &< 0.5 \end{aligned} \tag{4.4}$$

with $a$ being the largest length, $\lambda$ being the wavelength, $k$ being the wavenumber defined as $\frac{2\pi}{\lambda}$. Even if an antenna does not fulfill these equations, it is still possible for it to behave as an electrically small device as the surroundings and design can affect the antenna to a degree of it behaving electrically small[14]. The behaviour of an electrically small antenna is a gradual process so antennas not defined electrically small may still have similar behaviour.

If a device is found to be electrically small, this sets a limit on the minimum Q value for the antenna and therefore also the maximum possible bandwidth for the antenna. The minimum possible Q value for an electrically small antenna can be found from the CHU limit[8]. The Chu limit is a lower boundary for the Q value possible with the physical size of the electrically small antenna. The minimum Q value possible for an antenna is found by applying a sphere around the antenna with the minimum radius required to cover the entire antenna and ground for quarterwave antennas. A sphere applied on a dipole antenna can be seen on Figure 4.7.

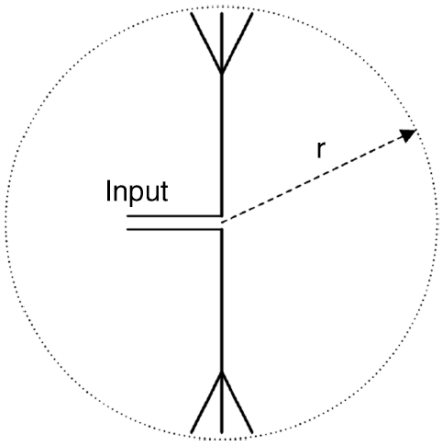


**Figure 4.7:** A figure showing how to find the radius in order to determine the Chu limit. The chu limit helps identify the possibility of certain requirements with the given antenna and groundplane. In case of quarter-wave antennas, the circulated area consists of the antenna and the entire groundplane.

With the minimum radius r determined, the Q limit can be found from the established Chu limit. The relation to find the Q limit for a lossless antenna is the following[14]:

$$Q \geq \frac{1}{(k \cdot a)^3} + \frac{1}{k \cdot a} \overset{ka<<1}{\approx} \frac{1}{(k \cdot a)^3} \tag{4.5}$$

with $k$ being the wavenumber defined as $\frac{2\pi}{\lambda}$ and $a$ being the radius found from Figure 4.7. The boundary given by Chu is based upon a simplified model and is considered the strictest of the models for the minimum Q[8]. As Q is inversely related to the bandwidth, the Chu limit is a quick way to determine whether an electrically small antenna can be created with the proposed requirements in regards to bandwidth at specific frequency and size. In case a Q value not fulfilling the requirement for bandwidth is found from the chu limit, the antenna can be denied with the current physical size.

When antennas are reduced in size, such as for electrically small antennas, the electrical length is reduced. A monopole is considered electrically short if the length of the antenna is less than a fourth of the wavelength. Electrically short antennas are ineffective radiators[15]. As the length decreases from the fundamental resonant length, the radiation resistance will decrease with the square of the electrical length[15]. This results in the other resistances in the antenna getting a larger fraction of the transmitted power that is dissipated as heat in the antenna on top of the s11 reflection loss. When an antenna is electrically short, it will have a capacitative reactance[15]. In order to cancel this out and get the antenna to resonate at the resonance frequency, an inductor is added in series. By adding the inductor, the antenna has been electrically lengthened. The inductor is added in series through a process of cutting and applying the inductor. Electrically lengthening an antenna like this does not change the radiation pattern[15], but it adds an additional lossy component that directly affects the efficiency of the antenna.

The PCB and ground plane of the RTX8950 is not considered small enough to be classified as electrically small from relation (4.4). The pcb is close to being considered electrically small and due to the process being gradual, it is therefore expected to have behaviour similar to electrically small. The behaviour consists of a decrease in radiation resistance, making it more difficult to reach a resistance of 50 Ω and having a lower efficiency.

## 4.5 Relation between ground plane and antenna performance

The size of a device is often a predetermined size that the PCB is designed around. The ground plane, antennas and the circuit is developed around the possible room for the PCB. The size of the device however sets a limit on the size of the PCB. The ground size affects the performance of the antenna by a large degree and its shape and size changes the performance of the antenna. For an asymmetric dipole, one of the two radiation arms is the ground plane where the size and shape affects the performance[8]. The same applies to quarter-wave antennas such as the monopole where the ground plane is a radiating element equivalent to the actual antenna in regards to radiated power and impedance. For a monopole, the ground plane is an essential part of the antenna that is a part of the radiating area and its size affects the frequency.

When an antenna is activated through current, the ground is excited at the same time and the modes intrinsic for the ground plane can be found[8]. A mode is a result of a modal analysis where the resonance of the object is checked. In the specific case of the ground plane the modes are the fundamental mode and higher order modes also known as harmonics. The specific modes on the ground plane determines the current distribution along the ground plane, with the frequency of the signal determining the mode. Resonant modes can occur when the dimensions of the ground plane or the antenna are a multiple of half-wavelengths at the operating frequency. In cases like this, standing waves are formed on the ground plane and the current distribution on the ground can vary in complex ways [8]. With a complex distribution of current, simulations and measurements are used to analyse the ground effect on the antenna. With a wider ground, the current is more evenly distributed, causing the antenna's characteristic to be less sensitive to the length of the ground[8]. In some cases, this distribution also creates a downward travelling wave. This downward travelling wave is responsible for causing the ground plane to radiate as an antenna. With a downwards travelling wave the additional radiation pattern caused by the ground plane will be tilted downwards[8]. The total radiated plot for a quarter-wave straight monopole should therefore have a gourd-like shape with two torus' on top of one another. Commonly, antennas are placed on the edge of the substrate in order to efficiently utilise the entire PCB, but for the case of the antennas in this section, it was found easier to match when positioned a bit within the substrate, but with the detriment of decreasing the efficient use of the full PCB.

### 4.5.1 IFA Antenna

This section aims to determine the relationship between the size of the ground plane and the antenna performance for the Inverted F antenna (IFA) through simulations in CST. The antenna was designed within CST for a center frequency of 1905 MHz. The antenna was designed following the equation from Balanis [14]. For the model the substrate is using the CST lossy FR4 with a relative permittivity of 4,3 and the substrate is a thickness of 1,55 mm.

$$L = \frac{c}{4 \cdot \sqrt{\varepsilon_r} \cdot f} = \frac{3 \cdot 10^8 \text{m/s}}{4 \cdot \sqrt{4{,}3} \cdot 1905 \text{ MHz}} = 19 \text{ mm} \tag{4.6}$$

A length of 19 mm was calculated for the radiating element of the antenna by using the equation. The shorting pin for the IFA antenna is of a smaller size compared to the antenna and is usually defined in a length of

$$W \leq (0.05 - 0.1)\lambda$$

Following the relation for the shorting pin [14], a length of 6 mm was found.

The IFA was connected to a ground plane spanning 160X40 mm consisting of 35 µm copper. As the CST model uses lossy copper and FR-4, the measured length from the the Balanis equation is not expected to be appropriate and therefore the antenna is matched in length to achieve a centering at 1905 MHz. The antenna model used for simulation is found on Figure 4.8.

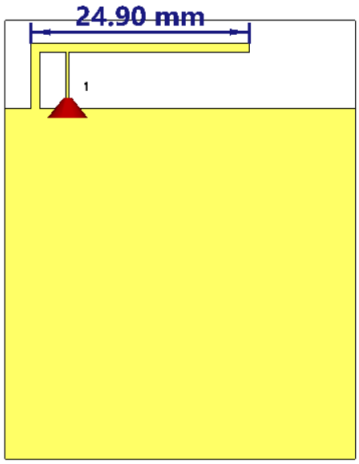


**Figure 4.8:** Simulated model of an IFA antenna. The antenna is placed away from the edge due to experiencing easier matching when designed. The model is simulated using FR4 substrate and lossy copper in CST.

The length of the antenna is found to be overall longer than the calculated by utilising the Balanis equation. The interdependence of the ground plane on the antenna is tested through the sweeping of an antenna matched to a center frequency of 1905 MHz. Using

CST parameter sweep, the length of the ground plane was swept in order to compare the different lengths with each others and thereby verify the effect of the ground plane length on the S11 and Total efficiency.

The plots for the length of 20, 80 and 160 mm were compared to determine the effect that the size of the ground plane has on the efficiency and s11 values. By applying both total efficiency and s11 in a plot, it is possible to compare the graphs to requirement T.4 and T.5 and confirm whether these requirements are fulfilled. The requirement lines are applied to the simulated result for the efficiency and s11 behaviour. Applying these lines we get Figure 4.9.

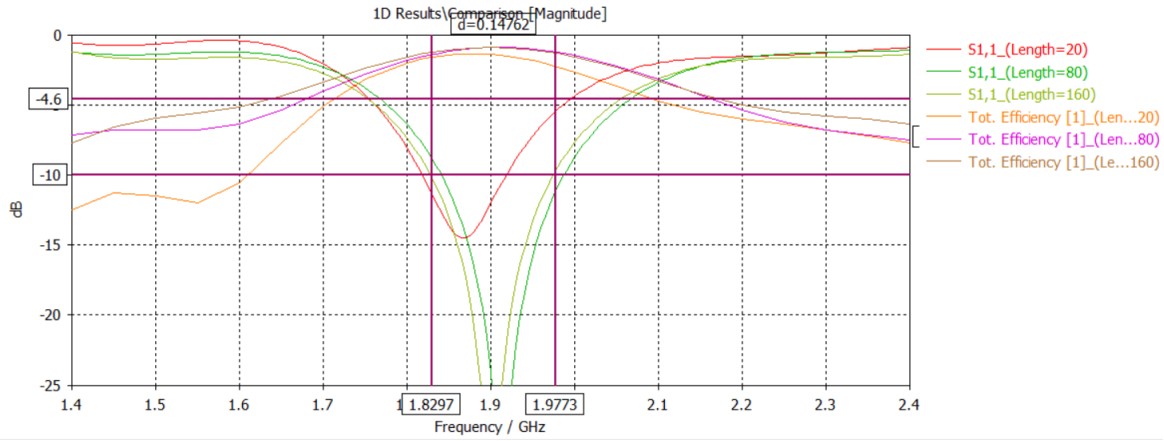


**Figure 4.9:** Plot of the ground sweep of the simulated IFA antenna. The horizontal lines show the requirements for the antenna. The bottom horizontal line is the s11 requirement, with top horizontal line being the efficiency requirement. The vertical lines measured the frequency spectrum that the ground extension of 160 mm would fulfil the requirements within.

The total efficiency of the antenna on Figure 4.9 shows that a larger ground plane has a better efficiency than a small ground plane if comparing with the total efficiency of the length 20 mm. To achieve the same center frequency for all antennas, an extension or reduction of the size of antenna would be necessary. This would have given a more reliable comparison. Our S11 limit requirement is -10 dB while our efficiency is minimum -4.6 dB. On Figure 4.9 these have been marked and the S11 limits for length 160mm have been lined in order to measure the bandwidth of the antenna. The bandwidth is measured to be 147 MHz, which is almost three times larger than the required bandwidth of 50 MHz, and the desired band is within the the bandwidth. The efficiency within the band lies at around -1 dB down to -2 dB in the edges of the band for both length 80 and 160 mm. This corresponds to an efficiency between 79% to 63% both of which is a good level for a product. It is important to note that this is without mechanics surrounding the antenna and PCB where the total efficiency would become reduced as a consequence of the damping occurring from the mechanics. Determining the directivity is also an important parameter for the model, and

it is visible on figure 4.10.

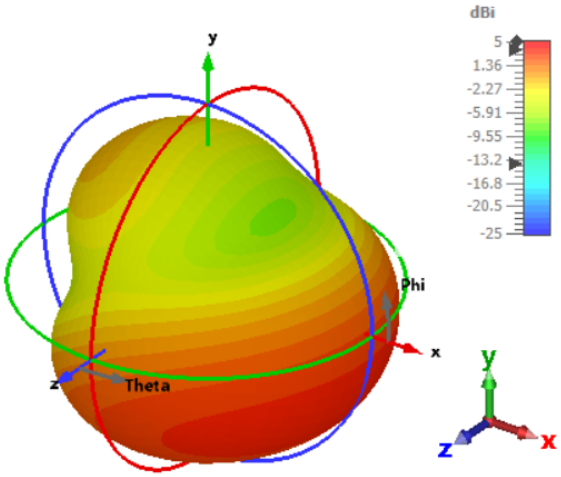


**Figure 4.10:** Radiation pattern of the simulated IFA at 1900 MHz. The directivity is at a value of 3,8 dBi at the bottom of the radiation pattern which is the area radiated by the ground plane.

The radiation pattern is found to have a directivity of 3,6 dBi with a ground length of 80 mm. Looking at the pattern it has an unique radiation pattern caused by the antenna arm and ground plane being in a different polarisation. The active element radiates vertically while the ground plane radiates horizontally. The relation between ground plane size and antenna performance have been confirmed for an IFA antenna and the same will be performed for monopoles for both the bent and straight variants of the monopole. The results of the simulations of the ground-effect on different other antenna-types can be seen in appendix A.

### Effect of relative permittivity on efficiency

The relative permittivity of a substrate is an important parameter to know as it can change the resonance frequency for the antenna depending on the permittivity. The relative permittivity used for the substrate in the simulations is the FR4 material in CST. The FR4 material is a classification of material and not a specific type so the relative permittivity in the substrate can range from 3,8 to 4,8[16]. The value in CST is at a value of 4,3 for the relative permittivity which is in the middle. The permittivity is swept from 3,4 to 4,8 to determine the effect it would have on the efficiency and resonance frequency for the simulated IFA. The results are available on Figure 4.11

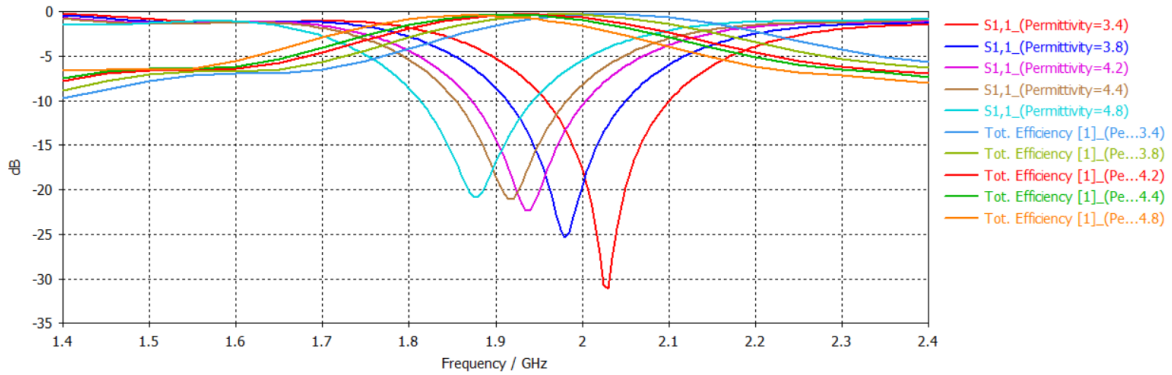


**Figure 4.11:** Sweep of the relative permittivity for the substrate from 3,4 to 4,8. The figure shows both efficiency and s11 response. The swept antenna is the IFA on Figure 4.8.

The figure reveals that the efficiency and resonance frequency is shifted according to the relative permittivity in the substrate. The higher the permittivity, the lower the frequency. This means that for an increase or decrease in permittivity will reduce the efficiency of the antenna in the form of shifted resonance frequency. A shifted resonance frequency means that less power is received on the antenna, and the antenna is worse at radiating the received power giving an overall decrease in efficiency. It is crucial to confirm the performance of an antenna when the PCB has been printed as each producer of PCBs may have individual differences in the relative permittivity of the PCBs.

### 4.5.2 Summary

Several types of internal antennas were modelled and simulated to confirm the effect of the ground size on the antenna performance. The results of the simulations are visible in section 5.3.1 and Appendix A. Determining the effect of gorund size on different types of antennas and finding the design difficulties of each type was the goal of this section. From the simulations it is clear that the size of the ground-plane affects the antenna to a large degree that is important to take into consideration when designing an antenna for the RTX8950 mechanic. From section A.2 and A.1 it could be confirmed that an electrically small ground required a longer monopole to achieve the same resonance frequency which confirms the relation between ground and performance. From designing the antennas, some types were easier to design and tune than others, while also using less space. From this, the IFA antenna type will be the primary antenna type focused on due to its omnidirectionality, additional matching possibility and compact size.

## 4.6 Effect of User on antenna performance

The surroundings of an antenna affects the performance of the antennas parameters. The surroundings are capable of changing the radiation pattern, reduce the gain and reduce

the efficiency. This would occur in the form of interference such as blocking or detuning when in close proximity. To determine the effect on the antenna performance that a body has, it is required to know about the different types of fields around an antenna as objects in each field affects the performance differently. Through this section, the field regions of an antenna are explained, after which the consequences of interference in each field is described.

### 4.6.1 Field regions

The field created by an antenna when excited by a current is separated into 3-4 different types of fields. While the fields are defined within a certain range from the antenna, the borders between each field is blurry as the transition between each field is gradual. The field of an antenna is separated into three zones which is the reactive near-field, the radiative near-field and the far field. In-between the radiative near-field and the far field, there is a transition zone that is defined as when the electromagnetic waves become self-propagating. Self-propagation is when a field consists of mutually reinforcing electric and magnetic fields. These fields oscillate in phase with each other, creating a self-sustaining wave that can propagate through space[17]. The different zones are defined in their range on Figure 4.12.

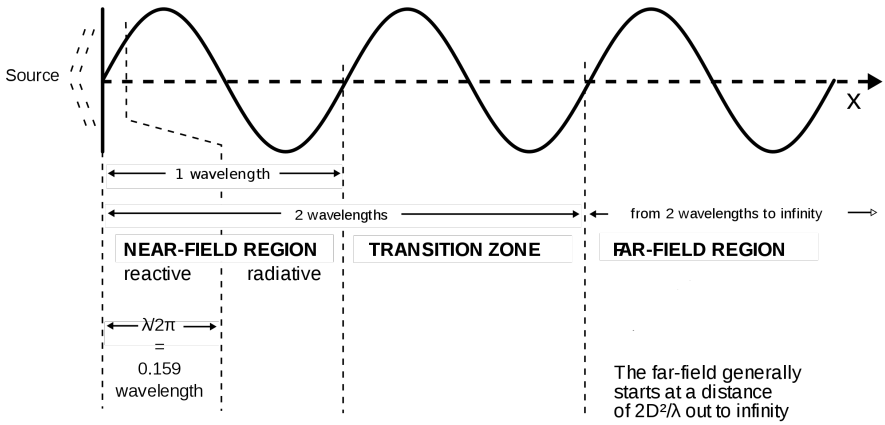


**Figure 4.12:** Field zone map showing the different zones of a near to far field field around a radiating element. The range from the radiating element and outwards for each field can be seen on the Figure. Credits to "OSHA, Dept of Labour, Public domain, via Wikimedia Commons"[17] for the figure.

The different regions have different electrical and physical behaviour which will be described below.

**Reactive near-field**

The reactive near-field is the field closest to the antenna and spans roughly $\frac{1}{6}\lambda$ around the antenna. The range is determined by the point where the field strength has decayed to an insignificant level. In the reactive near-field, the relationship between the strengths of the E- and B-field is often too complex to predict or measure accurately[17]. The E/H fields need to be orthogonal and in phase with each others in order to radiate or propagate. In the reactive near-field the E-field and H-field are 90 degrees out of phase thereby causing the field to be reactive[18]. An EM wave is transmitted towards far-space in the reactive region of the antenna, but as the name suggests, the field contains a reactive component. This reactive component causes the signal strength, direction and phase to be sensitive and vulnerable towards EM Absorption and re-transmission in the field. The reactive components strength decay at a level of $\frac{1}{r^3}$[17] thereby causing the field separation between reactive and radiative near-field as the reactive components become insignificant.

Several detrimental effects for the performance occur as a result of EM absorption. Instead of the energy being radiated as useful signals, it is dissipated as heat in the antenna structure or absorbed by nearby objects, including conductive or dielectric materials. One such example is the bio-tissue of the human head. Prolonged exposure to a high temperature potentially caused by heat dissipation can have a damaging effect on the antenna or the immediate surroundings[17].

EM absorption has the possibility to lead to changes in the electrical characteristics of the antenna in the form of detuning. Detuning alters the antenna's resonant frequency and impedance, which can lead to impedance mismatch and poor performance. If an object within the reactive near-field absorbs some energy it may introduce multi-path propagation effects leading to signal reflections, diffraction, and interference. This can lead to loss of range and performance for the product. It is crucial to tune the antenna in the environment that it is expected to operate in as a product. The tuning consists of eventually changing the antenna size but is more often done using a matching network.

**Radiative near-field**

For an electrically short antenna, the radiative field is a field stretching from $\frac{1}{6}\lambda$ to one wavelength $\lambda$[17]. Another name for the radiative near-field is the Fresnel region[19]. The radiative near-field decays by a degree of $\frac{1}{r^2}$. As the decay of the radiative near-field is less than the reactive, the reactive components have decayed enough for them to inconsequential. The magnetic (H) and electrical (E) components of the field have a complex relationship in this region, making it harder to predict measurements. Locally the fields may be in phase, but it is not applicable to the entire field[17]. The $E$ and $H$ relationship is easier to predict further out in the near-field, but it also allows for re-radiation.

Re-radiation can occur when a passive component such as a piece of metal is within the

radiative near-field. The component can function as an antenna by inductively absorbing part of the energy in the radiative near field and subsequently "re-radiate" it. This creates a new radiating surface to take into account when determining the radiation pattern. This radiating surface creates its own near-field and farfield which have the same conditions as the original radiator. It is possible to take advantage of this feature by placing passive components into the near-field to beamform. One example of this is the Yagi-Uda antenna[17].

**Transition zone**

For the electrically short antenna, the transition zone is a field stretching from $1\lambda$ to $2\lambda$[17]. The transition zone is where the characteristics of the near-field start to die out leaving the far field effect as the dominant interactions. The start of the transition zone is the initial point of balance between the electric and magnetic components of the emitted waves. Within this region, electromagnetic waves are beginning to propagate away from the antenna[17], with the $E$ and $H$ field now in phase. The further away from the antenna the signal comes, the closer it gets to being similar to far field. This zone can be considered either the furthest parts of the near-field or the closest parts of the far field, as this is the zone where the radiation changes into standard EM radiation.

**Far field**

The far field is the range from $2\lambda$ and outwards. This range is where the field has settled into normal EM radiation[17]. Normal EM radiation consists of radiating as transversal waves with the $E$ and $B$ fields orthogonal to each others and in phase. In the far field the radiation pattern has fully formed, allowing for easier measurement and mapping of the radiation pattern. CST can be used to simulate the far field to find the radiation pattern. The radiated power decreases as the inverse of the distance $\frac{1}{r}$ in the far field thus reaching out into the infinite[17]. In this region, the fresnel zone starts to be important, where interference in the form of obstacles can cause a reduction in range and cause multipath propagation[20].

### 4.6.2 Users effect on field regions

The antenna's performance is affected differently depending on the distance from the antenna to the user. The users effect on the performance increases the closer the user gets to the antenna. In the far field, the users primary effect is disruption of the fresnel zone which can cause loss of range, power and multi-path propagation.

Entering the radiative near-field, the user will affect the product in the form of altering the radiation pattern, reducing signal strength and causing interference. Signals may reflect off the body, scatter, or diffract around it leading to variations in the signal strength that can cause potential signal distortion. This can occur adue to the human body's ability to behave as an imperfect reflector. An imperfect reflector does not reflect all the energy which leads to loss of total efficiency.

The reactive near-field is the most vulnerable range and is where the human body can cause serious complications for the antenna performance. One of the more critical effects is the detuning of the resonance frequency. The product focused on in this case is the RTX8950 headset which is attached to the head. Due this, the head will be within the reactive near-field, thereby meaning that detuning and loss of efficiency is expected. Detuning of an antenna has the effect of shifting the resonance frequency, causing a loss of gain and as a consequence reduce the range of the product.

# Prototype development 5

In chapter 4, several types of antennas were simulated, antenna parameters were described, electrically small antenna was defined and the effect of user on antenna performance was researched. The next step is the design and development of antennas and measurement of them. Throughout this chapter, the current RTX8950 PCB will be simulated and measured with and without mechanic. The performance of the current choice of antenna will be documented. With a basis in the current PCB size and shape, an antenna will be designed and simulated. With the prototype antenna designed, the shape of the PCB will be modulated in the form of a ground extension during simulations to determine whether a modulated shape would improve the antennas performance.

## 5.1 Appropriate S11 measuring of Antenna

The return loss or s11 is one of the basic parameters for an antenna as was described in section 4.3. Measuring the S11 is important to determine the performance of the antenna. Measuring the antenna on the PCB for the RTX8950 requires an RF pig tail due to absence of a SMA connector. However applying a RF pigtail to a PCB such as the PCB on figure 4.2(a) introduces a comparatively large amount of ground known as the cable effect. The cable effect will affect the performance and the measurement of the antenna. The cable effect is a troublesome effect as it invalidates any precision required in measuring the actual performance of the antenna. The cable effect is diminished with large sized ground planes, but it is not a viable approach in the industry with the ground size being defined early on. For Quarter-wave antennas, the ground plane is used as emitter meaning that it helps define the resonance frequency. Addition of ground to the ground plane in the form of the RF cable will affect the resonance frequency unless it is mitigated.

There are mainly two options for mitigating the cable effect. One of the possible ways to mitigate the cable-effect is to solder the RF pig tail to the ground in a minimum of two locations. One soldering point close to the point of measurement also known as the feed-line and the other soldering point is applied to the ground close to the exiting point from the ground plane for the RF cable. This ensures that the current that was circulating through the RF cable reaches ground again, thereby lessening the impact of the RF cable on the Antenna. This will not remove all the current which means the cable effect is diminished but

not gone.

The second technique is often applied in combination with the previous one. This technique involves the usage of chokes often in the form of Ferrite beads. The two commonly used ferrite materials for the beads are manganese-Zinc (Mn-Zn) and Nickel-Zinc (Ni-Zn)[8]. Each material is used for different frequencies with Mn-Zn chokes being used at 1-30 MHZ and Ni-Zn being used for frequencies up to 1 GHz. Due to the mobile communication frequencies, only Ni-ZN is viable for usage. Ferrite material has a very high permeability and the permeability impacts the wire's inductance which in turn defines the wire's impedance from the relation J$2\pi fL$. The reason for Ni-Zn being used at a maximum frequency of 1 GHz is due to the permeability being connected to the frequency. An ideal choke would be pure reactance. If there is resistance in the choke it is lossy and will negatively affect the efficiency of the antenna. Utilising Ni-Zn chokes for frequencies above 1 GHz is in some engineer's opinion something that you should not, while others think differently[8]. They think that Ni-Zn Ferrite Chokes can be used for all mobile communication bands which is up to 2,17 GHz. Their reasoning for this is that at higher frequencies, the impedance in the choke is still relatively high. The loss in power caused by the ferrite choker is proportional to $\frac{V^2}{R}$. As the connection spot is kept far away from the antenna feed spot, the E-field should be less at the connection spot compared to the antenna feeding. The ferrite chokers resistance $R$ is significantly higher than the antennas and therefore the impact on the efficiency of the antenna should be reasonable[8]. Chokes are used as an auxiliary method of mitigating residual currents on the cable with most of it attempted diminished through optimal cable positioning. To determine if the cable effect has been reduced a hand is put onto the measurement cable. The measured s11 response should not change whether your hand is there or not. Ferrite chokes also provides a safety cushion in that if the efficiency is good with the chokes on, it can be expected that the efficiency of the antenna is better. Ferrite chokes do have the detrimental effect of potentially changing the resonance frequency, but it is to be preferred over an unstable s11 due to cable absorption, reflection and position.

These techniques are necessary for this project due to the small size of the PCB and product as the cable can have a large impact on the performance of the antennas. This will improve the stability and accuracy of the measurements, with the detrimental effect of a lower efficiency, a potentially shifted resonance frequency or a reshaped radiation pattern. This however is preferred to an unstable measurement constantly changing with the position of the RF pig tail.

## 5.2 Simulation and measurement of RTX8950 PCB

The mechanic will affect the performance of the antenna meaning that to determine the effect of the mechanic on the antenna it is necessary to measure and simulate the antenna

performance with and without mechanic. To measure the mechanic and PCB for determination of the radiation pattern and the S11 parameters, the PCB requires a RF-cable soldered to it. The presence of the RF cable in the reactive near-field means that it is expected that the s11 parameter and radiation pattern is affected by the presence of the RF cable due to the small ground plane on the PCB. While it is possible to get the radiation pattern from setting the device in Test mode, it would still require a measurement of the conducted power to get a gain-plot. The S11 would still be difficult to measure in the mechanic. The simulation of the PCB in and out of mechanic are performed first in order to get the expected plot. The PCB in the mechanic is simplified meaning that components and antenna match are not applied. As the pcb antenna is matched, its performance is expected better. The antenna is simulated after which the product is measured and a comparison is made.

### 5.2.1 Simulation of RTX8950 PCB without and with mechanic and battery

For simulation purposes CST is used as the simulation tool. The mechanic and PCB shape was obtained by RTX A/S and applied in CST. Simulating the current PCB with and without mechanic can give an idea to how the antenna is performing on the PCB and when it is encapsulated in the mechanic. The mechanic is defined as the whole RTX8950 device that is not the main PCB. This includes button PCB, battery, speaker and cables. The mechanic is expected to affect the performance of the antenna significantly due to presence of metal objects within the reactive near-field. The main affector in the reactive near-field is the presence of the metal encapsulated battery. A solid metal object positioned close to the PCB is certain to affect the performance of the antenna. Other viable effects is the presence of a PCB on top of the main PCB and the extension of ground through the ground wire connected to the microphone. The imported model of the mechanic and PCB contained placeholder material names giving them all a relative permittivity and permeability of 1. As it is unknown which type of plastic the mechanic utilises, an assumption for its characteristics was made. The assumption is that the plastic has EM properties similar to polypropylene with a permittivity of 2,1-2,3 with the applied value being 2,2[21]. These material properties were applied to all elements of the mechanic consisting of plastic. The rubber in the objects was applied with the CST rubber properties, the battery with lossy aluminium and wires and other connections being defined as lossy copper. The PCB for the RTX8950 in the model is a raw model consisting of a thickness, a sketch on the surface and some connectors applied on top of the PCB. In order to measure the antenna it was necessary to apply copper on the PCB and apply a copper island around the attachment point for the PCB. A standard thickness of 35 $\mu$m was applied and the antenna was fed similarly to the feed line on Figure 4.2(a). The configured PCB can be found on Figure 5.1(a) with (b) showing the mechanic.

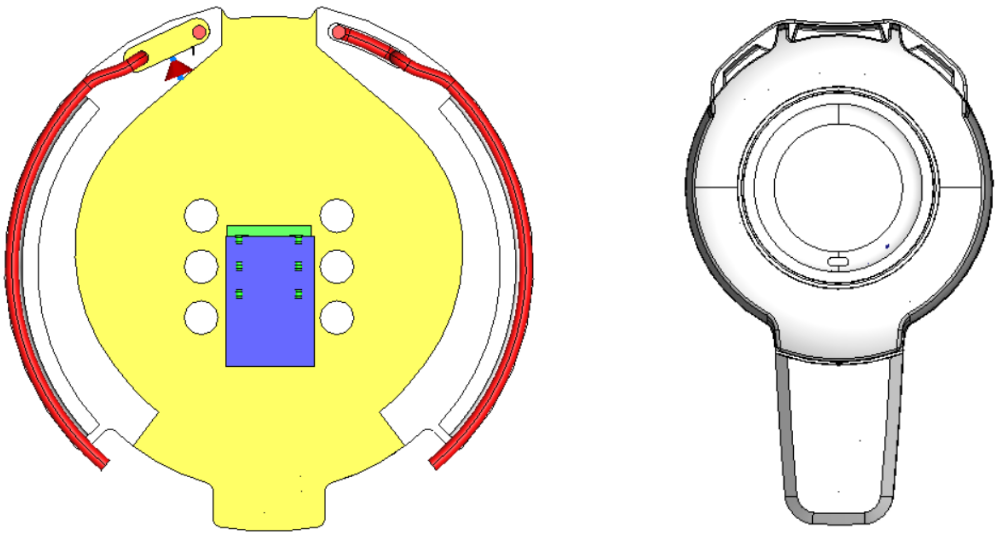

**Figure 5.1:** PCB and mechanic top view for the RTX8950 used for the project. The mechanic is used for simulating and measuring while the PCB is used as the platform for antenna design.

The frequency spectrum used in the CST simulation is set to be from 1,4 GHZ to 2,4 GHz with far field monitors measuring every 50 MHz with measurement points every 20 MHz in the frequency band [1,8;2] GHz to get more data-points in the desired frequency band. The simulated results of the RTX8950 PCB outside and inside full mechanic are shown on Figure 5.1 with a comparison between inside and outside performance on the antenna.

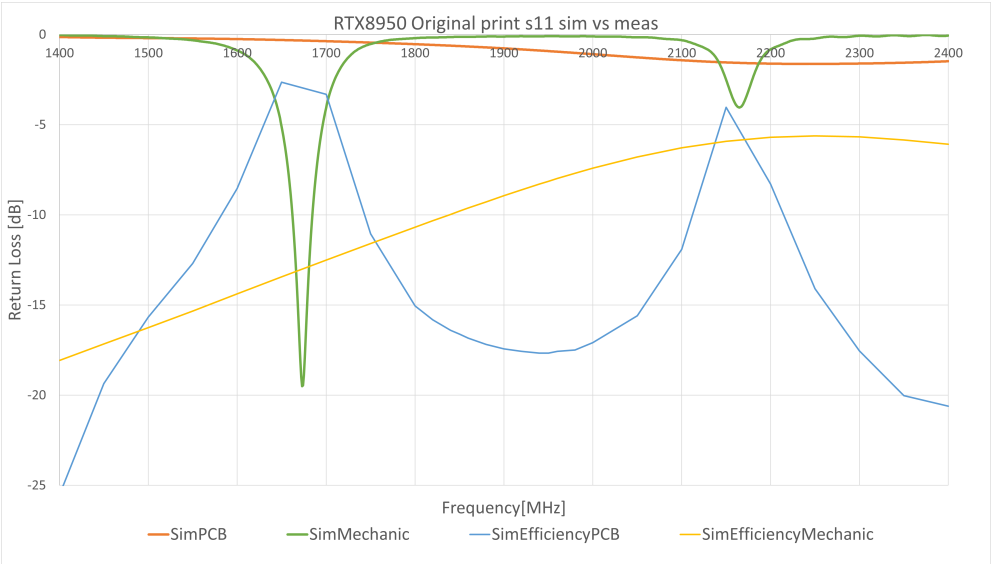


**Figure 5.2:** Simulation response of the original wire antenna on the RTX8950 PCB. The antenna is unmatched in the simulations.

From the simulated results of the PCB it is observed that the mechanic has a large effect on the antenna performance with the effect on the antenna being positive. The efficiency of the antenna is improved remarkably seen on Figure 5.2(a) due to improved s11 response. The effect of the mechanic is determined to have a critical effect on the antenna and will therefore be critical in designing the antennas.

### 5.2.2 Measurement of PCB in mechanic

It was confirmed in section 5.2.1 that the mechanic of the RTX8950 affects the antenna of the PCB to a degree that is critical to determine. This section will focus on the measured results of the RTX8950 PCB for one antenna. The purpose of this section is not to compare the measured and the simulated response of the antenna but to determine the antenna parameters. The parameters includes gain, efficiency and return loss. The matching components for the antenna are included in the measurement of the antenna's performance. In order to determine the antenna performance, passive antenna measurements are performed. Doing passive antenna measurements require a RF cable to measure. Measurements in this project are performed using SMA RF Pig tails that requires the necessary precautions described in section 5.1. The measuring setup can be observed on Figure 5.3 with the ferrite beads and RF pig tail soldered with the PCB both inside and outside mechanic.

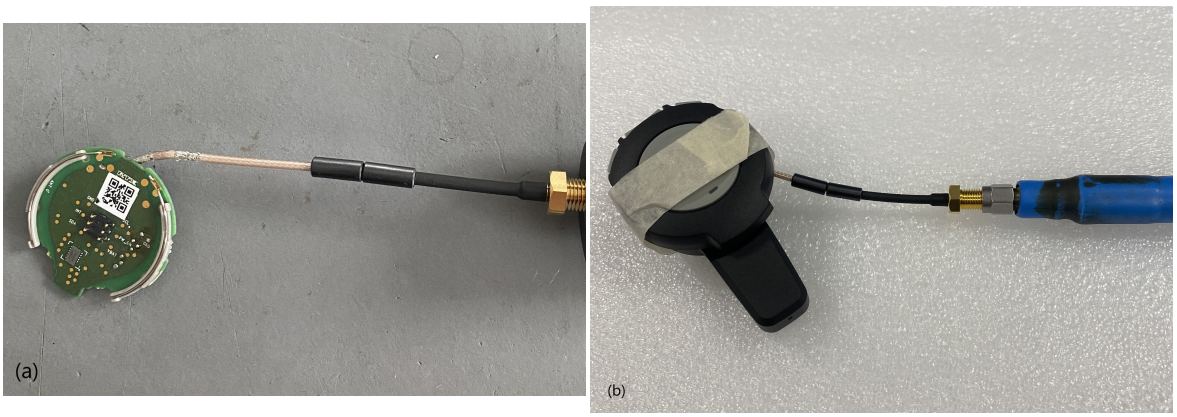


**Figure 5.3:** Measurement setups for the RTX8950 PCB and other prints. (a) is RTX8950 PCB without mechanic and (b) is inside mechanic.

The setups on Figure 5.3 are measured using the high frequency facilities at AAU. The first type of simulations performed at AAU facilities is a S11 measurement of the RTX8950 print with and without mechanic. To measure the s11 a Vector Network Analyser (VNA) is used. The VNA is calibrated and port extended using a RF pig tail similar to the one on Figure 5.3 to avoid phase shift. Figure 5.3 (a) and (b) are measured in free-space to avoid coupling with the objects in the vicinity. The PCB in the mechanic is measured in a head coupling configuration to determine the tuning or detuning caused by the head coupling. The re-

sults can be seen on Figure 5.4.

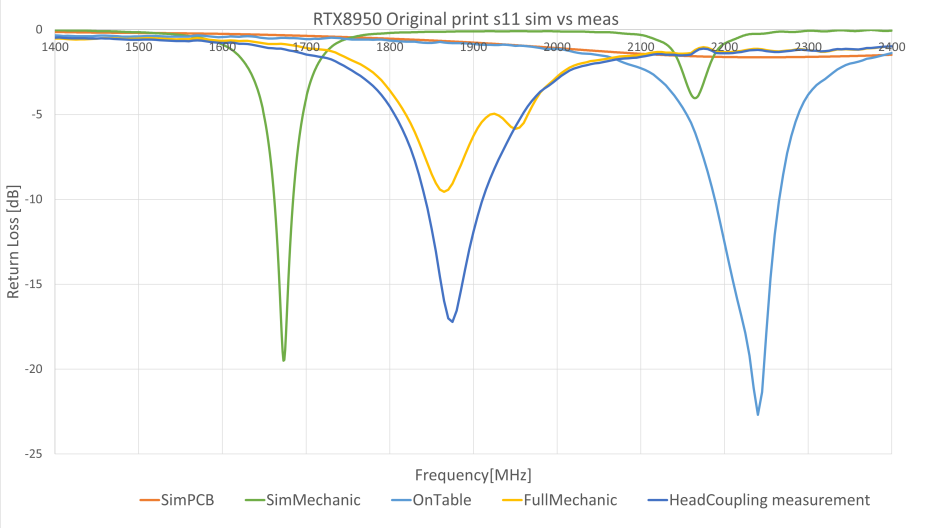


**Figure 5.4:** Measured response of the left antenna on the RTX8950 PCB. The response is measured through the antenna match on the antenna which explains the distance between simulated and measured antenna. The match was measured to a good response within the frequency spectrum in a head coupling configuration.

The s11 was measured through the match on the PCB. The match components are unknown but the match one reason for the s11 to have been matched to the frequency 1900 MHz. The response for the head coupling of the headset does not fulfil the bandwidth requirements but is a response that is in a good direction towards this. The PCB was measured in the Stargate at AAU to determine its directivity and efficiency. The setup for the RTX8950 mechanic in the Stargate is seen in Figure 5.5(a). Figure 5.5(b) contains the peak directivity and efficiency for the left antenna on the RTX8950 pcb. The testsetup will be used for the prototype antennas.

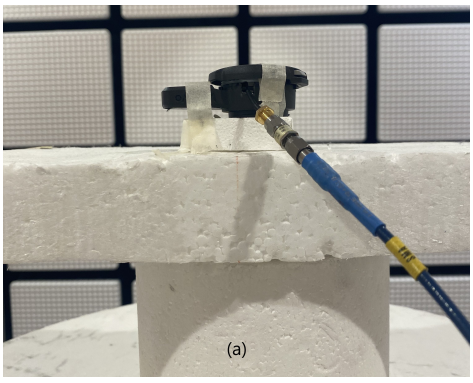


| (b) | RTX8950 Mechanic | |
|---|---|---|
| **Frequency** | **Directivity** | **Efficiency** |
| 1880 | 5,554 | -4,96 |
| 1890 | 5,62 | -5,057 |
| 1900 | 5,513 | -5,153 |
| 1910 | 5,129 | -5,4 |
| 1920 | 4,724 | -5,446 |
| 1930 | 4,408 | -5,623 |

**Figure 5.5:** Measurement setup for measuring in the AAU Stargate can be seen on (a). (b) contains the measured data specifically the directivity and efficiency of the antenna.

With the mechanic as a standalone, a gain of 0,6 dB down to a gain of -1,2 dB is obtained in the band. The behaviour in the frequency band is expected from looking at the s11 response for mechanic on Figure 5.4. The efficiency was measured to -5 dB, which is lower than requirement but not by a large degree. Tuning through head coupling could possible fulfil the requirement. The head coupling was not measured due to a loss of matching components and it being unknown which components the antenna was matched with. The mechanic and PCB were delivered from RTX A/S and it is uncertain if the antenna match is equal to the currently used match, so this is a comparison to the received PCB.

## 5.3 Design of prototype antennas

The PCB has a small circular size with a diameter of 3,1 cm. The possible amount of room for the antenna is small, meaning that a quarter-wave antenna is neccesary. The RTX8950 PCB contains two antennas but for prototype purposes, a single antenna is applied on the PCB. Due to the product requiring adequate amount of space for components, the size of the ground on the PCB is not viable for reduction, but modification through the extension of the PCB is possible. On Figure 5.6 we see the raw RTX8950 PCB with its ground and substrate.

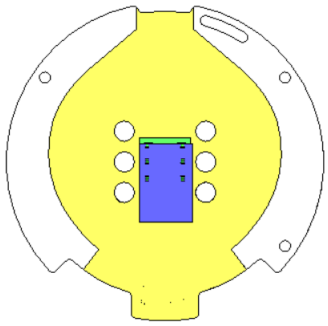

**Figure 5.6:** Raw PCB of the RTX8950 PCB with copper applied but antennas removed.

The curved space on each side of the Yellow area on Figure 5.6 is the area available for positioning antennas. The space is limited and was originally fit with bent wire antennas following the outer edge of the PCB. The curvature of the ground plane makes it impossible to make a typical straight antenna such as IFA or the monopole for a DECT antenna. It is possible to utilise an antenna type like the IFA in the case of only a single antenna on the PCB. The components can be moved to the other side of the PCB with the ground, and have more area for antenna development by reducing the circular part on the desired side.

There are options for putting an antenna near the edge of the PCB. These options include using miniaturised antenna methods, such as utilising serpentine method to make a meandered IFA antenna (MIFA) to reduce the physical size, or it can be obtained through

bending an antenna in either 90° or following the curvature of the PCB in similar fashion to the attached wire antenna seen on Figure 4.2(a). A detrimental effect of bending an antenna is an increase in Voltage standing wave [10] which in turn can decrease the radiated amount of power for the antenna.

It is unknown which type is the optimal for the specific size of PCB and copper plane. Several options for antenna type are explored for development of the optimal antenna on the PCB however all options are micro-strip antennas. Some of options explored were a bent IFA and a meandered IFA (MIFA) which will be described in the sections below. These antennas were designed with the premise of the head coupling shifting the frequency 50 MHz.

### 5.3.1 Curved IFA

One of the options explored in regards to developing an antenna for the PCB, was an antenna similar to the one already on the PCB seen on Figure 4.2(b). The antenna on the RTX8950 PCB is a bent wire antenna with the nearest equal on a PCB being a bent monopole. It is noticeable from the simulations of a bent Monopole in section A.3 that matching a bent monopole is difficult without utilising matching components. As the target is to have an antenna optimised for DECT frequencies the bent monopole is made into a curved IFA. A curved IFA will ensure easier optimisation for the antenna. The first iteration of the bent IFA antenna consisted of the antenna bent in a similar way to the wire antenna on the RTX8950. The designed antenna can be seen on Figure 5.7.

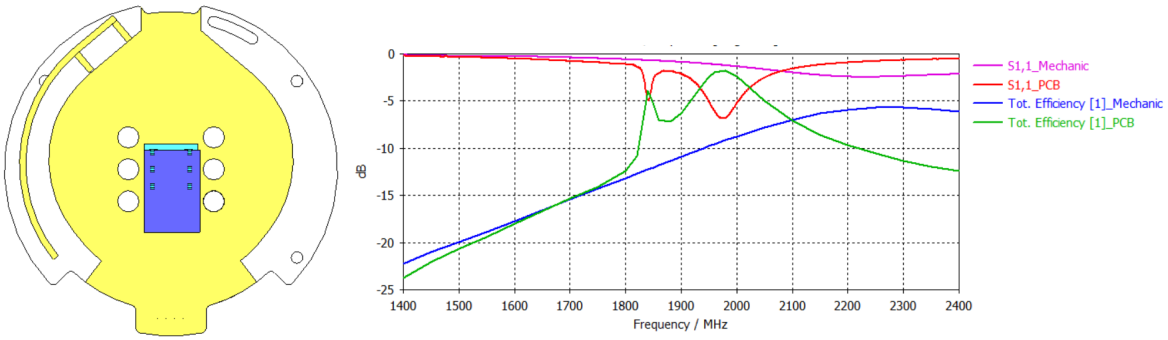


**Figure 5.7:** Curved IFA following the bend performance of the RTX8950 antenna with the s11 response shown on the plot. Antenna proved difficult to match through positioning

The antenna is simulated with and without the mechanic to determine its s11 and performance. It was attempted optimised with the design and response on Figure 5.7 being the final optimisation with the current design. The mechanical properties are the same as applied to the mechanical parts in section 5.2.1. The results of the simulation can be seen on Figure 5.7. The IFA parallel to the PCB seen on figure 5.7 turned out to be difficult to tune into an useful antenna without the use of components which was undesired for

prototypes. The S11 never got below -10 dB during tuning and with mechanic, but the efficiency looked fine at certain frequencies. This design was therefore considered unusable but the IFA antenna was still viable.

In section 4.5 the effect of the ground plane on the antennas performance was discussed. The specifics of the effect of the length and the width of the antenna were discussed. The length improves the antennas performance. The width of the ground makes the antenna more stable with changes to the length. The previous antenna on Figure 5.7 and on the RTX8950 has a peculiar relationship to ground due to the angle of entrance for the ground pin for the bentIFA and for the feed line for the wire antenna. In order to utilise the PCB to the biggest extent, the feed and the ground pin were rotated in order to have the longest possible ground for the antenna. This meant that the antenna had a need for a stronger bend during the start of the radiating part, with the rest of the radiating part bending slightly. Mentioned in section 4.5.1 the IFA's radiating element is made for a quarter-wave and is then adjusted to fit the resonance frequency. This includes adjusting the feed-line and ground pin sizes and positions. The first prototype of the antenna optimised in simulation in mechanic can be seen on Figure 5.8. The results of this antenna is seen on Figure 5.8.

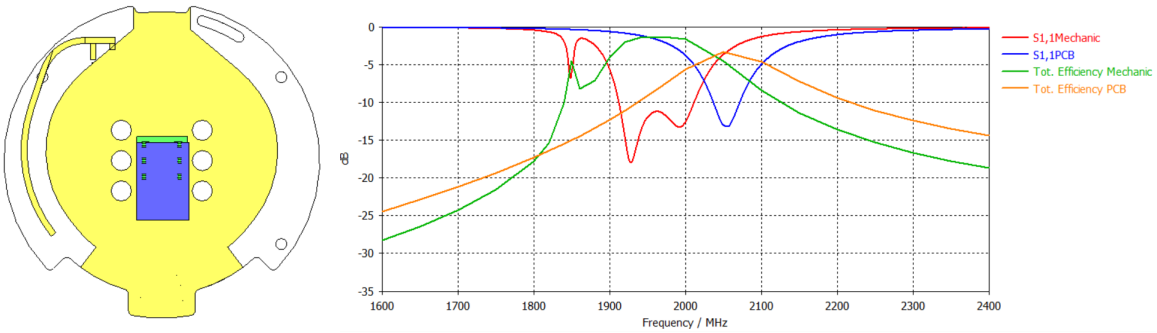


**Figure 5.8:** The resulting Curved IFA design and its corresponding s11 response.

Observed on the figure, the resonance frequency shifts noticeably when the mechanic is applied. This was an expected outcome with the antenna matched for a frequency of 2000-2100 MHz to counteract that. The resulting simulated result gives a bandwidth from 1915-2015 MHz. The resulting s11 bandwidth is still too high in frequency but as it was simulated on the basis of the simplified mechanic described in section 5.2, it was expected for the mechanic to have a higher effect when measured. The efficiency of the antenna is also reasonably within the requirement for the antenna in the mechanic sitting at a level of -2 dB. The simulated result of the antenna is within expected requirements and will therefore be printed on FR4 and measured.

### 5.3.2 Meandered IFA

Another design option that was simulated, is the meandered IFA(MIFA) antenna. A MIFA is often utilised when spatial constraints are tight for an antenna. The MIFA is used to preserve the electrical length within a smaller area. A way to obtain this is through splitting the antenna's radiating element into several connected pieces. The shape of the connected pieces can be many things but some examples of them are a square spiral antenna and a serpentine antenna with square corners. There are several options, and the options for the MIFA on the PCB were simulated. Utilising the experience with the size of ground in section 5.3.1 the positioning for ground and feed are utilised.The arrived choice of MIFA is closer in resemblance to a normal IFA than a MIFA. The curved space on the substrate for the antenna is not optimal for either MIFA or IFA, and therefore the MIFA method was used in order to bend the antenna on the available substrate. The model of antenna optimised for the specific frequency can be seen on Figure 5.9.

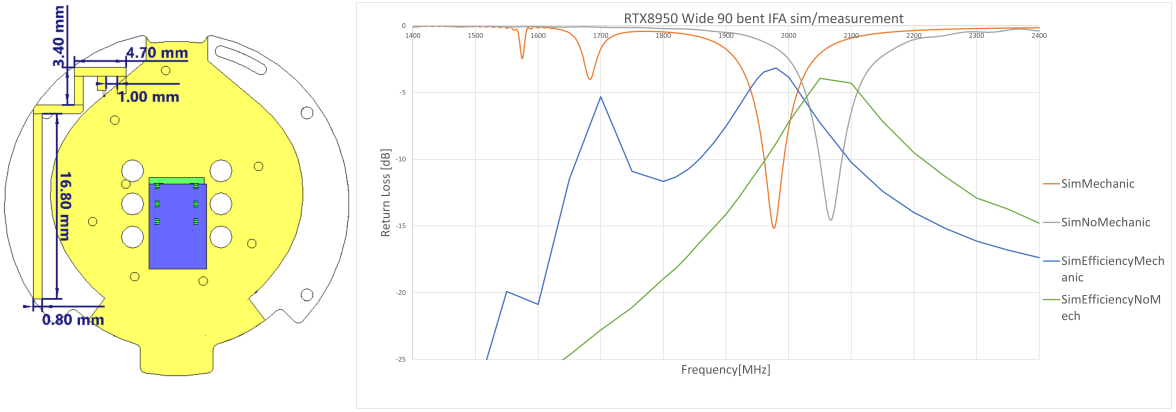


**Figure 5.9:** The MIFA antenna's design and corresponding simulated s11 response inside and outside mechanic.

The model is simulated using same mechanical properties as section 5.2. The results of the simulation can be seen on Figure 5.9. From the data, it can be concluded that the MIFA antenna is also a viable option for the developed antenna. The bandwidth however is lower for this antenna meaning that shifting in the frequency spectrum has a larger detrimental effect than seen on the curved IFA. A thinner version of the model was simulated and measured with the results being found in Appendix B.1.

## 5.4 Changing PCB shape

Two different prototypes were simulated in section 5.3.1 and 5.3.2 and are ready to be measured. Before measuring the antennas, an extension of the copper plan will be simulated.

The extension of ground is done with a basis in the designs in section 5.3.1 and 5.3.2. In section 4.5 it was confirmed that the length of the ground plane affects the performance of a quarter-wave antenna.

Observing the ground plane shape on figure 5.6a protrusion in the ground plane is observed which is connected to the PCB through cables to the microphone arm. A copper extension is available in the direction of the mechanical arm. The copper extension is applied in the form of copper piece having a width equal to the copper protrusion. The length is considered variable with a maximum length of 50 mm. The maximum length is to ensure the ground extension fits within the mechanic. With an increased ground plane, the radiating area will increase as well. This can help increase the efficiency, directivity and radiation pattern of the antenna, although it might also cause detrimental effects such as detuning of antenna. With a larger ground it should be easier to tune an antenna for a specific frequency [8]. The pre-simulated extended ground model can be seen on Figure 5.10.

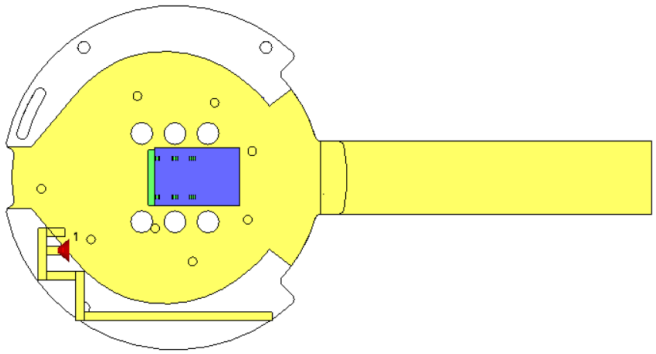


**Figure 5.10:** Ground extended PCB of the MIFA antenna model from Figure 5.9.

The model with the extended ground should make it easier to get a high directivity and efficiency for an antenna, but would require specific changes of the sizes of antenna to fit with each ground length. A sweep of the ground length from 5 mm to 30 mm can be seen in Figure 5.11 with the efficiency included to determine the performance. 5.4

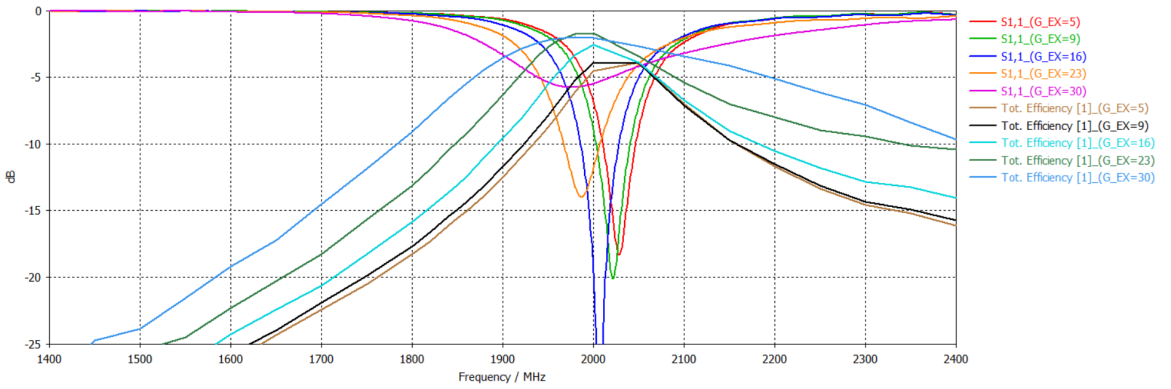


**Figure 5.11:** Ground extension length sweep plot. It shows the resonance frequency and efficiency for the antennas at certain ground extension lengths.

From this it can be seen that some lengths of the extension have a positive effect on the performance with the radiation pattern becoming more directive and radiating more power. This is visible on Figure 5.12 where a comparison of the radiation pattern between (a) no ground extension and (b) ground extension can be observed.

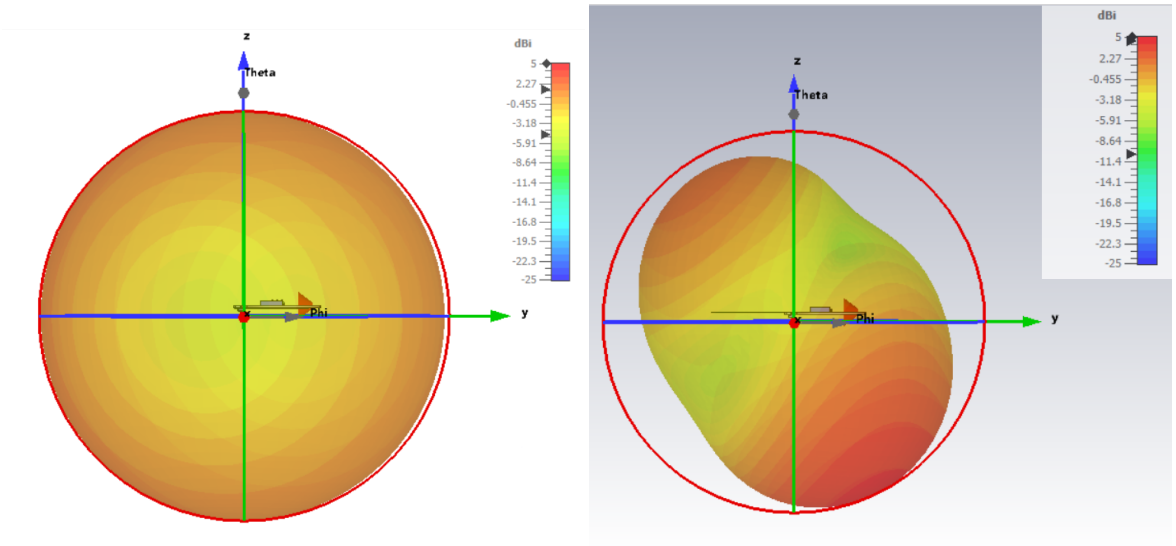


**Figure 5.12:** Comparison of the shape of the radiation-pattern with the introduction of a ground extension. The radiation pattern is elongated instead of an entire sphere which is visible on the left side. Left side is without ground extension and right is with ground extension which is visible from the PCB in the radiation pattern.

The comparison of the two at the frequency 1900 MHz in radiation pattern and efficiency shows that extending the ground plane to utilise the microphone arm has a positive effect on how good an antenna is achieve-able. The extension is applied as a part of the measure-

ments of the two antennas. As the results from Figure 5.11 are not expected to be equal to the measured response, the length of the ground extension will be the maximum length which is shortened with lengths equal to the step width in the figure.

## 5.5 Summary

Prototypes of antennas were developed through the chapter. They were developed after a measurement and simulation of the RTX8950 PCB in its mechanic. In order to get proper measurements of the original RTX8950 PCB given by RTX, appropriate fixation of RF pigtails was discussed with two techniques being used for measuring the RTX8950 PCB. The prototypes design is based upon reaching the desired requirements and achieving better results than the measured and simulated RTX8950 seen from Figure 5.4. The developed antennas are expected to achieve the desired performance and will be printed on a FR4 PCB with vias included to achieve proper grounding.

# Measurements and testing 6

The original antenna on the RTX8950 PCB has been measured and two prototype antennas were developed in chapter 5. The next step is to realise, measure, compare and optimise on the antennas. Both prototypes will be measured and the measured data is compared to the simulated results. The directivity and efficiency are measured and compared to the simulated results. The prototypes will then be measured with a ground extension length before comparing the data to the measured result. Both prototype antennas are compared to determine the optimal prototype. With the prototype decided, it will be compared to the measured RTX8950 data to determine the performance difference. The designed prototypes are printed using AAU facilities on FR4. One major source of error between the simulated and measured is the thickness of the PCB. The RTX8950 PCB is 0,82 mm thick while the FR4 sheets available at AAU is 1,55 mm thick. Difference between the PCB and the simulated in thickness is therefore previously known ahead of time as a source of error. The effects of a thicker PCB can be a detuning of antenna and reduction of efficiency due to loss incurred through surface waves[14]. In this chapter, the prototype antennas will be measured using several different test cases. The test cases consist of the following four.

1. PCB only measurement
2. PCB in mechanic in free-space
3. PCB in mechanic with head coupling
4. Ground extension in head coupling

Section 6.1 will describe the four tests.

In section 5.4 ground-extension was explored for potential improvement of the antenna. Ground-extensions will be applied as the last measurements for each antenna prototype to determine if any extension length has a positive effect on the antenna. The applied ground-extension is a crafted model of a flex-PCB. The crafted flex-PCB consists of polyimide tape in two layers with 35µm copper tape applied on the top. The ground extension is soldered to the position seen seen on Figure 5.11. The length of the extension is swept and measured with unequal intervals on a VNA. These intervals are unequal due to the extension being manually shortened.

## 6.1 Performance of test cases

This section describes how to perform each test case for the two prototype antennas. As each of the four tests is the exact same for the two prototypes, the tests will be described beforehand in this section. The S11 response is measured in the frequency-spectrum 1400 MHz to 2400 MHz. Two instruments are used for performing the test cases and they are a VNA and the Stargate at AAU. They are used for measuring different things. The VNA is responsible for measuring the S11 and impedance which is often used during optimisation of antenna performance. The Stargate measurements are responsible for determining the directivity, efficiency of the antenna at different frequencies. This includes derivative results such as the gain and radiation pattern.

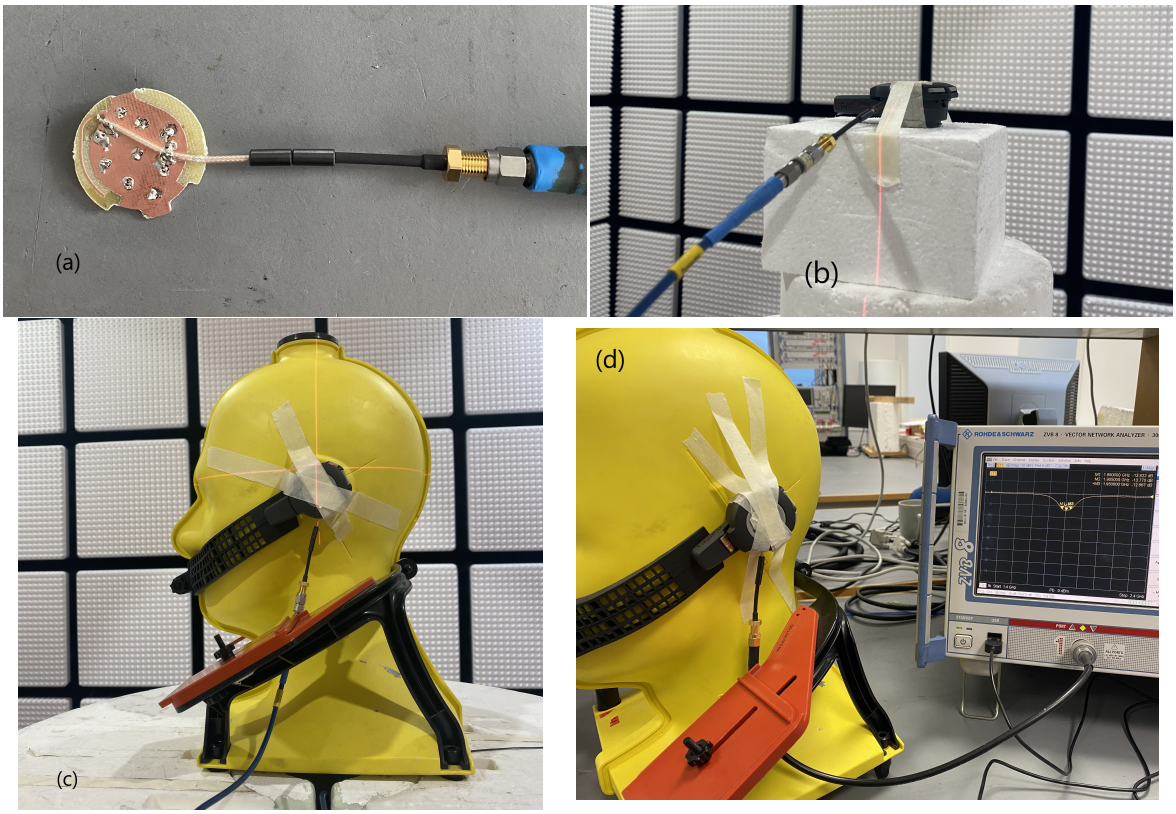


**Figure 6.1:** Measurement setups for the different measurement types. These are used by the different test cases. (a) is measurement of the PCB performance by itself. (b) is measurement of the performance of the antenna in free-space inside the mechanic. (c) shows the head coupling configuration. (d) shows the head-coupling configuration when measuring with a VNA.

**Test case 1** consists of only the PCB being measured. The VNA is calibrated with a port extension for the RF pig tails attached to the test case. The test case contains two scenarios, one on normal table and the other in free-space. The free space in the test case is foam

that have electromagnetic properties equal to free-space. This test case can be applies to tests using both the Stargate and a VNA. The test setup for VNA in non free-space is observable on Figure 6.1 (a) with the free-space variant visible on Figure 6.1 (b), except with no mechanic for the PCB.

**Test case 2** consists of placing the PCB inside the RTX8950 mechanic. The PCB is placed in mechanic with the pigtail protuding. It is positioned on free-space material. An example of this test setup can be seen on Figure 6.1(b). The same setup is used for both VNA and Stargate testing.

**Test case 3** consists of the PCB and mechanic being coupled to a head with electromagnetic properties similar to a real head. The target of the test case is the determination of the effect caused by head-coupling on the performance of the antennas.

Figure6.1(c) shows the position of where the the mechanic is attached on the head with a measurement cable connected. This allows for measurement of directivity, efficiency and S11 when the product is under normal usage. The test case is utilised for both the VNA and the Stargate, with Figure 6.1(d) showing one case of using the VNA to measure.

**Test case 4** contains a span of different measurements. The ground extension flex-PCB previously described is soldered on to the PCB with its length shortened and measured in several iterations. The desired cutoff per measurement is 5mm, but manual inaccuracy makes the individual length of the copper extension measured and recorded for every measurement. Figure 6.1(d) shows the VNA measuring the ground extended antenna performance. Test case 4 measures all the lengths of ground extension, compares the results and determine the optimal lengths. The optimal lengths are measured in the Stargate to determine their directivity and efficiency.

## 6.2 Curved IFA

The first prototype was designed in section 5.3.1 on the basis of maximising the ground length. The specific antenna in this design is a Curved IFA. The curved part of the antenna is the radiating arm with the resulting simulation results in section 5.3.1. The Curved IFA PCB was printed and the measurement guidelines from section 5.1 were applied to the PCB. The following PCB on Figure 6.2is obtained from applying the guidelines.

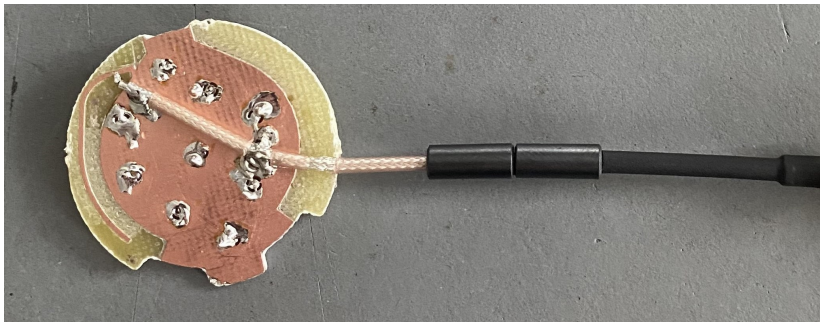

**Figure 6.2:** The printed Curved IFA with its soldered RF pigtail attached. The antenna is printed from the design on Figure 5.8.

The antenna shown in Figure 6.2 must undergo four test cases to assess its performance. The test method of the four test cases described in section 6.1 are performed on the curved IFA prototype. The order of test cases is 1, 2, 3 and 4. In case the results of test case 1 are insufficient, test case 4 can be performed to determine if the mechanic and head coupling causes the antenna to be within requirements before discarding the design. From measurements on the RTX8950 PCB in section 5.2.2 it is known that the mechanic shifts the frequency down approximately 70 MHz. This knowledge can be applied to test case 1 to determine if the response is at an appropriate frequency. Test case 4 can be used to optimise and improve the antenna in case the results from test case 1 and 2 are at an undesired level.

### 6.2.1 Measurement results

The first measurement performed on the curved IFA is test case 1. Test case 1 consists of measuring the PCB in free-space and afterwards measured inside the mechanic for the RTX8950. The results of the two measurements can be seen on Figure 6.3(a) and (b).

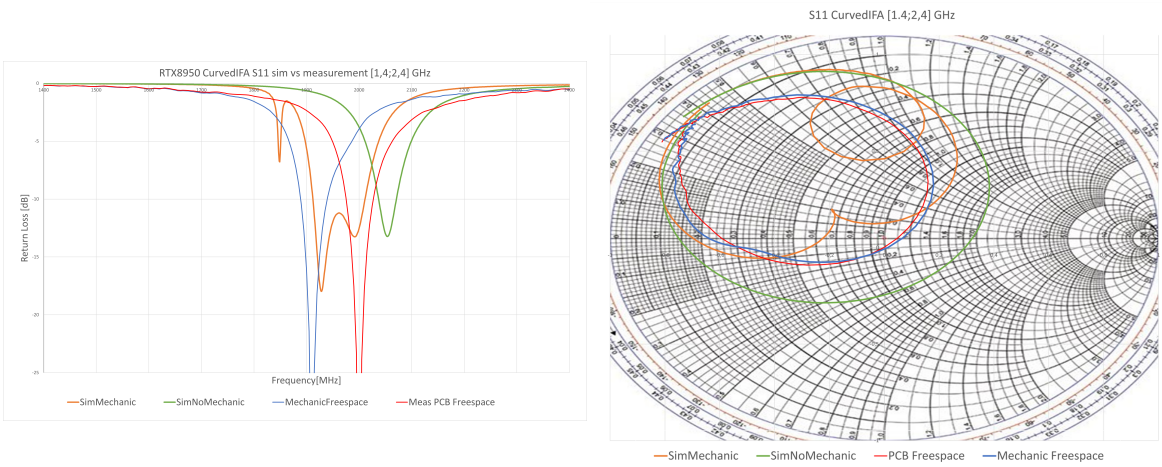


**Figure 6.3:** Measured Return loss and impedance results for the printed curved IFA antenna. On the figures is a comparison between the measured and the simulated. Test and measurement is available in appendix B.2.

Figure 6.3 shows a comparison of the simulated and the measured results of the antenna in free-space. The data shows that the distance moved is roughly equal between the measured and simulated but the measurements shows an overall lower frequency. The bandwidth was wider in mechanic when simulated and looking at Figure 6.3(b), the simulated mechanic result has a better pattern regarding having a wide bandwidth.

As the results from test case 1 and 2 are acceptable, with test case 2 results showing an s11 at 1900 MHz below -25 dB, the next step is to perform test case 3. Test case 3 is measuring the response when the PCB is head-coupled. In combination with test case 3, the directivity and efficiency of the antenna will be measured to determine the behaviour of the coupling with the head. On Figure 6.4 the resulting s11 measurement is compared to the free-space mechanic measurement.

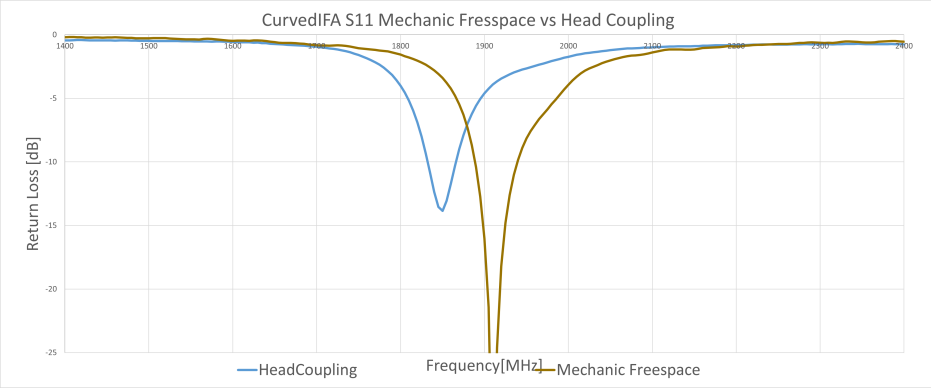


**Figure 6.4:** Comparison between the measurement of the curved IFA antenna in freespace in mechanic vs being in a head coupling configuration.

The coupling can be seen to have shifted the frequency down by 100 MHz, meaning that the head-coupled prototype is now too low in frequency to fulfil the requirements. To verify this it was measured in the Stargate to find the efficiency and radiation pattern. On Figure 6.5(a) and (b) we have the results of the Stargate measurement.

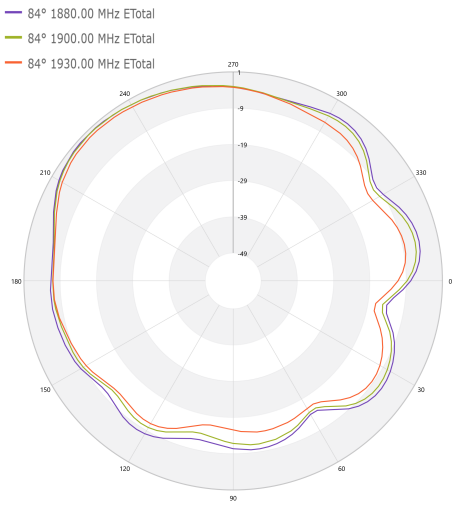


| | Mechanic | | Head coupled | |
|---|---|---|---|---|
| **Frequency** | **Directivity** | **Efficiency** | **Directivity** | **Efficiency** |
| **1870** | 6,979 | -5,37 | 6,589 | -6,859 |
| **1880** | 6,610 | -5,439 | 6,786 | -6,65 |
| **1890** | 5,934 | -5,689 | 6,946 | -6,8 |
| **1900** | 5,296 | -6,105 | 7,113 | -7,105 |
| **1910** | 5,155 | -6,65 | 7,256 | -7,577 |
| **1920** | 4,897 | -6,721 | 7,41 | -7,651 |
| **1930** | 4,534 | -7,19 | 7,486 | -8,07 |
| **1940** | 4,466 | -7,295 | 7,54 | -8,225 |

**Figure 6.5:** Radiation pattern plot for the three frequencies within the desired band for the head coupled measurement. The table contains the measured peak directivity at the different frequencies between the mechanic and the head coupled measurement combined with the efficiency at the different frequencies. It is observable that the head appears to reduce the efficiency as expected. Test and measurement is available in appendix B.2.

The data in Figure 6.5(b) shows the efficiency and directivity for the mechanic and head-coupled measurements. On Figure 6.5(a) the gain and its direction is visualised for the head coupled measurement. It can be read from the figure that the gain is at a value around zero, which is not unreasonable considering the frequency being out of band on Figure 6.4. It is visible how the radiation pattern level is lowered at angle 120 to 300, which is a reasonable span considered the close proximity to the head. This is likewise reflected in the data in the table. Comparing the directivity of the two measurements the directivity increases for the head coupled measurement. This is in line with the theory explained in section 4.6.2 where with a large object blocking an entire side of the antenna, it will radiate stronger in the opposite direction, thereby increasing its directivity. The efficiency is also known to decrease due to the head absorbing a part of the radiated power.

The results are in line with expected behaviour but the efficiency is below the requirement. The antenna is considered in need of an improvement to reach a centralised s11 in the frequency band. This is possible through matching with components or increasing the starting frequency of the antenna seen on Figure 6.3(a). Another option to this is explored in section 6.2.2 with an extension of the ground to research if the increase in ground plane will improve the performance.

### 6.2.2 Ground extension

Extension of the ground was confirmed to have general positive effects in section 5.4. The positive effect is tested on Curved IFA antenna to determine eventual improvements by utilizing the microphone arm. The test is case 4 seen in section 6.1 with Figure 6.1(d) showing the measurement setup. The copper extension was described earlier in the chapter, along with its width and positioning. The length of the extension was swept and the resulting s11 response for the lengths can be seen on Figure 6.6.

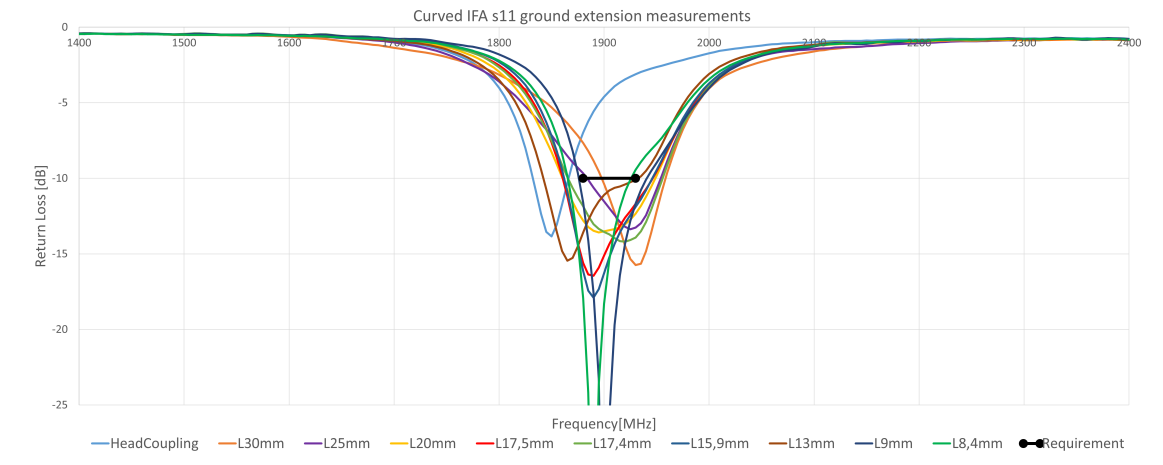


**Figure 6.6:** The measured s11 data when ground extensions of different lengths are soldered to it. L30mm equals a length of 30 mm ground extension for the different plots. Test and measurements are available in appendix B.3.

The figures suggest that the antenna will achieve a performance fulfilling the requirement of -10 dB in the frequency band defined by the black line on the plot. Only the head-coupling and length of 8,4 mm does not fulfil the requirement in the frequency band. From the data it can be confirmed that an extension of ground is beneficial to obtaining a better s11 response. Most of the ground extensions have a response that should improve the efficiency seen in the Table in Figure 6.5. The two ground extensions chosen for the matter of testing is a length of 9 mm and 17,4 mm. These two were chosen due to their different bandwidths. L9mm is a very sharp S11 with a peak below -25 dB having a bandwidth of around 60 MHz, while L17,4mm has a wider bandwidth of 85 MHz, but a peak of -14,2 dB. From the return loss measurement the L 17,4 mm is the preferred choice of length. With a wider bandwidth the antenna is less vulnerable towards frequency shifting caused by for example temperature changes. The better peak-value for the s11 of the L9mm has a smaller effect on the output power due to the logarithmic scale of the power. Less power is obtained between -10 and -20 compared to between 0 to -10. Both are tested in the Stargate with the results in Table 6.1.

| | Head Coupled | | Extension L 9mm | | Extension L 17,4mm | |
|---|---|---|---|---|---|---|
| **Frequency** | **Directivity** | **Efficiency** | **Directivity** | **Efficiency** | **Directivity** | **Efficiency** |
| **1870** | 6,589 | -6,859 | 6,435 | -7,15 | 7,2 | -5,942 |
| **1880** | 6,786 | -6,65 | 6,494 | -6,612 | 7,212 | -5,274 |
| **1890** | 6,946 | -6,8 | 6,555 | -6,488 | 7,211 | -5,147 |
| **1900** | 7,113 | -7,105 | 6,687 | -6,5 | 7,238 | -5,165 |
| **1910** | 7,256 | -7,577 | 6,871 | -6,66 | 7,25 | -5,209 |
| **1920** | 7,41 | -7,651 | 7,05 | -6,55 | 7,211 | -5,087 |
| **1930** | 7,486 | -8,07 | 7,176 | -6,746 | 7,155 | -5,251 |
| **1940** | 7,54 | -8,225 | 7,227 | -6,835 | 7,1 | -5,238 |

**Table 6.1:** The measured directivity and efficiency in head-coupling when comparing the head-coupling measurements with ground extension measurements.

Table 6.1 reveals that the performance of L9mm is similar to the head-coupled suggesting that the s11 may have been de-tuned to some extent, only allowing for a gain around 0,5 dB. The performance of L17,4 mm is better for the antenna, giving a gain of approximately 2 dB across the desired frequency band. The data concludes that the ground extension at a length of 17,4 mm is the optimal for the designed antenna on Figure 6.2. The radiation pattern for L17,4 mm can be seen on Figure 6.7, with the full test available in Appendix B.3.

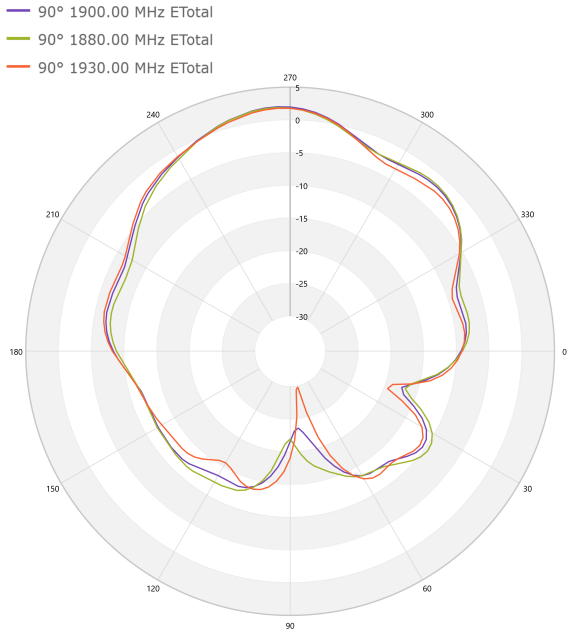


**Figure 6.7:** The gain radiation pattern of the ground extension length of 17,4 mm measured in Figure 6.6 with its data in Table 6.1. The plot is the directivity radiation plot with the efficiency in each frequency subtracted.

The angle from 340 to 120 clockwise shows a clear indication of the head altering the radi-

ation pattern through obstruction, absorption and re-emission of energy. The gain is reduced from -10 dB all the way down to -30 dB in the direction of the head which is expected. The L17,4 mm extension is therefore considered a potential end result for the prototype.

### 6.2.3 Curved IFA Double antenna

The original RTX8950 PCB on Figure 4.2(b) contains 2 antennas on the PCB. The option of adding an additional antenna to the Curved IFA PCB will be explored in this section with the purpose of eventually stabilising the antenna performance. The antenna on Figure 5.8 is applied on the other side of the PCB resulting in the PCB on Figure 6.8. The simulated results are visible on Figure 6.8.

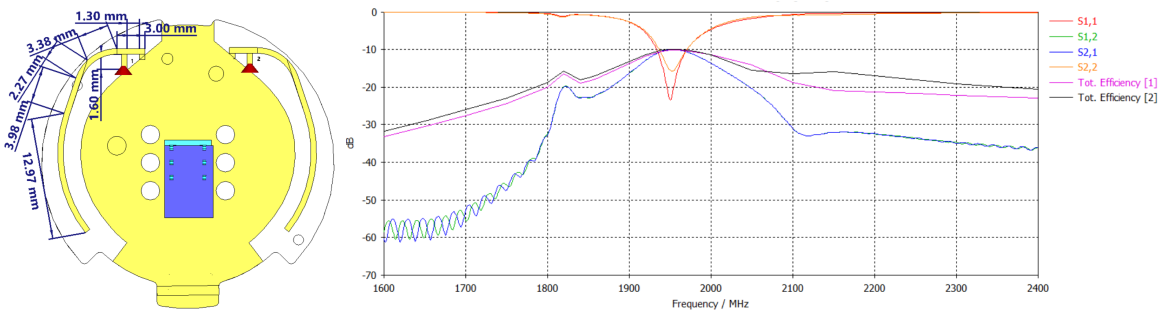


**Figure 6.8:** The curved IFA double PCB with its corresponding return loss plot. The antennas on the PCB is a mirrored copy of the one from Figure 5.8.

From the simulated results, we see a similar performance for both antennas, although the resonance frequency is too high. An attempt was made to include a bio-tissue head to cause coupling with the head as it was known for the head to reduce the frequency in frequency but no clear change was noticeable in the s-response. To confirm this performance, the antenna was printed on a PCB similar to the one on Figure 6.2 and a full 2-port measurement in head-coupling was performed. The data is compared to the simulated results and the result can be seen on Figure 6.9.

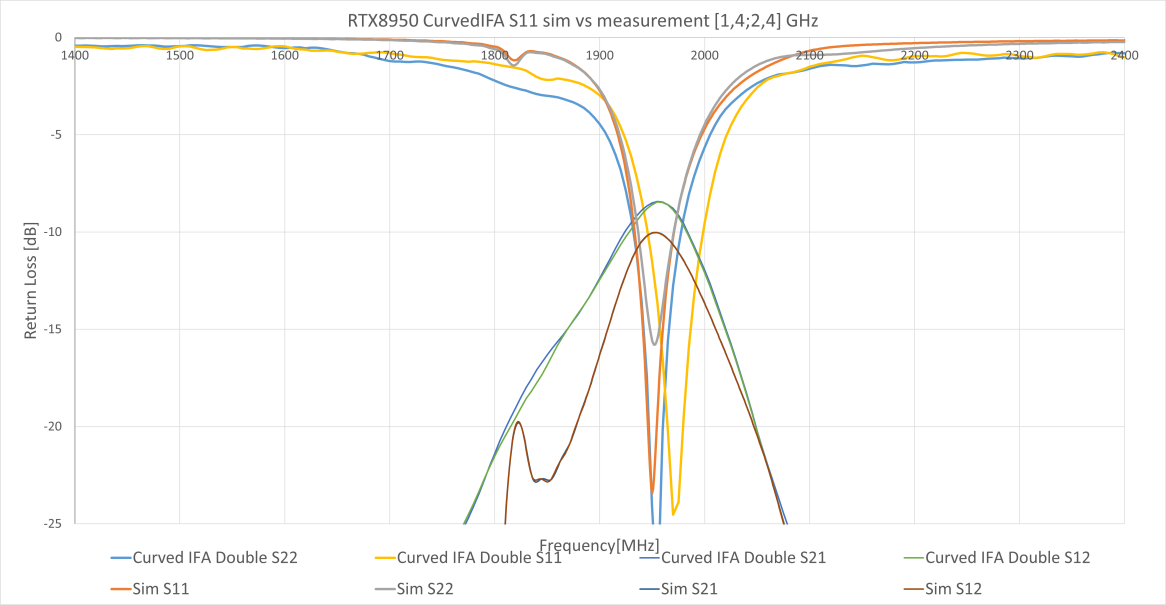


**Figure 6.9:** Comparison of simulated results vs measured of the curved IFA double antenna PCB. It is noticed how the coupling between antennas was higher for the measured and the frequency was shifted with approximately 10 MHz, which is acceptable. Measurement is available in appendix B.4.

The measurement was performed in a head coupling, but the smith chart did not move much when the PCB was removed from the head. From the data it is verified that the simulated model is appropriately similar to reality. This allows for the assumption that the antenna can be optimised in CST with the simulated and measured results almost entirely equal. The antennas are optimised for the center frequency of 1905 MHz. The S21 value is higher for the measured than the reality, meaning that a lot of the power is radiated from one antenna to the other. This coupling is undesired as high power transmissions will cause a lot of power to be received on the antenna, causing a potential disturbance on the RF switch. This is less of an issue as the antennas are connected through a single channel switched through an rf switch, but the issue does prevail. The optimised antenna design can be seen on Figure 6.10.

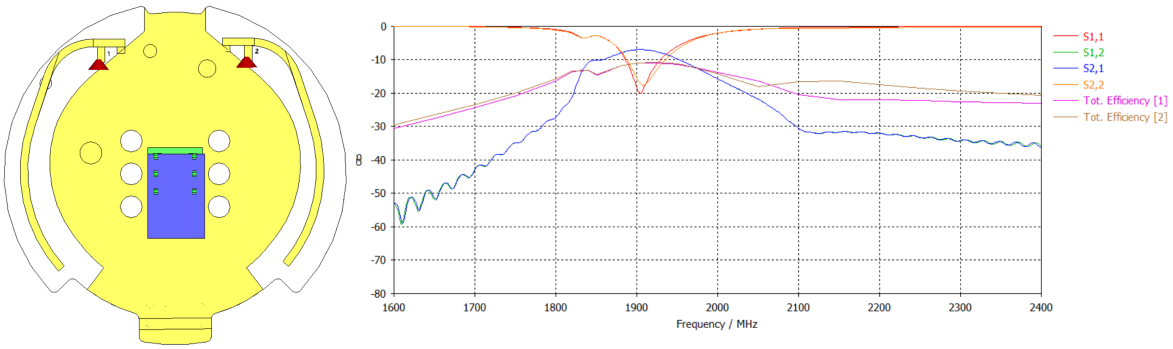


**Figure 6.10:** The optimised curved IFA double antenna PCB with its corresponding return loss plot. The frequency has been shifted to the desired resonance frequency at 1905 MHz.

The figure shows an equal s11 plot for either antenna without the use of matching components. It is also observed that the bandwidth is just barely outside the requirement. Due to lack of time, the optimised antennas were not measured for their performance on a PCB in the mechanic.

### 6.2.4 Requirements

With the prototypes performance tested, it is necessary to compare it to the requirements for the antenna in the project. Both the developed antenna and its ground extension are compared to the requirements to determine if it fulfils requirements. The results of this is compiled into Table 6.2.

| ID | Description | Requirement | Antenna | Ground Extended | Double Left | Double Right |
|---|---|---|---|---|---|---|
| T.4 | S11 ≤ -10 dB | 1880-1930 MHz | 1835-1865 MHz | 1870-1955 MHz | 1886-1930 MHz | 1887-1935 MHz |
| T.5 | Lowest efficiency | 35% (-4,6 dB) | -7,65 dB | -5,209 dB | not measured | not measured |

**Table 6.2:** A comparison of the curved IFA performance against the requirements described in chapter 3.

Requirement T.1 to T.3 are fulfilled through the use of the mechanic for measuring the antenna performance with the exception of the extended ground plane due to the nature of the measurement. In Table 6.2 we see that requirement T.4 is not fulfilled for the standalone head-coupled antenna and neither is the efficiency with no positive gain for the antenna. From the frequency band, it is visible that the aforementioned antenna needs resizing to work within the frequency band or it requires matching. The ground extension of the curved IFA does fulfil the T.4 requirement with a wider than needed frequency band. However the worst efficiency for the antenna is -5,2 dB in the frequency band which is less than the requirement. The head and the RF pig tail are reducing the efficiency, so it is pos-

sible for the efficiency to be 35% or above for the antenna by itself. The antenna however has 2 dB gain in the frequency band, making the lower efficiency less critical. The double curved IFA has a s11 response that just barely does not fulfil the bandwidth requirement on the optimised model. It can be seen that its a marginal difference, and the performance may be appropriate or requite a slight matching as is visible on Figure B.27(a). This is possible through the use of a DC-decoupling capacitor.

## 6.3 Meandered IFA

One of the developed prototypes is the meandered IFA. It was designed in section 5.3.2 and is a result of attempting to achieve the maximum ground-length while utilising an IFA antenna without curved segments. The PCB was printed with the measurement preparations following the guidelines in section 5.1. The printed PCB and attached pigtail can be seen on Figure 6.11.

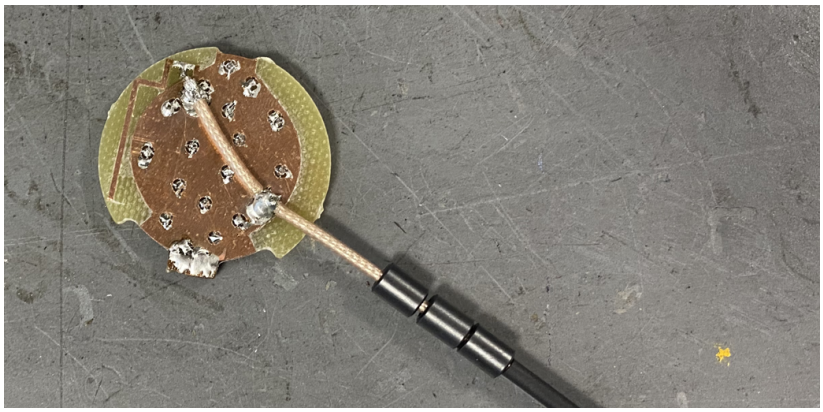

**Figure 6.11:** Printed MIFA PCB with the negation of pigtail effect in the form of ferrite beads and soldering points.

The antenna on Figure 6.11 will be measured for each test case described in 6.1 to determine its performance. The order of test cases is 1, 2, 3 and 4. In case the results of test case 1 are insufficient, test case 4 can be performed to determine if the mechanic and head-coupling causes the antenna to be within requirements before discarding the design.

### 6.3.1 Measurement results

The first test case for the MIFA is test case 1. The measurement consists of free-space and PCB in mechanic measurements which are the compared to the simulated results for the antenna. The results can be seen on Figure 6.12.

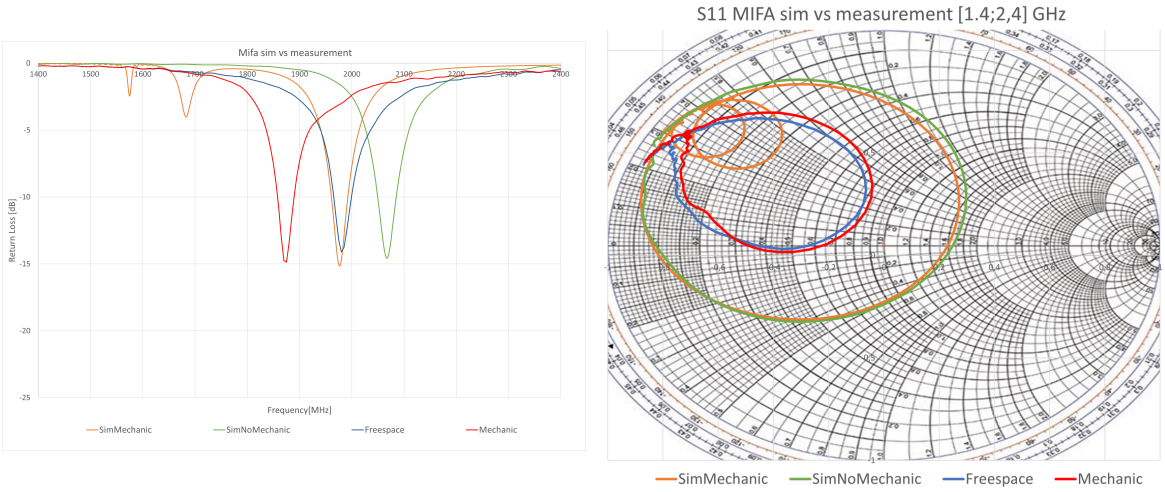


**Figure 6.12:** The measurement results of measuring the PCB MIFA in different configurations with a comparison between simulation and reality.

From the results in Figure 6.12 we see a comparison between the simulated and the measured for the MIFA in free-space. The return loss plot shows an undesired result for the measured antenna with the measured mechanics resonance frequency at 1870 MHz. It has the potential to achieve a radiated performance with a few dB gain when in free-space. The PCB is expected in head-coupling and the effect of it may shift the frequency down so it does not fulfil the requirement and may need to be redesigned. Test case 3 will be performed to determine the s11. The resulting s11 can be seen on Figure 6.13(a) with (b) containing radiated data.

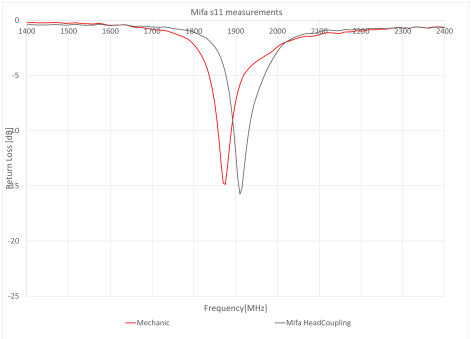


| | Mechanic | | Head coupled Left ear | | Head coupled right ear | |
|---|---|---|---|---|---|---|
| **Frequency** | **Directivity** | **Efficiency** | **Directivity** | **Efficiency** | **Directivity** | **Efficiency** |
| **1870** | 6,817 | -5,736 | 6,415 | -6,600 | 7,146 | -6,658 |
| **1880** | 6,512 | -5,621 | 6,578 | -6,154 | 7,129 | -6,129 |
| **1890** | 5,936 | -5,945 | 6,604 | -6,090 | 7,210 | -6,028 |
| **1900** | 5,551 | -6,529 | 6,513 | -6,144 | 7,394 | -6,075 |
| **1910** | 5,325 | -7,306 | 6,571 | -6,171 | 7,606 | -6,092 |
| **1920** | 5,114 | -7,608 | 6,718 | -5,965 | 7,787 | -5,917 |
| **1930** | 4,787 | -8,313 | 6,808 | -6,186 | 7,898 | -6,222 |
| **1940** | 4,188 | -8,619 | 6,828 | -6,328 | 7,972 | -6,381 |

**Figure 6.13:** Comparison of data between mechanic in free-space vs mechanic in head coupling. The resonance frequency is shifted slightly into the frequency band observed by the increase in efficiency in the frequency band for the head coupled along with an increase in directivity.

From this it is clear that the antenna needs an improvement. It does seem to imply that the head coupling has an improved directivity depending on which ear, causing a gain of ≈ 0,5

dB for left ear and ≈ 1-1,8 dB for the right ear.

### 6.3.2 Ground extension

The extension of ground is known to have general positive effects on an antennas performance. One of the effects is a slight shift in frequency as was noticed in section 5.4. The shift in frequency has the possibility to shift the frequency of Figure 6.13(a) to the desired frequency band. Test case 4 is performed with the described ground extension and position in section 6.1. The length of the antenna is swept with the resulting s11 response plotted in Figure 6.14.

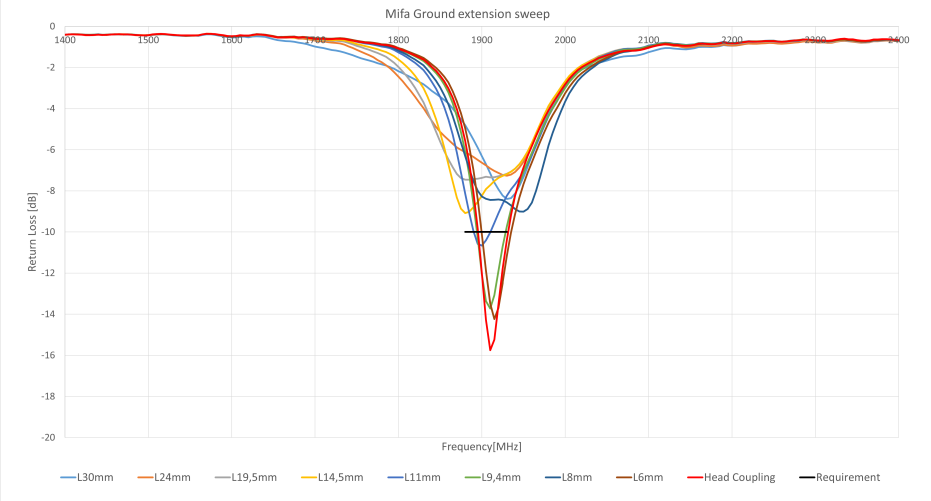


**Figure 6.14:** Measured MIFA s11 response from a ground extension sweep from length 30 mm to 6 mm. The black line is the bandwidth requirement.

The s11 response of the ground extension sweep is stable in its center frequency with a maximum shifting of ±50 MHz on either side of 1900 MHz. A response better than the standard head coupling antenna was not measured through a ground extension. It is therefore concluded that the ground extension is not necessary for the MIFA described in Figure 5.9. The measured sweep is verified through head-coupling radiation test in the Stargate and a ground extension of 14,5 mm. Compiling the results we have Table 6.3.

| | MIFA Left Ear | | MIFA Right Ear | | Ground Extension 14,5mm | |
|---|---|---|---|---|---|---|
| **Frequency[MHz]** | **Directivity** | **Efficiency** | **Directivity** | **Efficiency** | **Directivity** | **Efficiency** |
| **1870** | 6,415 | -6,600 | 7,146 | -6,658 | 6,435 | -7,159 |
| **1880** | 6,578 | -6,154 | 7,129 | -6,129 | 6,495 | -6,612 |
| **1890** | 6,604 | -6,090 | 7,210 | -6,028 | 6,555 | -6,488 |
| **1900** | 6,513 | -6,144 | 7,394 | -6,075 | 6,687 | -6,499 |
| **1910** | 6,571 | -6,171 | 7,606 | -6,092 | 6,871 | -6,664 |
| **1920** | 6,718 | -5,965 | 7,787 | -5,917 | 7,053 | -6,550 |
| **1930** | 6,808 | -6,186 | 7,898 | -6,222 | 7,176 | -6,746 |
| **1940** | 6,828 | -6,328 | 7,972 | -6,381 | 7,227 | -6,835 |

**Table 6.3:** Measured directivity and efficiency in the Stargate for the MIFA antenna. The test can be found in Appendix B.3.

From the table, it is observable that the standard antenna has a better performance than the ground extension, and the ground extension is therefore ignored.

### 6.3.3 Double MIFA on PCB

Another option explored is the addition of an extra antenna to the PCB. The original RTX8950 PCB on Figure 4.2(b) contains 2 antennas and this is attempted. Here the effect of an additional antenna on the PCB is explored for the MIFA. The antenna on Figure 5.9 is mirrored to the free space on the PCB. With a mirror copy of the antenna, the antennas are configured to match the frequency band and a port is placed on each antenna. The configured model can be seen on Figure 6.15(a) with the simulated results of the antennas on Figure 6.15(b).

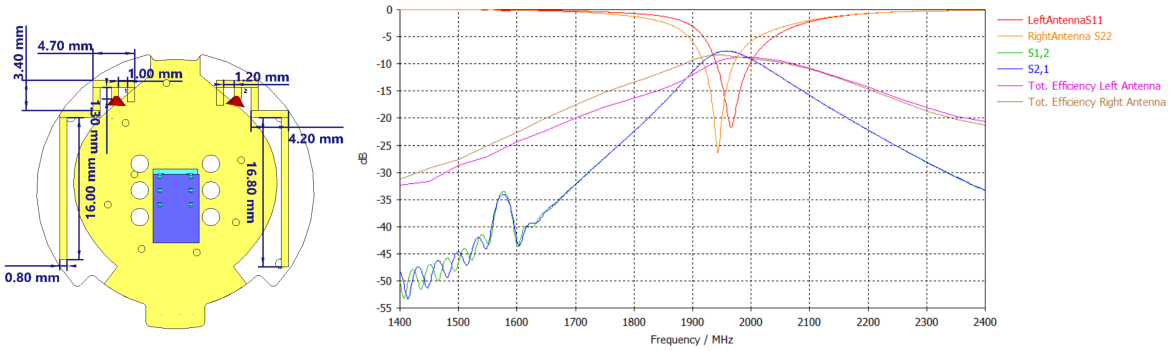


**Figure 6.15:** The MIFA double antenna simulation results and model. Here the optimised MIFA was mirrored and applied to the other side of the PCB on the assumption of head coupling shifting the frequency. The return loss can see a shift between the two antennas, but with a too high frequency.

With two antennas on the same PCB, there is a need to measure both at the same time to perform S2.1. It is desired to have a lot of isolation between the two antennas with a preferred level of around -10 dB and below. The simulated results for the model can be seen on Figure 6.15(b). The resonance frequency for both antennas are too high in the frequency

spectrum, but due to experiences with detuning caused by head, the antennas were configured at this. To verify if the antenna gets de-tuned from head coupling, a bio-tissue head was applied in CST. The head did not cause detuning of antenna but it caused reduction in efficiency and change of radiation pattern as expected. This performance was verified using a printed dual antenna MIFA PCB where the coupling with the head did not de-tune it as was observed in the simulation. This is contrary to the behaviour observed for the single antenna on Figure 6.13(a). The PCB was measured and compared to the simulated s11 and s22 through a full 2-port measurement. The antennas were measured in the Stargate to determine the directivity and efficiency. For the Stargate measurements, only 1 pig-tail was soldered on the PCB at a time to avoid interference from the other pig tail. The results can be seen on Figure 6.16.

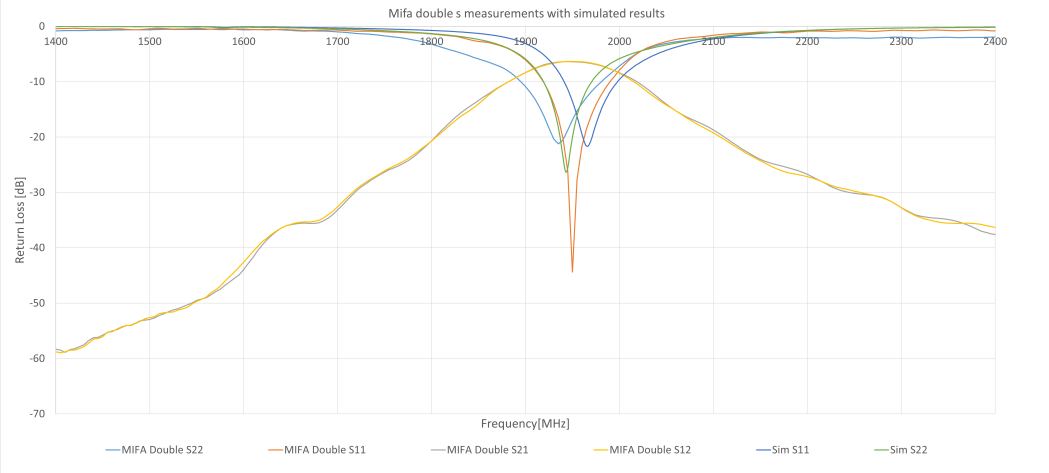


**Figure 6.16:** Comparison between simulated and measured return loss for the MIFA double antenna pcb.

The measured results are verified to be similar to the simulated for the antenna. The lack of detuning from bio-tissue in simulation was confirmed on the measured PCB in reality. The results of the Stargate measurements are summed up in Table 6.4.

| | MIFA Left antenna Left | | MIFA Left antenna Right | | MIFA Right antenna Left | | MIFA Right antenna right | |
|---|---|---|---|---|---|---|---|---|
| **Frequency [MHZ]** | **Directivity** | **Efficiency** | **Directivity** | **Efficiency** | **Directivity** | **Efficiency** | **Directivity** | **Efficiency** |
| **1870** | 6,450 | -9,612 | 7,288 | -9,233 | 6,362 | -6,839 | 6,375 | -6,868 |
| **1880** | 6,269 | -8,020 | 6,979 | -7,761 | 6,336 | -6,509 | 6,348 | -6,538 |
| **1890** | 6,275 | -7,173 | 6,817 | -7,080 | 6,288 | -6,242 | 6,304 | -6,274 |
| **1900** | 6,378 | -6,682 | 6,865 | -6,692 | 6,223 | -6,113 | 6,238 | -6,150 |
| **1910** | 6,527 | -6,357 | 7,131 | -6,463 | 6,165 | -6,028 | 6,183 | -6,075 |
| **1920** | 6,829 | -5,951 | 7,456 | -6,157 | 6,127 | -5,989 | 6,126 | -6,050 |
| **1930** | 6,957 | -5,772 | 7,663 | -6,127 | 6,094 | -6,227 | 6,095 | -6,301 |
| **1940** | 7,237 | -5,526 | 7,872 | -5,696 | 5,949 | -6,493 | 5,960 | -6,583 |
| **1950** | 7,593 | -5,535 | 8,057 | -5,367 | 5,855 | -7,004 | 5,857 | -7,101 |
| **1960** | 7,889 | -5,661 | 8,176 | -5,206 | 5,745 | -7,426 | 5,769 | -7,526 |
| **1970** | 8,202 | -6,146 | 8,246 | -5,224 | 5,732 | -8,180 | 5,760 | -8,281 |
| **1980** | 8,532 | -6,491 | 8,322 | -5,340 | 5,700 | -8,735 | 5,727 | -8,830 |
| **1990** | 8,789 | -7,108 | 8,291 | -5,799 | 5,731 | -9,324 | 5,726 | -9,416 |
| **2000** | 9,208 | -7,859 | 8,483 | -6,322 | 6,020 | -10,300 | 6,017 | -10,388 |

**Table 6.4:** Summation of the directivity and efficiency results for the MIA double antenna. The perceived higher frequency is visible on the left antenna having an improved efficiency at frequencies 1920-1980 MHz.

As was expected from the s11 simulations, the frequency lies in the higher spectrum of the band, with only a part of the bandwidth being within requirements for "MIFA Double S22" on Figure 6.16. This also shows in Table 6.4 where the left antenna gets a gain between 2 and 3 dB in the frequency spectrum [1940;1990]. As was expected, the performance on the right antenna was worse, meaning that both antennas indeed need an improvement, but from how similar simulation and measurement were, a simulated antenna will be developed.

The model was optimised to the known degree possible without utilising components. The following Figure 6.17 shows the optimised model and its s11 response.

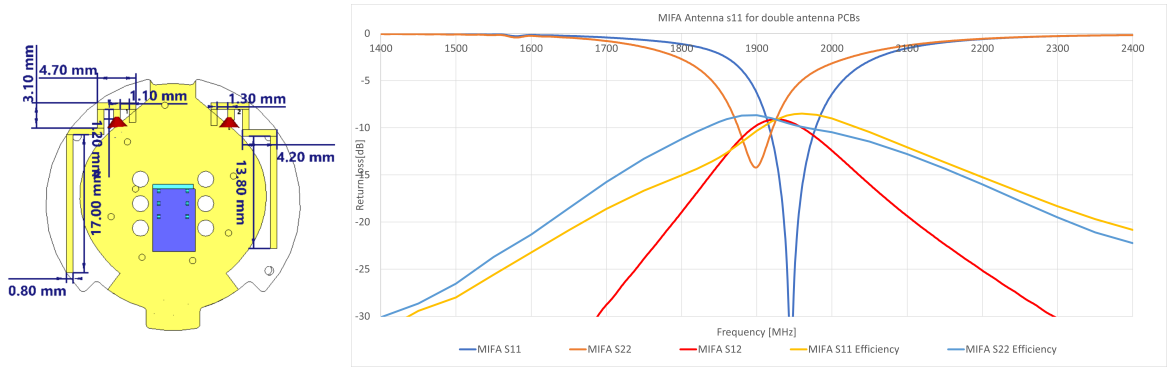


**Figure 6.17:** The optimised design of the MIFA double antenna with its corresponding S11 plot is visible on the figure.

The S11 response was not possible to optimise further into the same frequency at 1905 MHz center frequency by utilising the straight design. The left antenna is not within the correct frequency band and will require to be matched into the frequency band using components.

### 6.3.4 Requirements

The prototype has been tested for its performance, and a comparison of the results with the requirements are put forth for the antenna. The developed antenna is compared to the requirements to determine the usability of the antenna. The results of the comparison are compiled in Table 6.5.

| ID | Description | Requirement | Antenna | Double Left | Double Right |
|---|---|---|---|---|---|
| T.4 | S11 ≤ -10 dB | 1880-1930 MHz | 1895-1930 MHz | 1920-1980 MHz | 1876-1921 MHz |
| T.5 | Lowest efficiency | 35% (-4,6 dB) | >-6,154 dB | not measured | not measured |

**Table 6.5:** Comparison of requirement to the developed antenna prototypes without matching network. The Double left and right are not applied for requirement T.5 due to the efficiency not having been measured on the optimised PCB antennas. The single MIFA antenna is the PCB on Figure 5.9.

The performance of the antenna observed in Table 6.5 does not fulfil the S11 requirement and neither does it fulfil the efficiency requirement. The antenna would therefore need some antenna matching. On the positive side, it has a gain of 0,5-1,8 with the RF pigtail and ferrite beads reducing the efficiency. It is expected for the efficiency to increase with the removal of ferrite beads and pigtail. Looking at the performance of the double antennas, there is a need to match either of the antennas in order to obtain an antenna that can fulfil the requirements. They are however expected to have a good gain following the directivity on appendix Figure B.24.

## 6.4 Comparison between prototypes

The prototypes were developed and tested in previous sections and the two prototypes are compared in this section. This comparison looks at the data from Table 6.2 and 6.5 combined with the actual gain obtained in the frequency band. This is performed for both the single antenna on the PCB and the double antenna models individually to keep them separated in order to determine which antenna is best if one or two antennas are desired. The measured S11 response is compared and the head coupling measurements of efficiency and directivity are compared respective to normal coupling and the highest peak value measured. The data and plots are combined into Figure 6.18 for the single antenna designs.

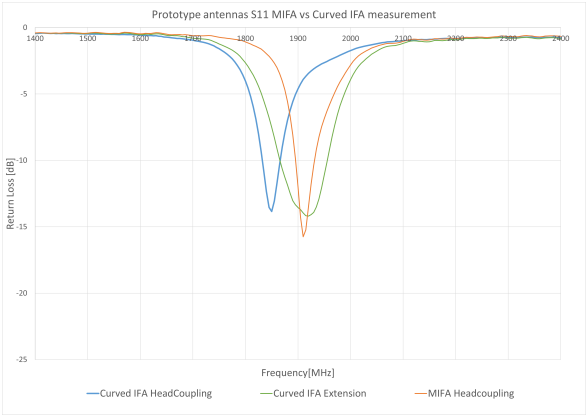


| | Curved IFA | | Curved IFA extension | | MIFA Headcoupling | |
|---|---|---|---|---|---|---|
| **Frequency** | **Directivity** | **Efficiency** | **Directivity** | **Efficiency** | **Directivity** | **Efficiency** |
| **1870** | 6,589 | -6,859 | 7,2 | -5,942 | 7,146 | -6,658 |
| **1880** | 6,786 | -6,650 | 7,212 | -5,274 | 7,129 | -6,129 |
| **1890** | 6,946 | -6,800 | 7,211 | -5,147 | 7,210 | -6,028 |
| **1900** | 7,113 | -7,105 | 7,238 | -5,165 | 7,394 | -6,075 |
| **1910** | 7,256 | -7,577 | 7,25 | -5,209 | 7,606 | -6,092 |
| **1920** | 7,410 | -7,651 | 7,211 | -5,087 | 7,787 | -5,917 |
| **1930** | 7,486 | -8,070 | 7,155 | -5,251 | 7,898 | -6,222 |
| **1940** | 7,540 | -8,225 | 7,1 | -5,238 | 7,972 | -6,381 |

**Figure 6.18:** Comparison of return loss and directivity and efficiency between the single MIFA and curved IFA prototype antennas. The curved IFA with an extension in ground has the best performance, but for the antennas and PCB alone, the MIFA antenna is superior.

From the data on figure 6.18 it can be read that the performance of the antennas is considerably lower than the required efficiency, but with the directivity of 7-8 dBi the bad efficiency is mostly negated in regards to obtaining an antenna with a maximum gain of 3 dB. The optimal antennas from the single antennas is the Curved IFA antenna developed in Section 5.3.1 under the premise that the ground is extended. The extended ground setup has a gain of up to 2 dB gain. This premise would require additional changes to the mechanic to perform. In case such is not possible the MIFA is the preferred antenna for the single antenna PCB.

The configured PCB antennas for the double antenna PCB's are available on Figure 6.19 for the simulated responses.

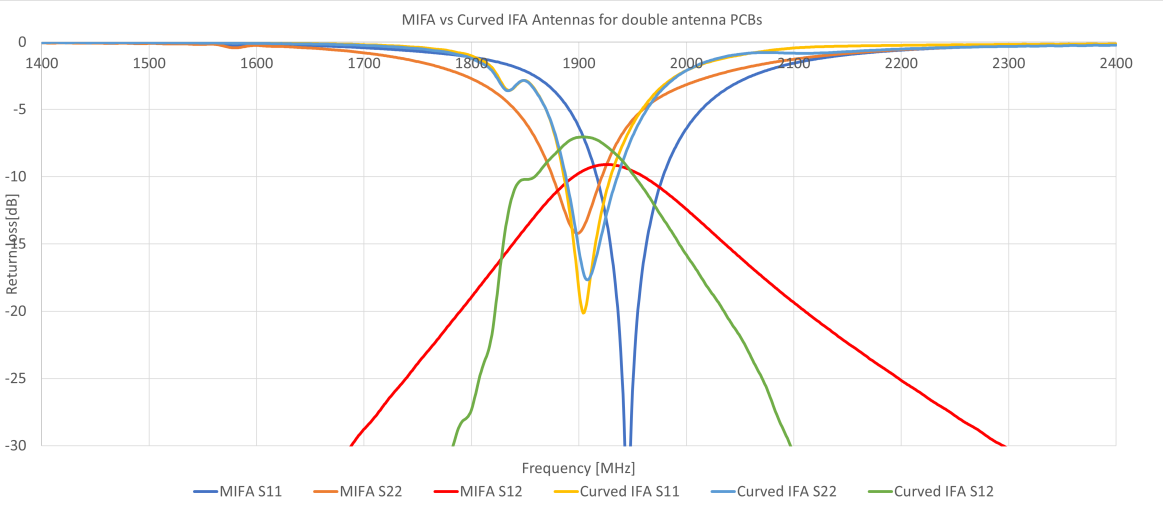


**Figure 6.19:** Comparison of the return loss for the double antenna PCB prototypes combined with isolation between the antennas.

From each respective section in the sections for the double antennas, an unoptimised version of the antennas were measured to determine if the head coupling affected the performance of the antenna. The head coupling was found to not affect the performance of the antennas. The data in Table 6.4 shows that the antennas perform optimal in the frequency band that the unoptimised antenna is within. It is uncertain if similar performance will occur when measuring the optimised antenna. From the similarity between simulation and measurement on Figure 6.10 and 6.15 it is concluded that the antennas are comparable from the simulations. From figure 6.19 we conclude that if two antennas are utilised, it is optimal to use the curved IFA antenna. While its actual efficiency is unknown the design-type has more room for physical adaptability. Additionally, with the required serial DC-coupling capacitor of 10 pF, the match is shifted closer to 50 Ωin accordance with Figure B.26.

## 6.5 Comparison between prototype and RTX8950 PCB

Antenna prototypes were selected and designed in this chapter with the aim of enhancing performance and creating a matching network-free antenna with high gain. To achieve the goal, the current antenna in the RTX8950 was measured to assess its performance and optimise accordingly. This section presents a comparison of the results obtained with the selected prototype. The comparison is not full due to the lack of Stargate measurements of the RTX8950 in a head-coupling setup.

The first prototype compared is the single curved IFA. From table 6.1 we got a gain of 2 dB in the entire spectrum. This was under the assumption that the PCB had an extended

ground of 17,4 mm. Without extension, the gain was less than the RTX8950 and MIFA. With an extension the curved IFA is better in regards to gain. Combining the s11 plots for the antennas we have the comparison on Figure 6.20.

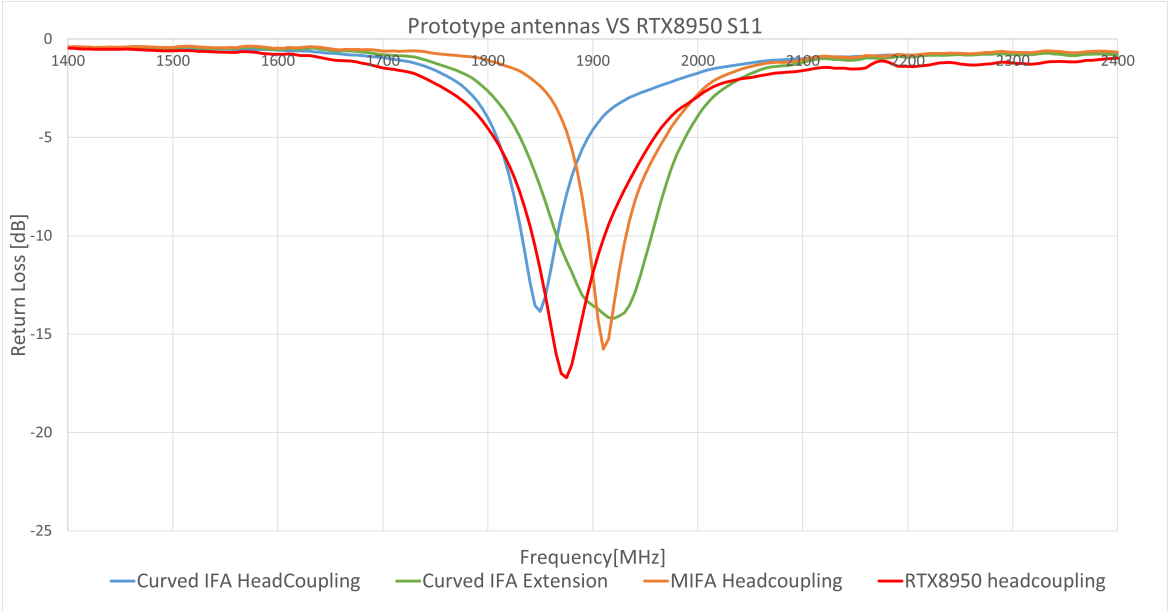


**Figure 6.20:** Comparison of the return loss of the single antennas with the measured head coupling response of the RTX8950 PCB.

The comparison shows that the Curved IFA Extension has the best s11 response in case a single antenna is needed. The RTX8950 PCB however is a double antenna PCB, and it has not been possible to obtain an antenna with a performance remarkably higher than the RTX8950 for it to warrant the use of only one antenna on the PCB.

Comparing the performance of a single antenna with that of two antennas may not be entirely practical, but in this case, it is deemed viable because the RTX8950 PCB incorporates two antennas. The performance will be assessed by comparing the measurements of the RTX8950's left antenna on the PCB. Due to no measurements of the optimised curved double IFA PCB, the measured response of the RTX8950 is compared to the optimised s11 response. The comparison is observably on Figure 6.21.

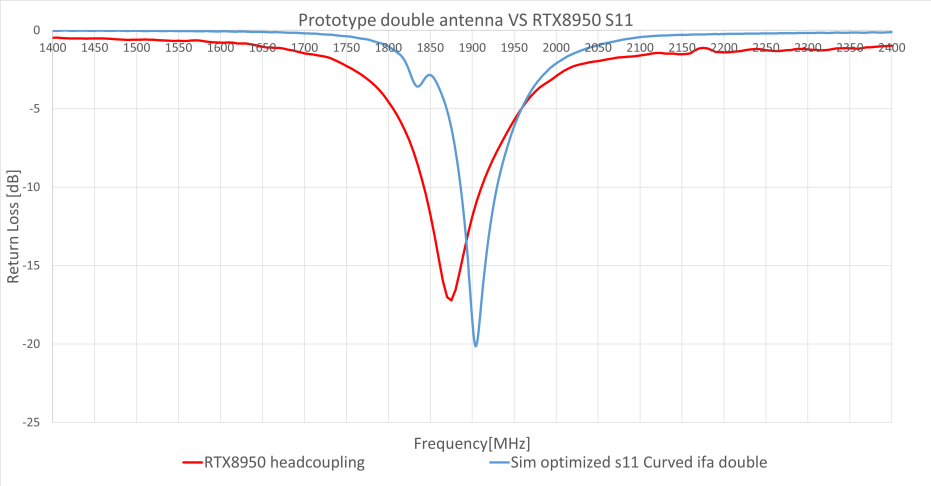


**Figure 6.21:** Comparison of the return loss of the double antenna with the simulated response of the optimised double curved IFA antenna. Only one response of the curved IFA double is applied due to their close similarity observed in Figure 6.10.

Observing the performance on Figure 6.21, the Curved double IFA has the s11 response closest to the requirement, but RTX8950 has a larger bandwidth. From the requirement for the antenna, The double antenna is found to have the most optimal response, which makes it viable as replacement antennas for the PCB.

# Conclusion 7

The project has delved into the challenge of designing an antenna tailored for the constraints of limited space. Within the constraint of the limited space, prototypes of antennas were developed. The purpose of the project was to develop an antenna and gain experience within the development and behaviour of antennas, considerably focusing on the antenna type known as quarter-wave antennas and how the ground-shape changes the performance of the antenna. The project started out with a general focus on the theory behind antennas. This included basic knowledge about the DECT protocol that is behind the requirements for the antenna, an overall look at the parameters important for an antenna and theory behind relation between ground plane size and antenna performance. The effect of body blocking in the different field regions was described and was experienced during the measurements of the prototypes in chapter 6. The body blocking and detuning was taken into consideration when designing the antennas but using actual simulated bio-tissue was only taken into consideration in the form of a head model during simulations of the double antenna PCB. The detuning caused by biological tissue was determined from measurements on the RTX8950. The frequency shift caused by bio-tissue was taken into account for the single antennas, which gives the response of Figure 6.13. The response does not fulfil the requirement, but is close to the requirement without the use of matching network components and without extension of ground.

The two chosen prototypes for further development were the curved IFA for the single antenna and the double antenna. The double antenna was not measured, but it is expected for the antennas to equal the performance of the simulated double antenna. For the curved IFA single antenna, the performance can only be considered acceptable for the requirements if the ground is extended by a copper extension of 17,4 mm. This gives an efficiency of -5,2 dB which does not fulfil the efficiency requirement, but it obtains a gain of 2 dB which is the reason behind the acceptance of the single antenna.

Overall the efficiency measured on the prototype antennas is lower than the requirement. The comparison of the prototype antennas to the requirement reveals that none of the antennas are fulfilling the requirement. Some of the efficiency loss is possible to explain but not to the extent of how much. As the antennas are known to couple with the head, they were tuned with head detuning into consideration. However the head-coupling causes a

loss in efficiency due to absorption in bio-tissue. This will reduce the efficiency of the antenna when in use but still requires the head coupling for the s11 performance. From the data, it is concluded that the double antenna curved IFA is the optimal antenna requiring the least optimisation with a DC decoupling capacitor improving the performance. The actual gain and efficiency is unknown but from the S11 response, it is expected for the antenna to achieve a good performance across the frequency band on both antennas.

# Discussion 8

As part of the project focused on antenna design and the grounds effect on the performance of an antenna, there was developed antenna prototypes for the PCB on figure 4.2(a). Through the project there has been a development and research into the basic antenna properties, different types and techniques to improve the antenna performance.

Through the report, several compromises and choices were taken to design the antenna and some of these compromises and other choices will be discussed. One of the concepts to discuss is the efficiency of the antenna. The requirement was set to -4,6 dB in efficiency but neither of the antennas fulfilled this requirement. When they were measured, each antenna required an RF pigtail and it required additional techniques to remove the Pigtails effect from the measurement of the s11 response. In order to do that, RF Ferrite pearls were utilised to increase the impedance of the cable and thereby reduce any surface currents that would travel across the RF pig tail. By applying ferrite pearls a loss of efficiency is introduced which naturally decreases the total efficiency of the antenna.

The ground plane for the RTX8950 PCB is a size of 3,1 cm in diameter and is close to the definition of electrically small ground from Section 4.4. The addition of a comparatively large conductive area, in the form of the soldered part of the RF pigtail, to the electrically small PCB will increase the overall copper to radiate from. This is especially the case for quarter-wave antennas such as the IFA as the ground plane is an important part of the antennas performance. The ground plane is another part of the radiating element and introduces a relatively large ground piece. If the ground plane is increased in size the pigtails increase in ground is comparatively smaller. Combined with this, the efficiency of the antenna can also increase with a larger ground size and change the overall radiation pattern for the antenna. This is observable in the radiation patterns seen on Figure 5.12 with the data from Table 6.1.

The ground extension of the PCB was rectangular with its size arbitrarily decided from the width of the protrusion on the RTX8950. This meant that the ground when extended was equal to a rectangular. The width of the ground extension could have been decided through simulations and measurements which could have been a point of improvement in case of further development. The same applies to the general shape of the ground extension.

Shaping the ground extension differently may optimise the antenna through the extension of the ground. The position of the IFA prototypes feed lines were found in an attempt to get the longest ground plane to achieve the optimal antenna utilising the entire length of the ground plane while designing antennas for 1900 MHz. This achieved an instantaneous increase in the performance during the development of the curved IFA antenna while allowing for easier length extension of ground. One thing to improve for the antennas however is their position on the PCB. The optimal choice for antenna placement would have been along the edge of the RTX8950 PCB as it would have reduced coupling effect between ground plane and antenna. It would have been possible for the curved IFA but for the MIFA this was not a possibility due to its straight nature.

One thing of improvement for further development of antennas is an earlier introduction of a bio-tissue model of a head into the simulations. Through the early stages of the single antenna MIFA and curved IFA, the antennas were designed from the knowledge obtained by the shift caused by head-coupling of the RTX8950 antenna that was measured. This is far from an optimal design method as it is unknown how much the exact amount of shift is which may also change depending on the directivity and shape of the antenna. The results from the method were reasonable but for proper design, including a bio-tissue head model into the simulation would have given more consistent results from the measurement that should allow for easier optimisation. Despite the tuning, a matching network is still expected to be needed to some extent due to the differences between the used FR4 and the actual PCB for the product. The difference lies in both the thickness and the differences in the electromagnetic properties of the FR4 material. There will be differences between the PCB's from different PCB producers, and therefore a small tuning is still expected to be needed.

One of the options for designing a single antenna on the PCB was realised too late for there to be time to utilise it. If it was known or defined that only a single antenna would be needed then it would have been possible to utilise the entire ground plane. For the developed prototypes, one of the RTX8950 antenna slots was available and unused for the prototypes meaning this was a just a piece of substrate. If the ground plane had covered that, the components could have been moved and the antenna would have had more design freedom and an IFA for the frequency would have been a possibility as well. It was possibly a consequence of the thought, that a singular antenna would not be able to achieve so well a performance that it would not require two antennas. This could have led to more diverse antenna-designs and possibly enough room for a slit PIFA.

Another aspect that would have optimised the design-process of the antennas would have been through utilising machine-learning to optimise antennas. Especially the ground shape would have been interesting to get a machine learning process to optimise on. This would mostly be on the concept of the ground extension and the shape that would optimise an antenna. Complex shaping of antenna would however require a lot of parame-

ters which would increase the time needed to optimise the ground shape. The machine learning would be capable of optimising the antenna with several parameters. Machine-learning would be an interesting direction to take the project had there been more time.

# Bibliography


[1] Pengjian Gao, Jia Li, and Weibing Wang. *Ground Plane Effects on Monopole Antenna Performance*. https://www.mdpi.com/2079-9292/12/12/2681. (Accessed on 12/09/2023). 2023.

[2] Antennatestlab. *Return Loss and VSWR*. https://antennatestlab.com/antenna-education-tutorials/return-loss-vswr-explained. (Accessed on 19/09/2023).

[3] Etsi. *Digital Enhanced Cordless Telecommunications (DECT); Common Interface (CI); Part 2: Physical Layer (PHL)*. https://www.etsi.org/deliver/etsi_en/300100_300199/30017502/01.09.00_40/en_30017502v010900o.pdf. (Accessed on 10/09/2023). 2005.

[4] Oliver Falkenberg Damborg. *Praktikforløb i RTX: Med position i RF afdeling*. Tech. rep. Aalborg University, 2023.

[5] wikipedia. *Digital enhanced cordless telecommunications*. https://en.wikipedia.org/wiki/Digital_enhanced_cordless_telecommunications. (Accessed on 28/09/2023).

[6] wikipedia. *Phase-shift keying*. https://en.wikipedia.org/wiki/Phase-shift_keying. (Accessed on 17/09/2023).

[7] Hans Ebert and Povl Raskmark. *Grundlæggende Transmissionsledningsteori*. Aalbord :Aalborg University, 1988.

[8] Zhijun Zhang. *ANTENNA DESIGN FOR MOBILE DEVICES. IFA p. 141*. Singapore: John Wiley & Sons (Asia), 2011. ISBN: 978-0-470-82446-7.

[9] https://www.antenna-theory.com/. *Antenna Efficiency*. https://www.antenna-theory.com/basics/efficiency.php. (Accessed on 12/10/2023).

[10] ScienceDirect. *Voltage-Standing-Wave Ratio*. https://www.sciencedirect.com/topics/engineering/voltage-standing-wave-ratio. (Accessed on 18/10/2023). 2022.

[11] wikipedia. *WiFi Antenna Types*. https://www.accessagility.com/blog/wifi-antenna-types. (Accessed on 16/10/2023).

[12] wikipedia. *Microstrip antenna*. https://en.wikipedia.org/wiki/Microstrip_antenna. (Accessed on 15/9/2023).

[13] wikipedia. *Horn Antenna*. https://en.wikipedia.org/wiki/Horn_antenna. (Accessed on 17/10/2023).

[14] Constantine A. Balanis. *Antenna Theory: Analysis and Design*. Fourth. John Wiley & Sons, 1997.

[15] wikipedia. *Electrical Length*. https://en.wikipedia.org/wiki/Electrical_length. (Accessed on 19/10/2023).

[16] Peterson Zachariah. *FR4 Dielectric Constant and Material Properties*. https://resources.altium.com/p/fr4. (Accessed on 24/11/2023). 2021.

[17] wikipedia. *Near and Far field*. https://en.wikipedia.org/wiki/Near_and_far_field. (Accessed on 26/10/2023).

[18] everythingrf. *What are Near Field and Far Field Regions of an Antenna?* https://www.everythingrf.com/community/what-are-near-field-and-far-field-regions-of-an-antenna. (Accessed on 26/10/2023). 2018.

[19] Cadence. *The Near-Field vs. Far-Field Regions of an Antenna*. https://resources.system-analysis.cadence.com/blog/msa2021-the-near-field-vs-far-field-regions-of-an-antenna. (Accessed on 26/10/2023).

[20] wikipedia. *Fresnel zone*. https://en.wikipedia.org/wiki/Fresnel_zone. (Accessed on 18/10/2023).

[21] J. Krupka a et al. *Low loss polypropylene-silicon composites for millimetre wave applications*. https://www.sciencedirect.com/science/article/abs/pii/S0025540817335225. (Accessed on 18/10/2023). 2018.

# Appendices

# Ground plane relation to antenna performance for antenna types A

This appendix contains the different antenna types that were simulated for the performances relation to ground size. This performance includes return-loss, efficiency and radiation pattern.

## A.1 Straight monopole antenna

As was shown in section 4.5, the size of the ground plane affects the antenna in regards to frequency and efficiency. With that in mind, the same will be confirmed for a simple monopole. This will be confirmed in two cases, one with a monopole on a large ground and a case with a large monopole on a small ground.

The antenna was designed by finding the length required for a quarter-wave antenna on a FR-4 substrate. The length was found by applying the substrate value and the desired frequency. Utilising equation 4.6 the length of the radiating element is found to be 19 mm. If the substrate is ignored from the equation, we get a length of 39 mm. Applying the length to the dipole antenna on a ground plane of 40x120 mm, we get the antenna design seen on Figure A.1. The length of the antenna is swept to determine the appropriate length when using lossy materials for copper and substrate. The Length sweep is shown in Figure A.1.

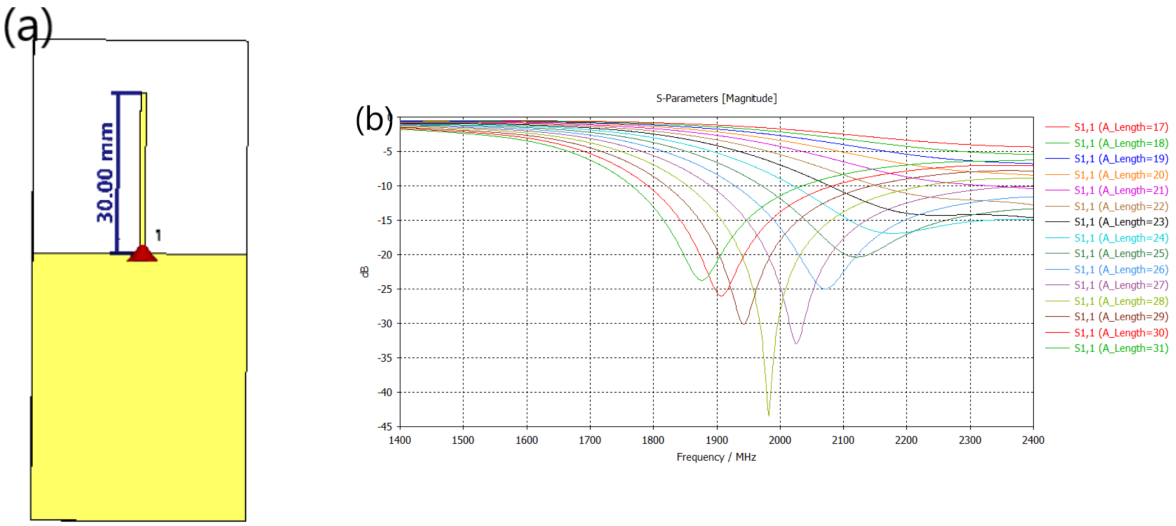


**Figure A.1:** Simulation model and results of the straight monopole. (a) shows the model that is simulated. (b) shows the results of a length sweep of the monopole. The length is found most suitable at a length of 30 mm.

The length of the antenna is determined to be 30 mm to get a centered S11 response. With the Antenna designed the length of the ground was swept to determine if the effect seen in section 4.5.1 is present for the straight monopole. The Ground length was swept on Figure A.2.

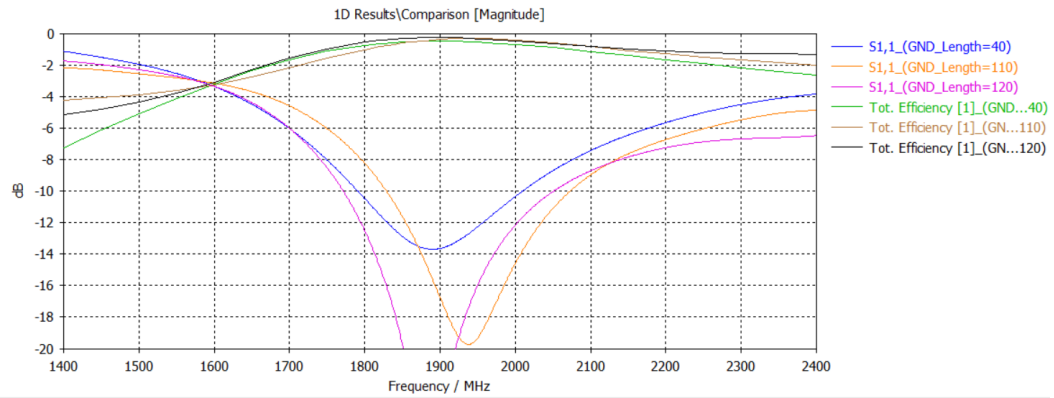


**Figure A.2:** Sweep of ground length for the straight monopole. three measurements are taken out in order to see the effect of ground length on the antennas performance.

The plots shown on Figure A.2 are excerpts that were found to have a frequency similar to the required band. Only a few excerpts were chosen as the frequency shifted in a 500 MHz band around the center frequency of 1905 MHz as was previously experienced for the IFA antenna. The same behaviour as the IFA antenna is noticeable for the straight monopole antenna, with the efficiency of the antenna becoming smaller as the size of the antenna lessens. Looking at the radiation pattern for the length of 120 we get figure A.3.

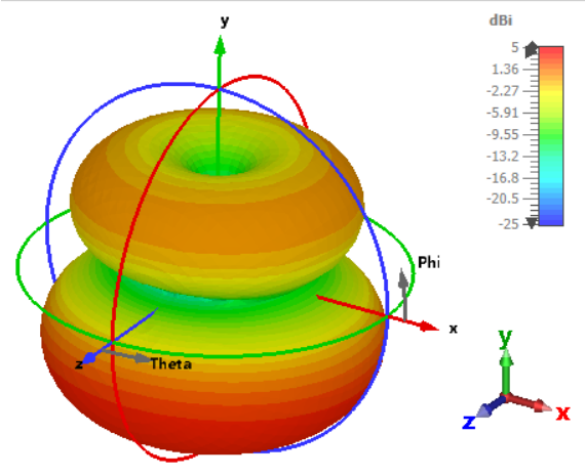


**Figure A.3:** Radiation pattern of the straight monopole with the large 120 mm ground.

On the figure, the effect of the ground plane is remarkably visible as the second torus on the lower half of the radiation pattern. It can be observed how the ground plane has the highest directivity. The downwards behaviour of the torus is caused by the downward standing wave causing the radiation pattern to bend downwards, giving a "slim" section between the ground plane and antennas radiation torus.

## A.2 Electrically small ground Monopole

Another interesting case is about what would happen to a straight monopole if the ground plane is defined as electrically small. From section 4.4 it is known that if the largest size is smaller than $0.1\lambda$, then it is defined as electrically small. The wavelength at frequency 1900 MHz is found to be 15,78 cm and an electrically small size is a size smaller than 15,78 mm. The ground length was defined to be 15 mm. Simulations were made to determine the appropriate length of the antenna, which can be seen on Figure A.4.

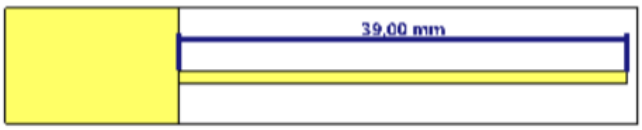


**Figure A.4:** Model of the straight monopole on an electrically small ground plane.

The monopole's length became 9 mm longer with the smaller ground as compared to the monopole on figure A.1. The monopole was previously 30 mm long, which had a s11 peak at roughly 1900 MHz seen on Figure A.2. Keeping this length with small ground, it can be seen on Figure A.5 that the antenna has shifted 400 MHz upwards in frequency thereby having a peak at 2260 MHz.

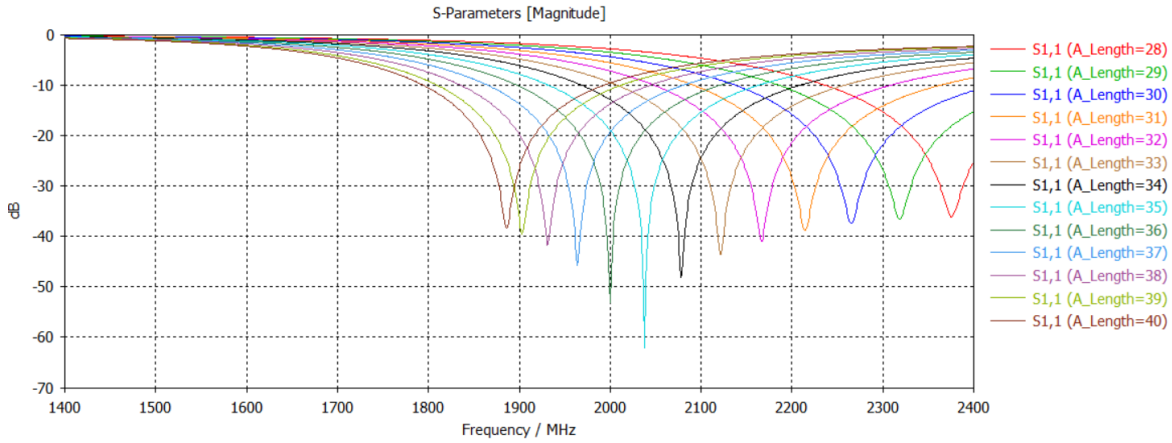


**Figure A.5:** Length sweep of the straight monopole on the small ground plane. Compared to Figure A.1(b) the neccesary length is increased by 9 mm to achieve the same resonance frequency.

The length of the antenna was swept and a length of 39 mm was determined from simulation results for the monopole. By having an electrically small ground the antenna had an increase in size by 30% in order to obtain a performance similar to the one with a 40x80mm

ground. The resulting length of the antenna resulted in Figure A.6 with the efficiency added to the plot.

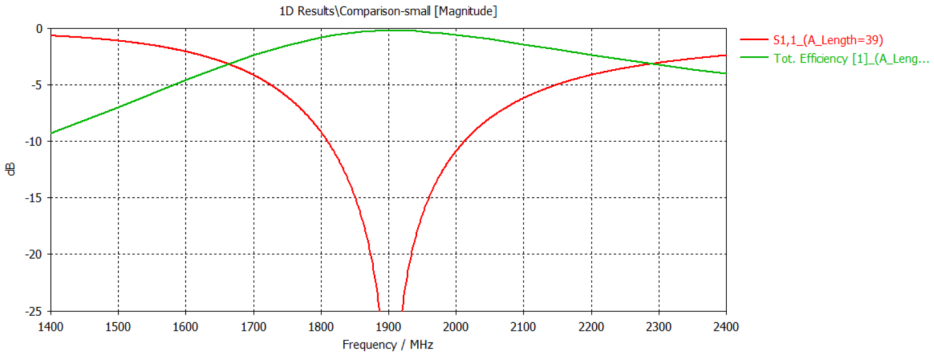


**Figure A.6:** S11 and efficiency response of the small ground monopole at a length of 39 mm. The total efficiency is measured to be -0.2 dB with the peak of the S11 being below -25 dB.

The total efficiency can be read to be around -0.2 dB, which is a good efficiency for this band, however efficiency and s11 is not enough information to determine the antennas performance which is why measuring the far field is important. The far field was simulated in CST with the plot seen in Figure A.7.

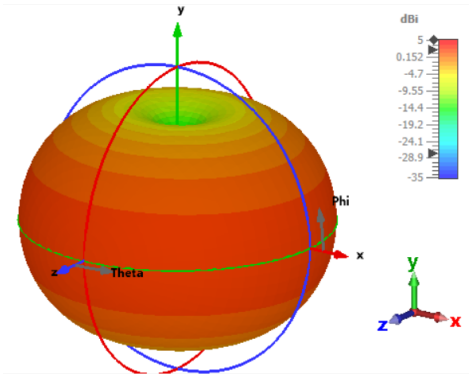


**Figure A.7:** Radiation pattern of the Electrically small ground monopole with the S11 response visible on Figure A.6. The frequency of the radiation pattern is 1900 MHz.

The plot shows a torus shape common for monopoles with a directivity of 2 dBi. Common for monopoles is that the ground radiates as a part of the antenna, but with the smaller ground, the radiation pattern is not altered with an additional torus as was seen on Figure 4.4 which is the radiated pattern of the antenna on Figure A.1. Balanis mentions that a smaller ground will result in a smaller possible gain [14] which is visible when comparing the two figures, where a difference of 2 dBi in directivity exists compared to the directivity of around 3-4 dBi on Figure A.3.

## A.3 L antenna

Another type of monopole is the bent whip antenna also known as an L-antenna. As the name suggests it is a whip antenna that is bent in a 90° angle to form an L-shape. The antenna should have a length similar to the straight monopole. The design can be found on Figure A.8. The length is necessary to sweep to determine the length needed for the correct resonance frequency, but the distance between the antennas arm and the bend affects the impedance in accordance to the distance. The smaller the distance, the smaller the real part of the impedance [8].

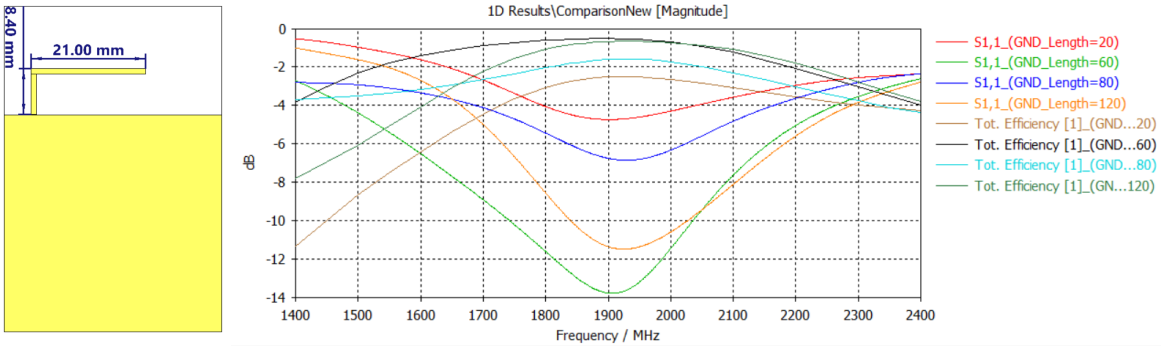


**Figure A.8:** Model of the L-antenna which consists of a bent monopole. The bend makes the antenna more likely to couple with the ground plane which affects the performance. The performance of the model can be seen on the s11 plot showing the response at different ground lengths.

The antenna was swept to determine the frequency of the antenna. The antenna was determined to a length of 21 mm for the bent piece and 7,4 mm for the straight part of the antenna for a total internal center length of 28,4 mm which is not too dissimilar to the response of the straight monopole in section A.1. The response of ground length 60 and 120 has a response that fulfils the requirements for the antennas, but only to the degree of reaching -14 and -11,5 dB which is not a lot of room from the requirement. One beneficial effect however is the amount of bandwidth obtained from the antennas which span in the size of around 200 MHz.

It looks optimal for larger ground planes but is expected to require additional components. The L antenna is not that different from the IFA in design but with the design option of the shorted pin, an component is introduced. The shorted pin of the IFA in section 4.5.1 is equivalent to an inductor[8], thereby making for a smaller loss in saving a component. Verifying the radiation pattern we have Figure A.9.

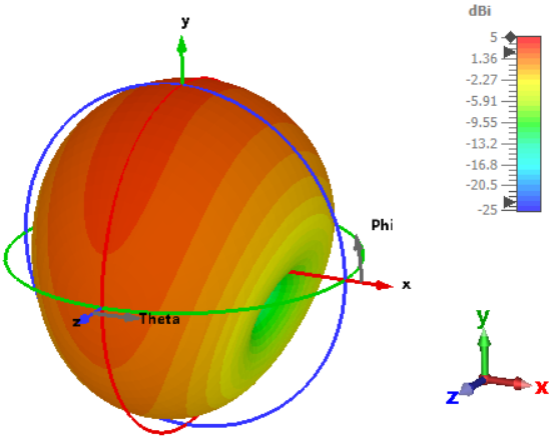


**Figure A.9:** Radiation pattern at 1900 MHz for the L antenna with a ground extension of 60 mm. The z axis is the POV on the figure of the antenna.

The radiation pattern reveals a directivity of around 2,5 dBi and it is noticeable how the pattern has rotated by 90° as a consequence of the antenna being bent in an L-shape.

## A.4 PIFA antenna

Similar to the IFA antenna, the planar inverted F antenna(PIFA) has a shorting pin and a feed-line connected to it. The resonance frequency for a PIFA is found from the size of the antenna plane, specifically from the ground pin until the distance furthest away from it by following the edge. The PIFA can be designed in several ways. One way is to have the antenna suspended above the ground plane with the ground and feed-line keeping up the antenna. To obtain this behaviour the antenna is thicker than normal micro-strip antennas. Another PIFA type is to have the antenna mounted on the substrate with a ground plane on the other side connected through vias from the ground pin. For the simulations a suspended type PIFA was designed with the design available on Figure A.10.

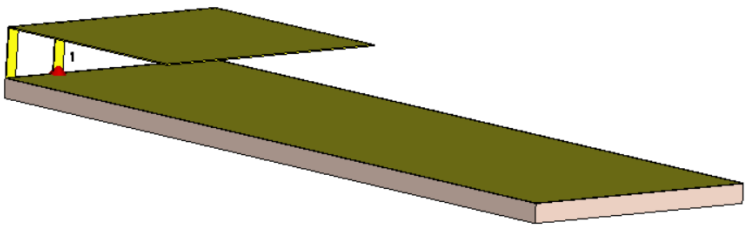


**Figure A.10:** PIFA antenna model. The PIFA consists of a thicker sheet of copper floating through the ground and feed line connected to the PCB.

The PIFA designed on Figure A.10 is designed to have equal width to the ground with the length then being swept for the ground. The width, length, height and distance between feed and ground were all swept to find an antenna with a s11 measurement within the DECT band. The plots for the length of 60 and 120 mm were compared to determine the effect that the size of the ground-plane has on the efficiency and s11 values for the PIFA antenna. The simulated s11 and total efficiency can be seen on Figure A.11.

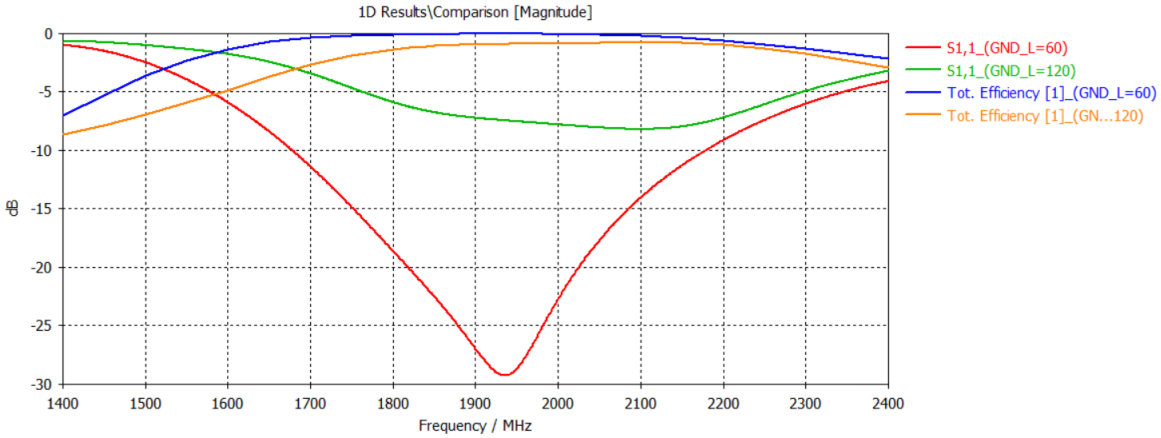


**Figure A.11:** s11 response of the PIFA antenna with a swept ground length.

The s11 response on the plot for the PIFA antenna is can be read to obtain a good response at a length of 60 with a significantly worse at 120 in length. The efficiency for either ground lengths is above the requirement, but the s11 for a length of 120 mm is not fulfilling the requirement of an s11 of -10 dB and below. The radiation pattern of the PIFA can be seen on Figure A.12.

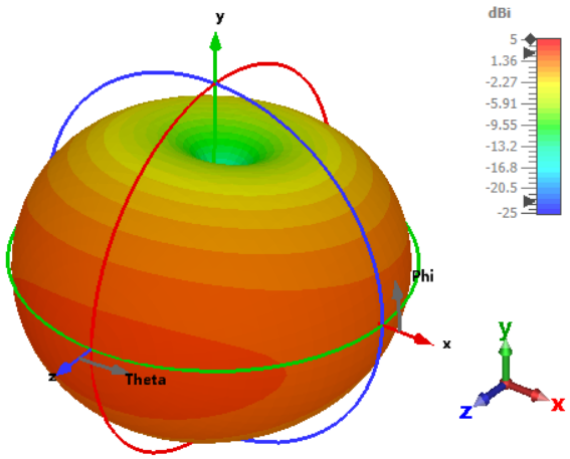


**Figure A.12:** Radiation pattern of the PIFA simulated on Figure A.10.

The radiation pattern for the PIFA reveals a pattern not unlike the other types of antennas, but with the exception of having a wider radiation pattern in the direction that the PIFA is towards. The directivity is at a value of 2,7 dBi giving the PIFA a similar directivity to the other quarter-wave antennas simulated.

## A.5 Wire IFA

A different type of antenna that may be viable is the wire IFA. The wire IFA is similar to the normal IFA antenna with a similar design and use of shorting pin. The difference between the IFA and the wire IFA is that the wire IFA is a non-planar IFA, meaning that it protrudes from the PCB. The design is similar to a PIFA antenna except the lack of a plane for the antenna. The wire IFA is designed from the design of the IFA on Figure 4.8. The wire IFA is available on Figure A.13.

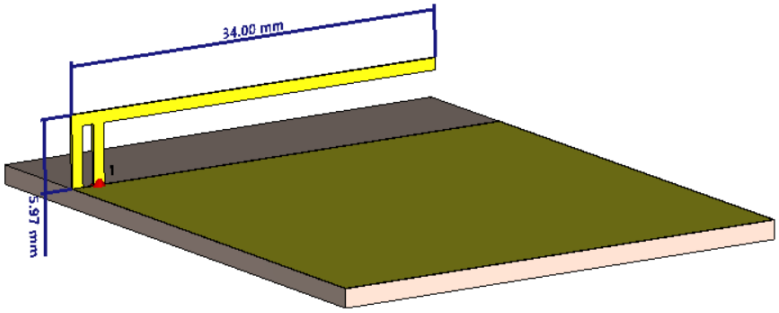


**Figure A.13:** Model of the wire IFA antenna that is matched for the resonance frequency 1900 MHz.

Observed if comparing the wire IFA to the PCB IFA is that the antenna is longer for the wire IFA to achieve the resonance frequency. This is expected to be caused by the fact that the relative permittivity is lower in air compared to the substrate as the permittivity would lower the frequency. This was verified for the IFA where a higher permittivity reduced the frequency. The ground is also swept for the wire IFA to confirm the behaviour on this antenna. The ground sweep is available on Figure A.14.

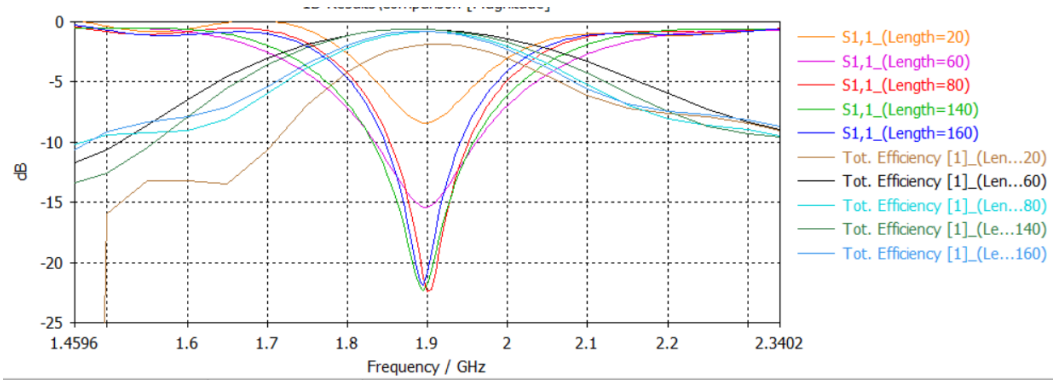


**Figure A.14:** Ground sweep of the wire IFA antenna. Select lengths have their efficiency and return loss plotted.

The ground sweep shows that the wire IFA antenna only seems to be affected by the reduction at smaller ground lengths. Like for the other types, it has a decreased efficiency and return-loss as the ground plane becomes smaller. The wire IFA seems more resilient to changes in ground length and less shifting in frequency with the ground length.

The wire IFA is of the same shape as the IFA antenna and it is therefore expected for the radiation pattern to achieve a pattern similar to one another. The radiation pattern can be seen on Figure A.15.

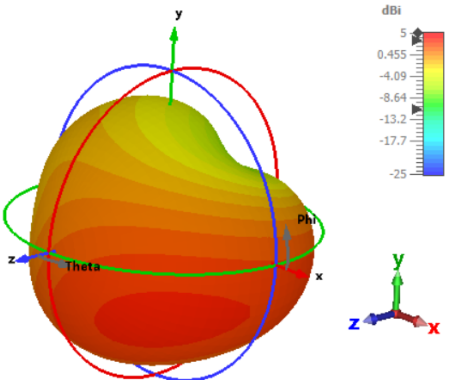


**Figure A.15:** Radiation pattern for the wire IFA antenna. The pattern is reminiscent of an IFA antenna with a large groundplane.

The radiation pattern has a pattern reminiscent of the IFA antenna radiation pattern which makes sense. The directivity is also appropriate, with one weak angle, being the tip of the antenna.

# Designed antennas: simulations and measurements

B

This appendix contains the test journals for the designed antennas in chapter 5 where this appendix contains the simulated results and the measured results for the prototypes when realised.

## B.1 MIFA antenna simulation

This section will contain the simulations and measurements of the MIFA antenna utilised on the PCB shape from Figure 5.6. The simulation of the antenna and its performance will be measured and tested. The antenna was realised on PCB and then measured with a VNA and afterwards in the Stargate at AAU University. Note that the measurements were preliminary measurements to determine the direction to go with the antenna performance when comparing simulation and PCB.

| | |
|---|---|
| **Conducted by** | Oliver Falkenberg Damborg |
| **Date** | 28 / 11 / 2023 |
| **Purpose** | To design and confirm antenna performance between simulation and realisation |

### B.1.1 Device Under Test (DUT)

The configured antenna can be seen on Figure B.9.

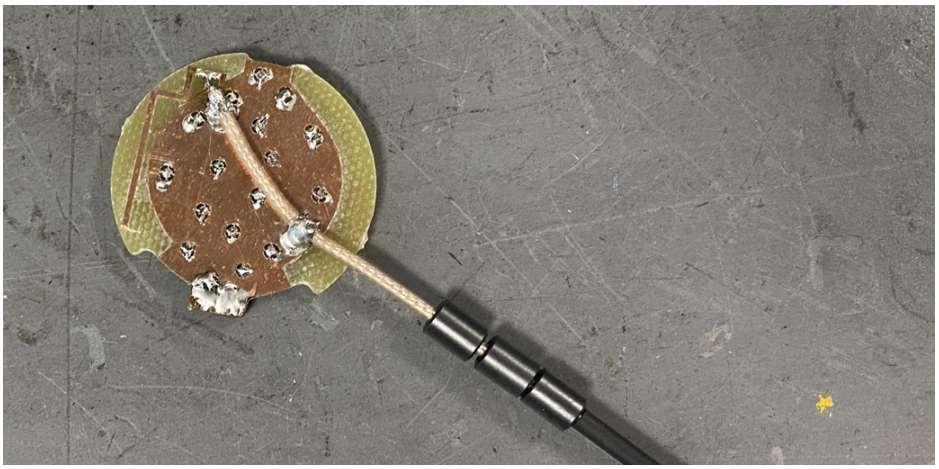

**Figure B.1:** Soldering setup of the RF pig tail on the DUT for measurements.

The printed antenna-design can be seen on Figure B.9 which was realised using a PCB printer. One thing to note is that the FR4 plates available were of 1,55 mm thickness whereas the PCB for the RTX8950 is 0,82 mm thick. This introduces an error that is expected to affect the resonance frequency to some degree. The Antenna was milled in two different thickness' to determine the optimal one. On Figure B.2 we see the Thin antenna PCB on the Left and the thick antenna PCB on the right.

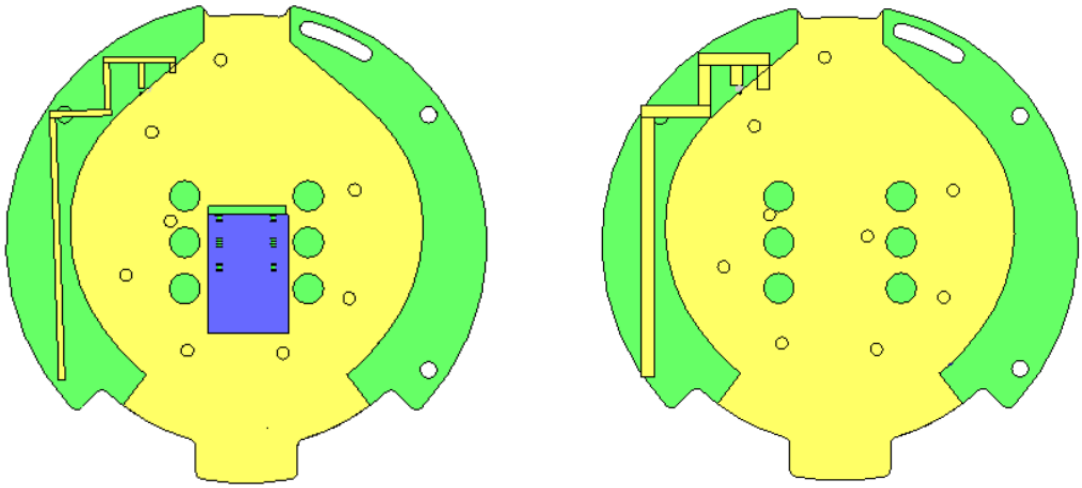

**Figure B.2:** The two models of PCB antennas that are tested. Left is defined as thin and the right is defied as thick antenna.

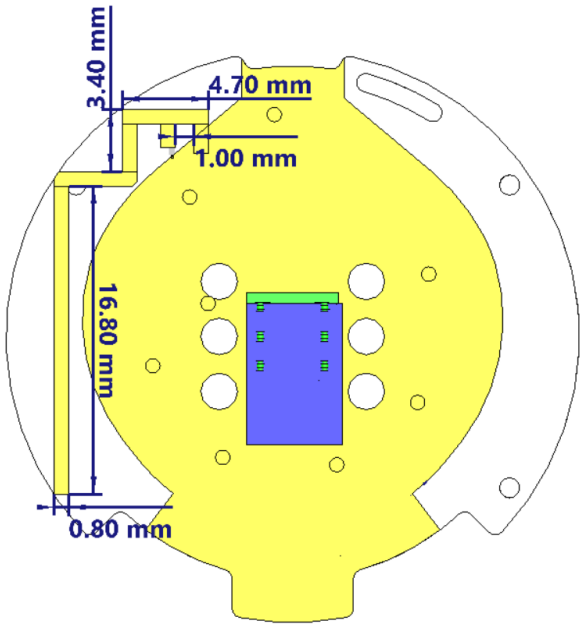


**Figure B.3:** The model for the final optimised antenna. This antenna is tested after the two antennas on Figure B.2 as it is an optimised design of the antennas.

### B.1.2 List of equipment

| Equipment | Manufacturer | Type | Specification | AAU no. |
|---|---|---|---|---|
| Calibration Kit | Agilent Technologies | 85033D | Range: 0 Hz to 6 GHz | — |
| Network Analyzer | Agilent Technologies | E5062A | Range: 300 kHz to 3 GHz | 56983 |
| Multiprobe system | Microwave Vision Group | Stargate 24 | Range: 400 MHz to 10 GHz | — |

**Table B.1:** List of equipment that was used in test.

### B.1.3 Test setup

The testsetup consisted of four different setups for each PCB.

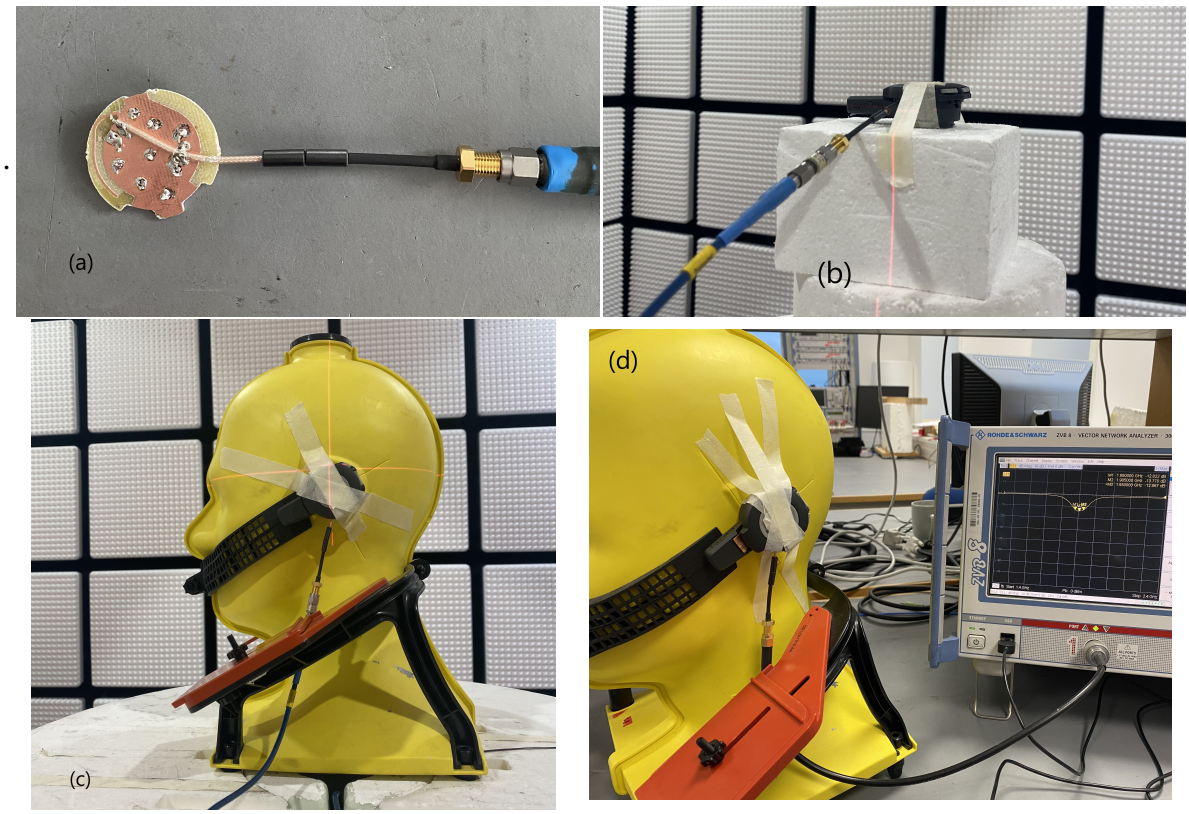


**Figure B.4:** Measurementsetups for the different measurement types. (a) is measurement of the PCB performance by itself. (b) is measurement of the performance of the antenna in freespace and inside the mechanic. (c) shows the head coupling configuration. (d) shows the headcoupling configuration when measuring with a VNA. All testcases are applicable for both types of test. The two types are VNA measurements and radiation measurements.

### B.1.4 Procedure

The procedure for the test is the following.

1. Simulate antenna outside mechanic.
2. Simulate antenna inside mechanic
3. Solder RF pigtail to feed line following the guidelines in section 5.1.
4. Measure PCB only using calibrated and port-extended VNA using setup (a).
5. Measure PCB in mechanic with VNA using setup (b).
6. Once model has been optimised, measure in head-coupling using setup (c) or (d).
7. Repeat step 4-6 but in the Stargate.

### B.1.5 Results

#### Preliminary results

This section contains the data from measurements before the antenna was optimised. This was the first test.

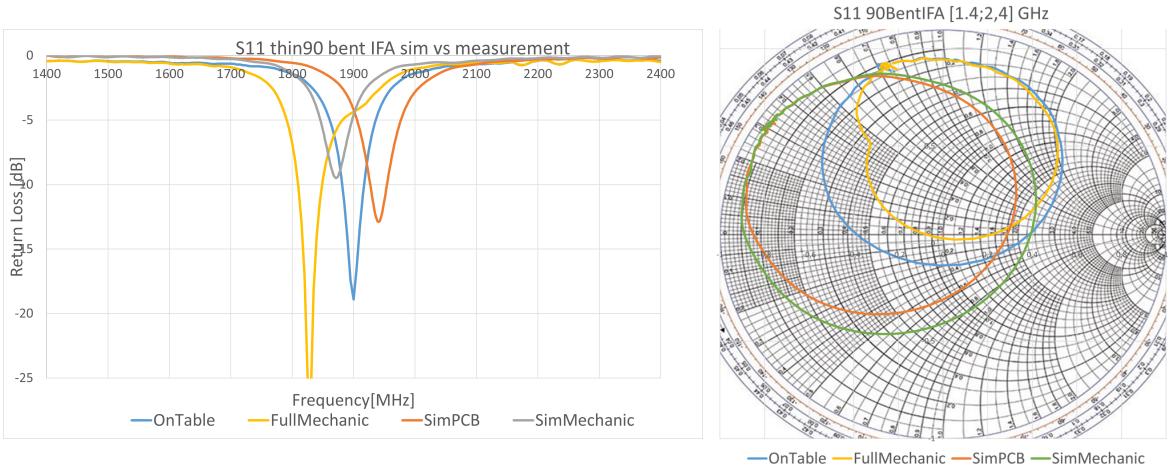


**Figure B.5:** Simulated VS reality for the thin antenna. This antenna is a prototype before it has been properly configured.

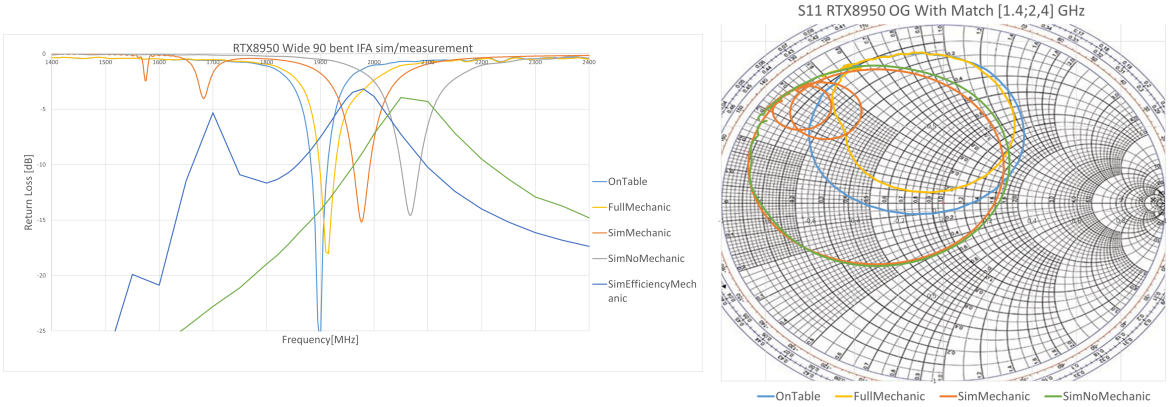


**Figure B.6:** Simulated VS Reality for the wide MIFA antenna with smith chart and s11 plot.

## Chosen type results

From the preliminary results, the wide MIFA antenna has been chosen for measurement. The wide MIFA will be measured in the AAU Stargate.

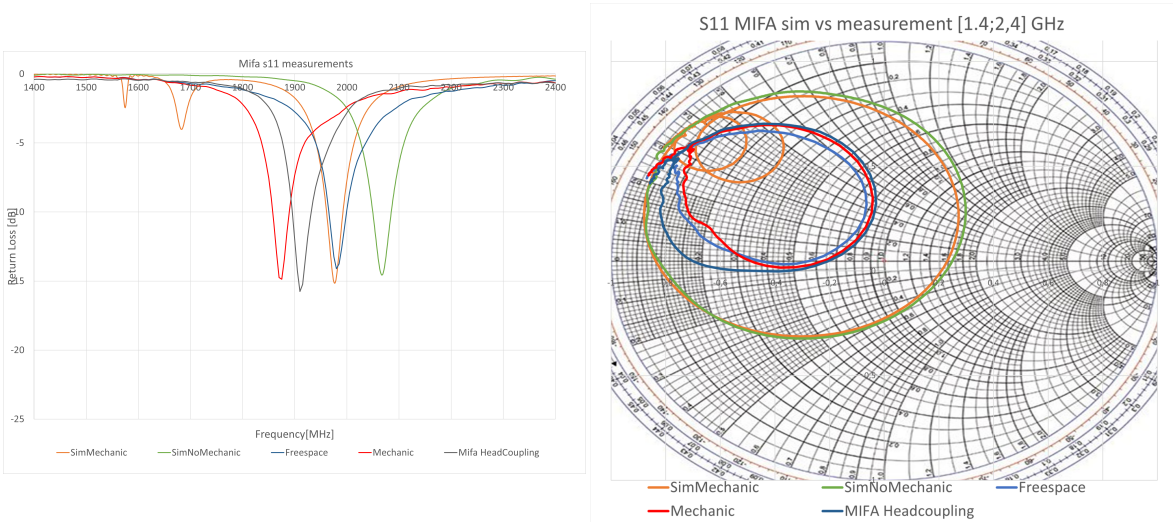


**Figure B.7:** Simulated VS Reality for the chosen MIFA with smith chart and s11 plot. The MIFA Head-coupling is the measurement of the antenna performance in the head-coupling expected for normal usage of antenna. A shift in frequency for resonance frequency is observed.

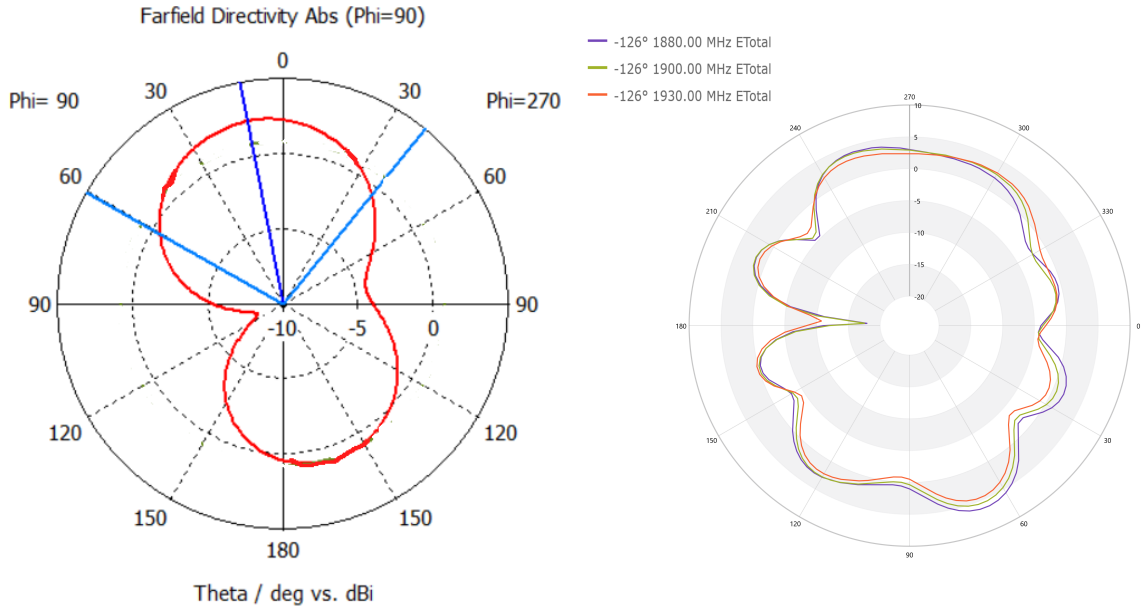


**Figure B.8:** Simulated VS Reality for the thick antenna at 1900 MHz. Left plot shows the simulated radiation pattern and right plot shows the measured radiation pattern.

| Parameter | Frequency | Simulated PCB | Simulated Mechanic | Measured MIFA | MIFA in Mechanic | MIFA Headcoupling |
|---|---|---|---|---|---|---|
| **Directivity** | 1880 MHz | 1,42 | 2,96 | 6,273 | 6,844 | 6,578 |
| | 1900 MHz | 1,43 | 2,98 | 6,353 | 6,451 | 6,513 |
| | 1930 MHz | 1,43 | 3,01 | 6,227 | 5,377 | 6,808 |
| **Efficiency** | 1880 MHz | -15,147 | -8,798 | -13,703 | -6,609 | -6,154 |
| | 1900 MHz | -14,111 | -7,515 | -12,572 | -7,636 | -6,144 |
| | 1930 MHz | -12,218 | -5,338 | -10,330 | -8,380 | -6,186 |

**Table B.2:** Summed table of the resulting directivity and efficiency for the Wide MIFA antenna.

### B.1.6 Assumptions and sources of error

The PCB had a thickness of 1,5 mm meaning that they're almost twice the thickness of the original RTX8950 PCB. Another aspect is the port extension. This could have turned the S11 slightly on the smith-chart, seeing as the difference for the simulated thin and thick are equal between simulated and measured.

## B.2 Curved IFA antenna simulation and measurements

This appendix contains the simulations and measurements of the Curved IFA antenna utilised on the PCB shape from Figure 5.6. The simulation of the antenna and its performance will measured. The antenna was realised on PCB. It was then measured with a VNA and in the Stargate at AAU University.

| | |
|---|---|
| **Conducted by** | Oliver Falkenberg Damborg |
| **Date** | 28 / 11 / 2023 |
| **Purpose** | To design and confirm antenna performance between simulation and realisation including head-coupling. |

### B.2.1 Device Under Test (DUT)

The simulated and configured antenna can be seen on Figure B.9.

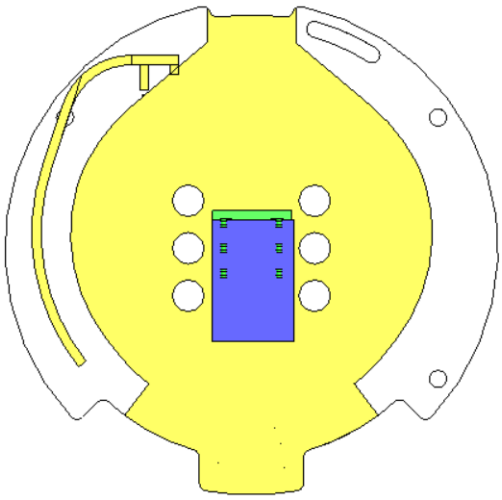

**Figure B.9:** Model of the Curved IFA antenna prototype developed with an approximation in frequency shift caused by head coupling.

The simulated antenna design can be seen on Figure B.9 which was realised on a PCB printer. On Figure B.10 we see the PCB for the Curved IFA.

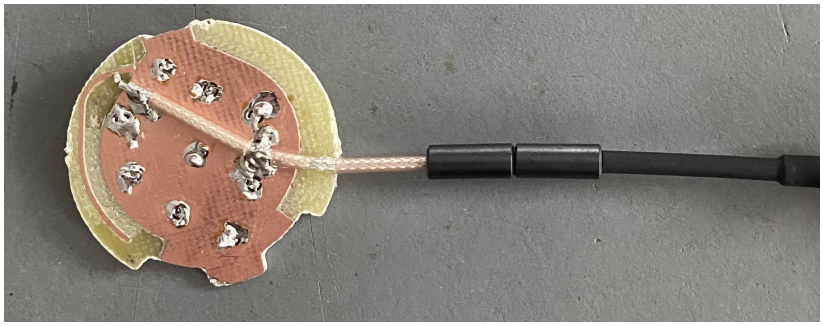

**Figure B.10:** Measuring setup showing the soldering points of the RF pig tail on the antenna and ground plane.

### B.2.2 List of equipment

| Equipment | Manufacturer | Type | Specification | AAU no. |
|---|---|---|---|---|
| Calibration Kit | Agilent Technologies | 85033D | Range: 0 Hz to 6 GHz | — |
| Network Analyzer | Agilent Technologies | E5062A | Range: 300 kHz to 3 GHz | 56983 |
| Multiprobe system | Microwave Vision Group | Stargate 24 | Range: 400 MHz to 10 GHz | — |

**Table B.3:** List of equipment that was used in test.

### B.2.3 Test setup

The test setup consists of two different setups for each PCB. Figure B.11(a) shows the measurement setup for VNA and stargate. Figure B.11(b) shows the head-coupling setup for measurement with VNA.

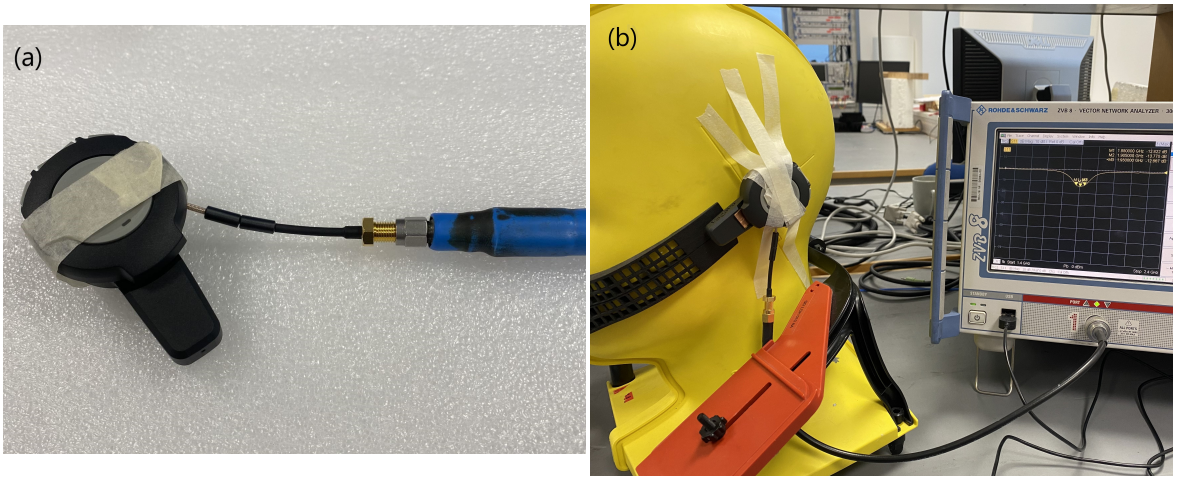


**Figure B.11:** Test setups for the measurement of the Curved IFA. (a) shows the PCB encapsulated in mechanic for measurements of PCB performance in mechanic. (b) shows the head-coupling of the mechanic for VNA and Stargate measurements.

### B.2.4 Procedure

The procedure for the test is the following.

1. Simulate antenna outside mechanic.
2. Simulate antenna inside mechanic.
3. Solder RF pigtail to feed-line following the guidelines in section 5.1.
4. Measure PCB only using calibrated and port-extended VNA.
5. Measure PCB in mechanic with VNA.
6. Measure PCB in Mechanic in head-coupling setup using VNA and Stargate.

### B.2.5 Results

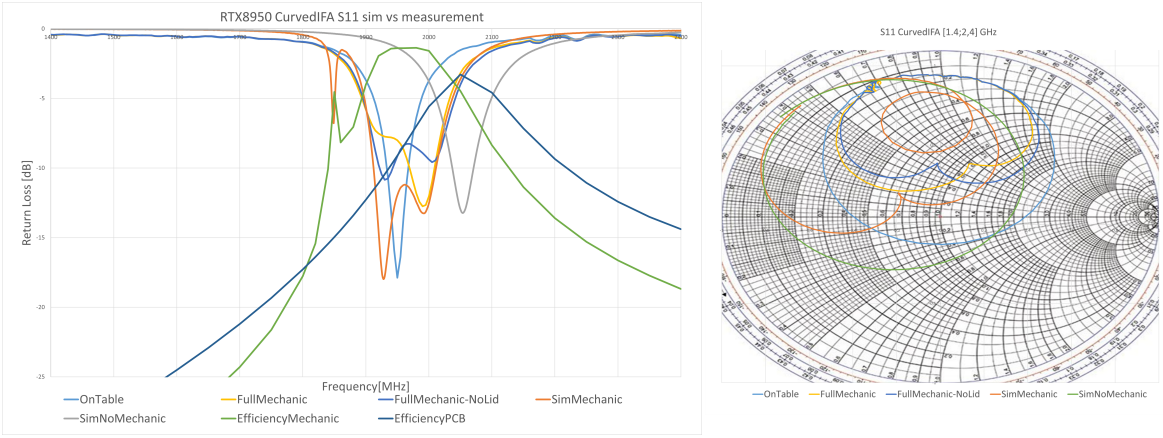


**Figure B.12:** Simulated VS Reality for the Curved antenna. This figure contains the s11 response of the antenna compared to the simulated result. One of the peaks is very similar between the simulated and measured in the mechanic which is the yellow and orange curves albeit in the higher frequency band only.

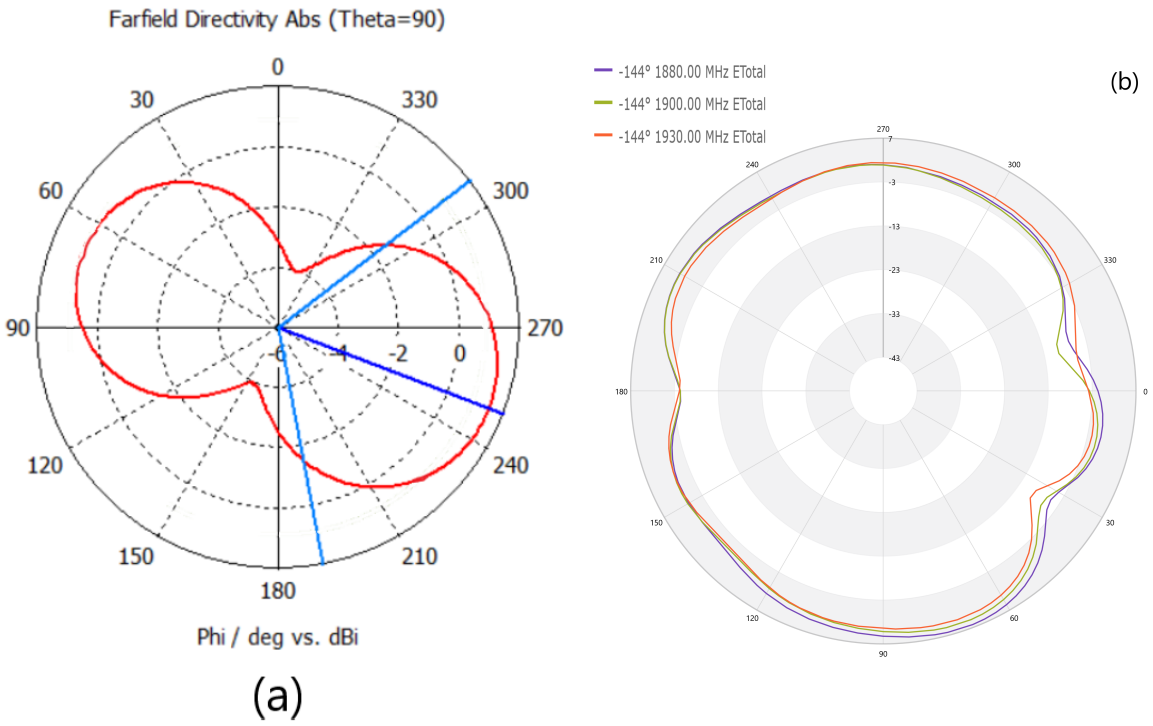


**Figure B.13:** The radiation pattern of the directivity. (a) is the simulated directivity of the PCB with a peak value around 2 dBi. (b) is the measured radiation pattern. In Table B.4 the peak directivity values are found for the three frequencies.

| Parameter | Frequency | Simulated PCB | Simulated Mechanic | Measured No Mechanic | Measured in Mechanic |
|---|---|---|---|---|---|
| **Directivity** | 1880 MHz | 1,461 | 3,347 | 6,814 | 6,01 |
| | 1900 MHz | 1,463 | 3,43 | 7,006 | 5,181 |
| | 1930 MHz | 1,467 | 3,338 | 6,856 | 4,956 |
| **Efficiency** | 1880 MHz | -13,410 | -7,050 | -15,320 | -7,122 |
| | 1900 MHz | -12,278 | -3,99 | -14,476 | -5,687 |
| | 1930 MHz | -10,44145 | -1,687 | -12,909 | -4,747 |

**Table B.4:** Results of measuring the curved IFA antenna in mechanic and without. A clear sign of improvement of the mechanic is the increased efficiency while the directivity drops due to losses in the mechanic. These antennas were measuring using a RF pigtail without ferrite beads, thereby causing some shifting or efficiency deterioration.

### Head-coupling results

The PCB and mechanic were then measured in a head-coupling setup and compared to the mechanic response seen on Figure B.14. The results are then compared and compiled

into a table.

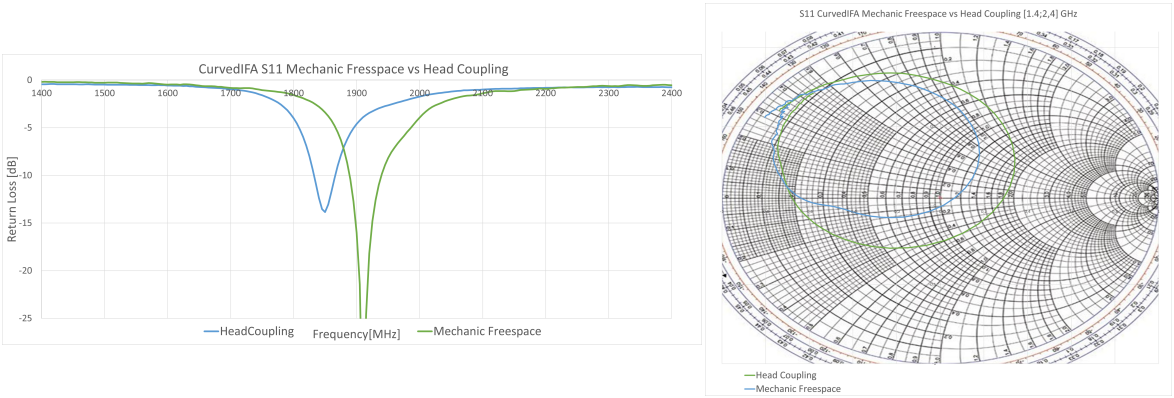


**Figure B.14:** S11 results of a comparison between the mechanic in free-space and the head coupling of the antenna while in mechanic. The frequency is visibly shifted down in the frequency spectrum, causing it to be out of band.

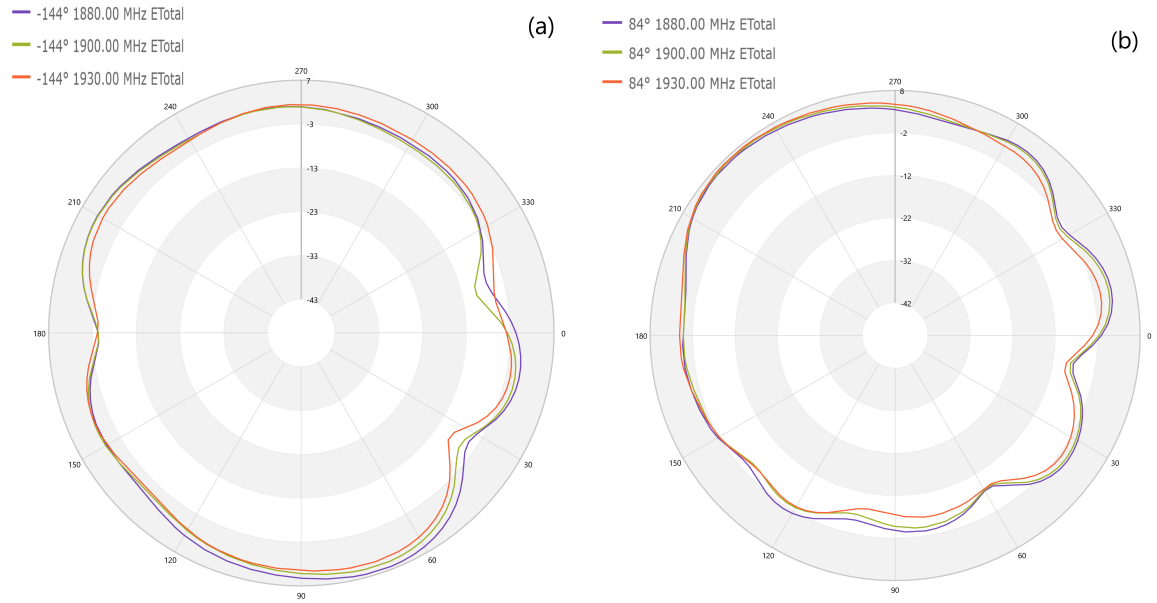


**Figure B.15:** Mechanic radiation pattern VS head coupling radiation pattern for the curved antenna. (a) shows the radiation pattern for PCB in mechanic and (b) shows the radiation pattern for a head coupling. It can be observed that (b) is more directive and have a lower overall directivity. One half of (b) is remarkably lower than the rest, which is a contribution to the positioning of the head reducing the directivity in that direction.

| Parameter | Frequency | Measured No Mechanic | Measured in Mechanic | Measured in Head Coupling |
|---|---|---|---|---|
| **Directivity** | 1880 MHz | 8,315 | 6,61 | 6,7859 |
| | 1900 MHz | 8,171 | 5,396 | 7,113 |
| | 1930 MHz | 8,828 | 4,534 | 7,486 |
| **Efficiency** | 1880 MHz | -8,19 | -5,439 | -6,65 |
| | 1900 MHz | -7,03 | -6,105 | -7,105 |
| | 1930 MHz | -5,138 | -7,19 | -8,07 |

**Table B.5:** Results with head coupling compared to no mechanic and so on. All these measurements areincluding the RF pigtail being isolated through the use of ferrite beads.

### B.2.6 Assumptions and sources of error

The PCB had a thickness of 1,5 mm meaning that they are almost twice the thickness of the original RTX8950 PCB. This will cause a difference due to this possibly introducing additional loss in the form of surface waves. Another important thing to note is that the measurements without head-coupling were without ferrite beads and two points of soldering to remove the RF pigtail effect on the S11 response.

## B.3 Ground extension determination

| | |
|---|---|
| **Conducted by** | Oliver Falkenberg Damborg |
| **Date** | 13 / 12 / 2023 |
| **Purpose** | To measure the difference between different ground plane extensions, possibly getting a better result than the original groundplane. |

### B.3.1 Device Under Test (DUT)

The configured antenna can be seen on Figure B.9.

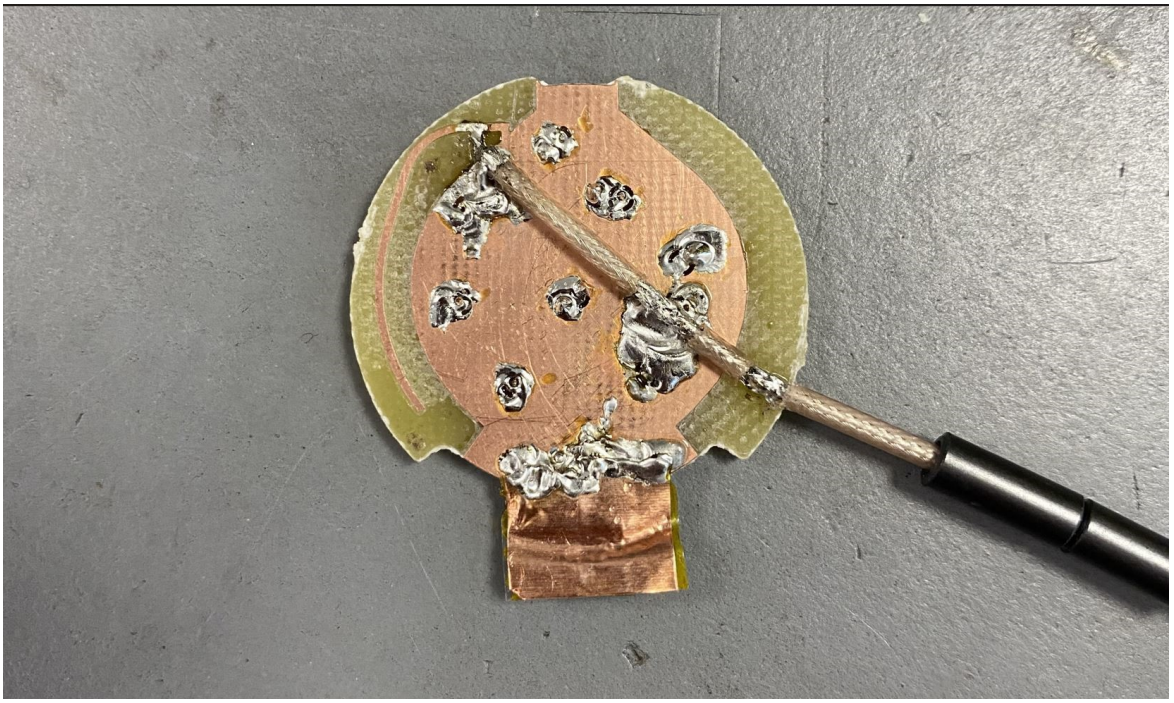

**Figure B.16:** Example showing the soldering and the specific antenna that will be measured through this test. Applied on the PCB is a short piece of ground extension to research the effect of this on the performance of the antenna.

The actual ground extension starts at a length of 30mm which is reduced for each measurement. This occurs for both antenna types in this test.

### B.3.2 List of equipment

| Equipment | Manufacturer | Type | Specification | AAU no. |
|---|---|---|---|---|
| Calibration Kit | Agilent Technologies | 85033D | Range: 0 Hz to 6 GHz | — |
| Network Analyzer | Agilent Technologies | E5062A | Range: 300 kHz to 3 GHz | 56983 |
| Multiprobe system | Microwave Vision Group | Stargate 24 | Range: 400 MHz to 10 GHz | — |

**Table B.6:** List of equipment that was used in test.

### B.3.3 Test setup

The test setup consisted of two setups. The Stargate and a VNA.

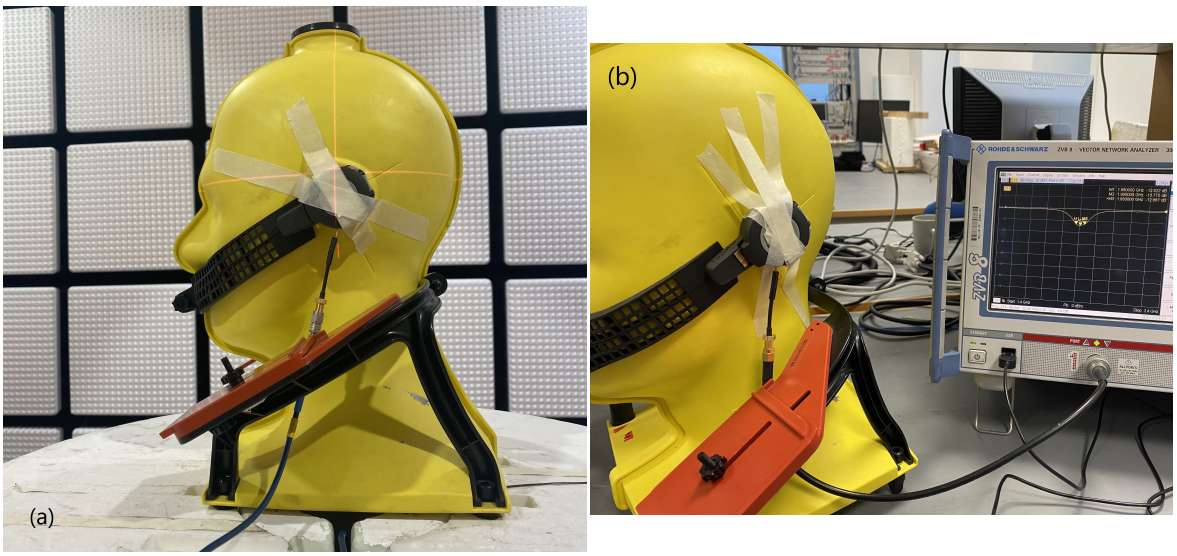


**Figure B.17:** The test setups for measuring the ground extension effect. This test is solely in head coupling configuration. The figures show the measurement setup in the Stargate and when measuring using a VNA.

### B.3.4 Procedure

The procedure for the test is the following.

1. Simulate the effect on the radiation pattern that the ground extension applies.
2. Solder RF pigtail to feed line following the guidelines in section 5.1.
3. Apply 30 mm ground extension following the position and description in section 5.4.
4. Measure PCB in mechanic on RF head using calibrated and port-extended VNA.
5. Cut a piece of ground-extension off. Desired is approximately 5 mm.
6. Measure length and note new length.
7. repeat step 3 to 6 until no more ground extension.
8. Repeat for both antenna prototypes.

### B.3.5 Results

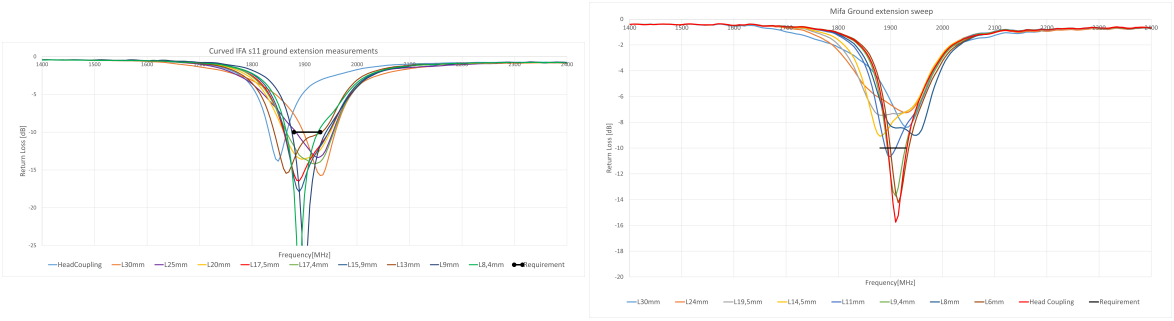


**Figure B.18:** S11 of the ground extension sweep. Left shows the Curved IFA ground extension s11 results. Right shows the MIFA antennas ground extension s11 results.

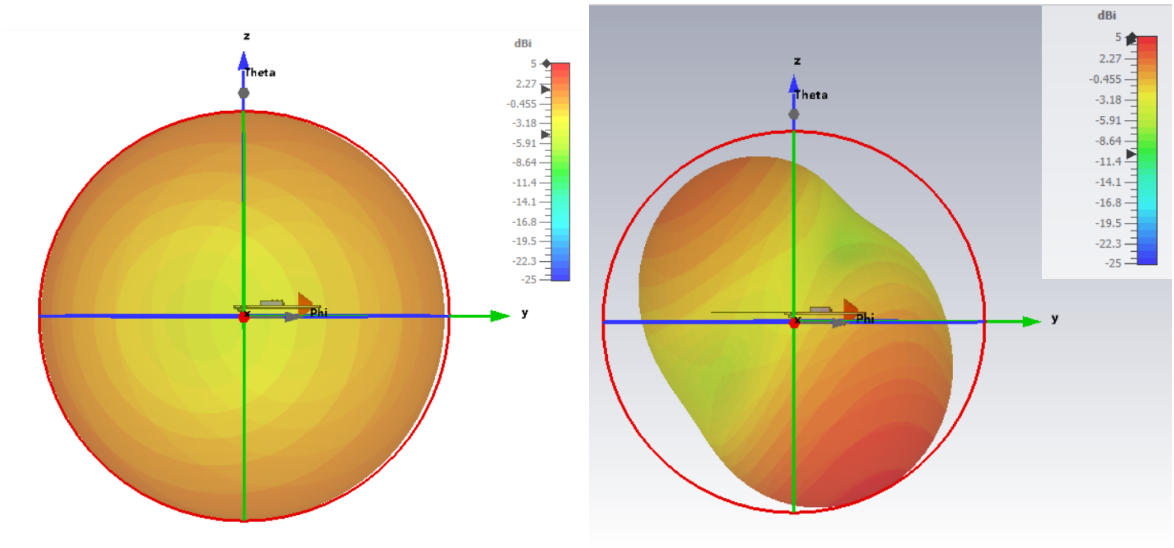


**Figure B.19:** Simulated effect of ground extension on the directivity of an antenna as well as the radiation pattern. Left side is the Curved IFA antenna without ground extension. Right is the Curved IFA antenna with 30 mm ground extension.

### B.3.6 Assumptions and sources of error

Due to the handmade nature of the ground extensions, there will be individual differences between each ground extension and the expected from the simulation. The path for the ground extension in reality means that at long lengths, the extension is unprotected by mechanic and bent slightly at the PCB due to mechanic squeezing it. The reduction in length of the extension is also imprecise due to it occurring using a scissor. A scissor is an imprecise reduction in length if specific desired lengths were needed. This however was a test of the performance at different lengths.

## B.4 Double antenna simulation and measurements

| | |
|---|---|
| **Conducted by** | Oliver Falkenberg Damborg |
| **Date** | 15 / 12 / 2023 |
| **Purpose** | To design and confirm antenna performance for a simulated result and then improve upon it. |

### B.4.1 Device Under Test (DUT)

The configured antenna can be seen on Figure B.9.

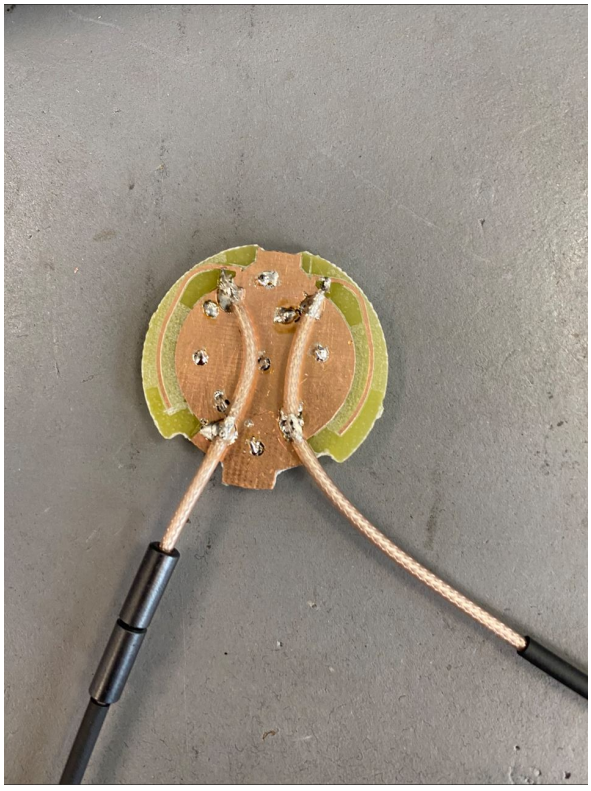

**Figure B.20:** Soldering setup of the RF pigtail on the DUT for measurements.

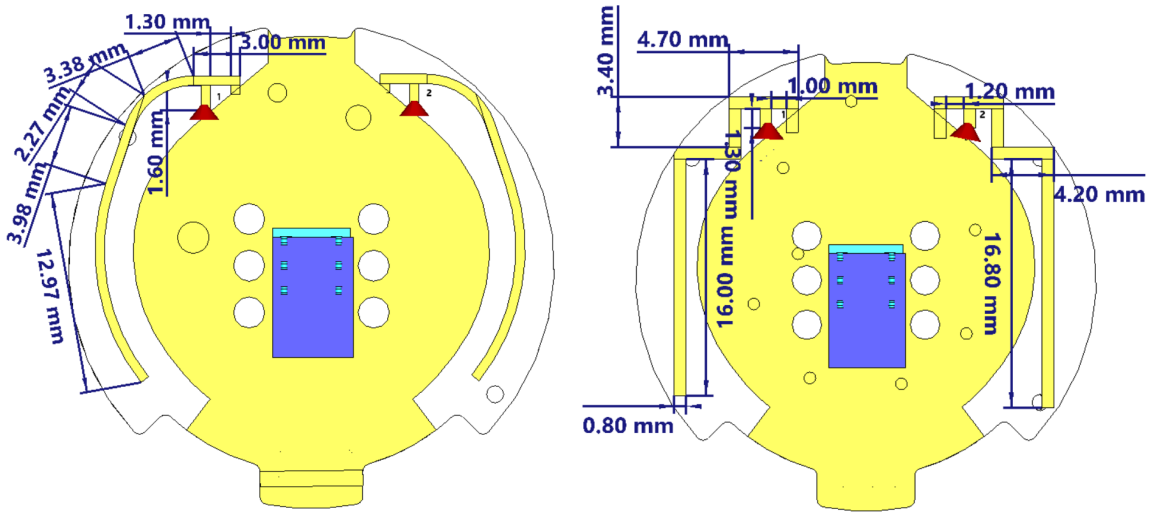


**Figure B.21:** The two simulated antennas that will be measured on. To the left is the double curved IFA. To the right is the double MIFA.

### B.4.2 List of equipment

| Equipment | Manufacturer | Type | Specification | AAU no. |
|---|---|---|---|---|
| Calibration Kit | Agilent Technologies | 85033D | Range: 0 Hz to 6 GHz | — |
| Network Analyzer | Agilent Technologies | E5062A | Range: 300 kHz to 3 GHz | 56983 |
| Multiprobe system | Microwave Vision Group | Stargate 24 | Range: 400 MHz to 10 GHz | — |

**Table B.7:** List of equipment that was used in test.

### B.4.3 Test setup

The testsetup consisted of two different setups for each PCB.

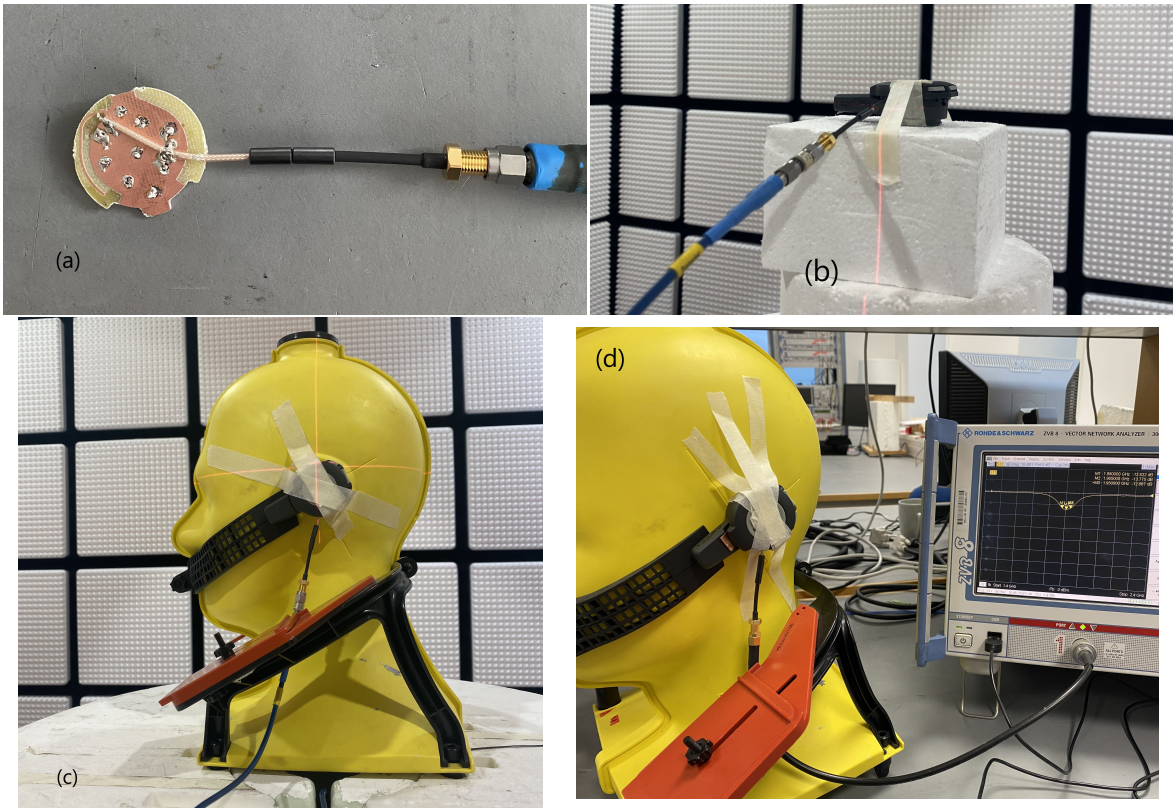


**Figure B.22:** Measurement setups for the different measurement types. These are used by the different test cases. (a) is measurement of the PCB performance by itself. (b) is measurement of the performance of the antenna in free-space inside the mechanic. (c) shows the head coupling configuration. (d) shows the head-coupling configuration when measuring with a VNA.

### B.4.4 Procedure

The procedure for the test is the following.

1. Simulate antenna outside mechanic.
2. Simulate antenna inside mechanic in head-coupling.
3. Solder RF pigtail to feed line following the guidelines in section 5.1.
4. Measure PCB in mechanic with a full 2-port VNA with port-extension on both ports in head-coupling.
5. Remove one RF pigtail. Put in mechanic, apply head-coupling and measure in Stargate.
6. Remove pigtail and solder to other antenna and measure in Stargate.

### B.4.5 Results

The first results were from the simulation of the double antennas before they were optimised in order to verify the simulation model was correct with the use of a Bio-Tissue coupling component.

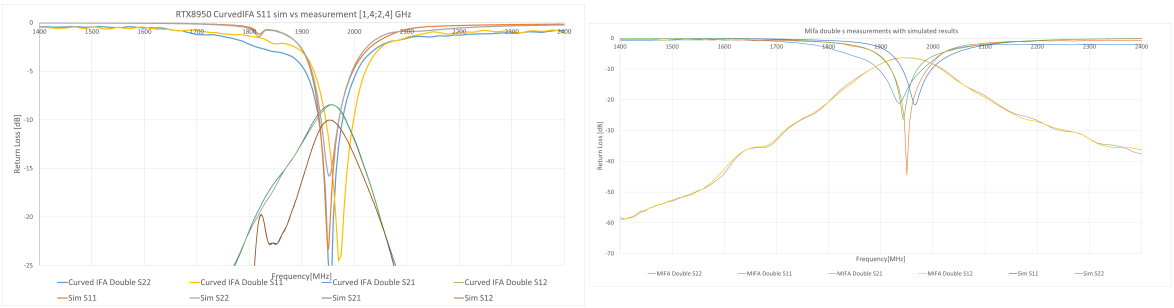


**Figure B.23:** Simulated VS Reality for the double antennas. Left shows the S11 return loss for the Curved IFA double antenna PCB. The simulated and the measured are read to be close in value. Right shows the s11 for the MIFA double antenna PCB when comparing between simulated and measured. The measured MIFA is further from each others than the simulations suggested but otherwise a close relation between simulated and measured.

The MIFA double antenna PCB was measured in the Stargate:

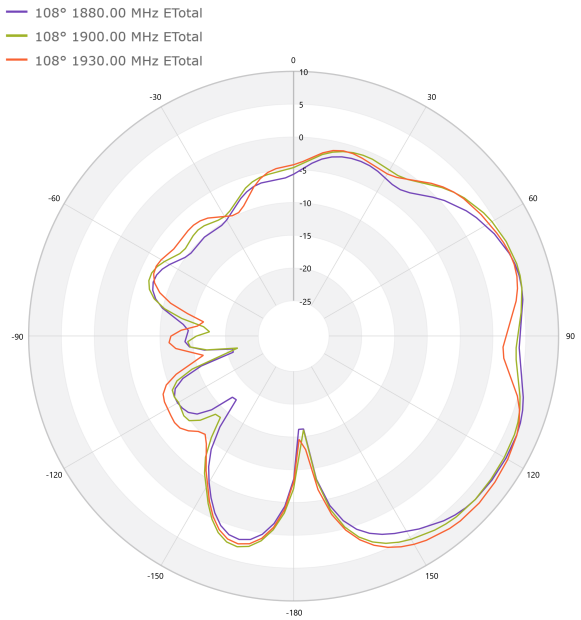


**Figure B.24:** Radiation pattern of the measured MIFA double antenna. The measured antenna is the left antenna head-coupled to the right ear radiating in the Stargate. The radiation pattern clearly reveals the reduction of directivity caused by the head-coupling.

| | MIFA Left antenna Left | | MIFA Left antenna Right | | MIFA Right antenna Left | | MIFA Right antenna right | |
|---|---|---|---|---|---|---|---|---|
| **Frequency [MHZ]** | **Directivity** | **Efficiency** | **Directivity** | **Efficiency** | **Directivity** | **Efficiency** | **Directivity** | **Efficiency** |
| **1870** | 6,450 | -9,612 | 7,288 | -9,233 | 6,362 | -6,839 | 6,375 | -6,868 |
| **1880** | 6,269 | -8,020 | 6,979 | -7,761 | 6,336 | -6,509 | 6,348 | -6,538 |
| **1890** | 6,275 | -7,173 | 6,817 | -7,080 | 6,288 | -6,242 | 6,304 | -6,274 |
| **1900** | 6,378 | -6,682 | 6,865 | -6,692 | 6,223 | -6,113 | 6,238 | -6,150 |
| **1910** | 6,527 | -6,357 | 7,131 | -6,463 | 6,165 | -6,028 | 6,183 | -6,075 |
| **1920** | 6,829 | -5,951 | 7,456 | -6,157 | 6,127 | -5,989 | 6,126 | -6,050 |
| **1930** | 6,957 | -5,772 | 7,663 | -6,127 | 6,094 | -6,227 | 6,095 | -6,301 |
| **1940** | 7,237 | -5,526 | 7,872 | -5,696 | 5,949 | -6,493 | 5,960 | -6,583 |
| **1950** | 7,593 | -5,535 | 8,057 | -5,367 | 5,855 | -7,004 | 5,857 | -7,101 |
| **1960** | 7,889 | -5,661 | 8,176 | -5,206 | 5,745 | -7,426 | 5,769 | -7,526 |
| **1970** | 8,202 | -6,146 | 8,246 | -5,224 | 5,732 | -8,180 | 5,760 | -8,281 |
| **1980** | 8,532 | -6,491 | 8,322 | -5,340 | 5,700 | -8,735 | 5,727 | -8,830 |
| **1990** | 8,789 | -7,108 | 8,291 | -5,799 | 5,731 | -9,324 | 5,726 | -9,416 |
| **2000** | 9,208 | -7,859 | 8,483 | -6,322 | 6,020 | -10,300 | 6,017 | -10,388 |

**Table B.8:** Measurements from utilising the Stargate to measure efficiency and directivity for the double MIFA PCB. The data from this table is the unoptimised antenna that requires optimisation in order to achieve a frequency response within the requirements.

The antennas were optimised and this can be seen on Figure B.25 and B.26.

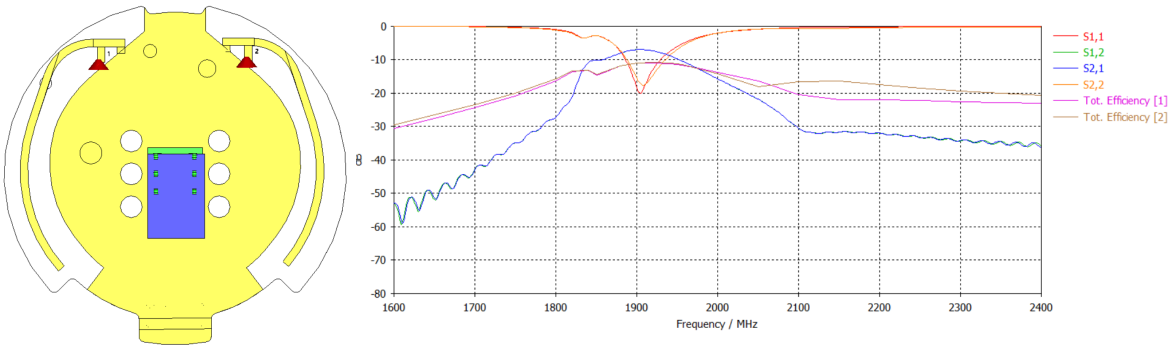


**Figure B.25:** The optimised design of the double curved IFA antenna with its corresponding simulated S11 plot.

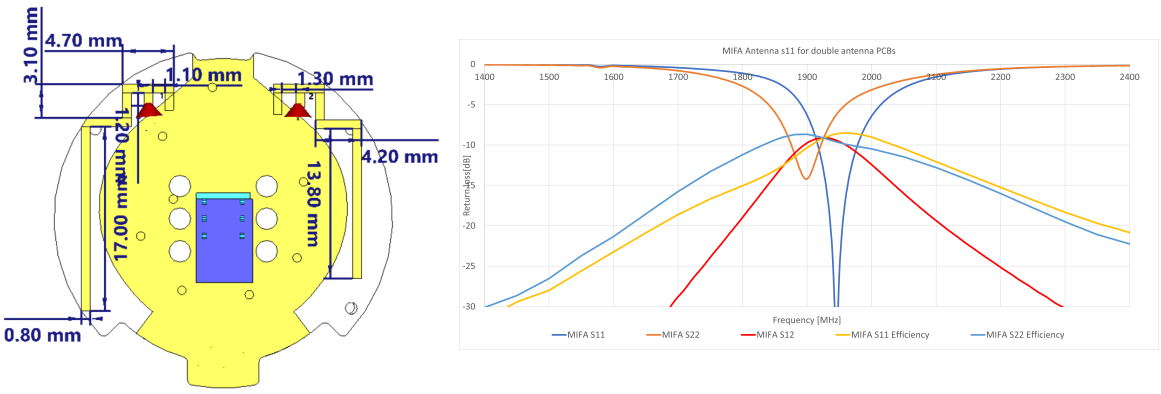


**Figure B.26:** The optimised design of the MIFA double antenna with its corresponding simulated S11 plot.

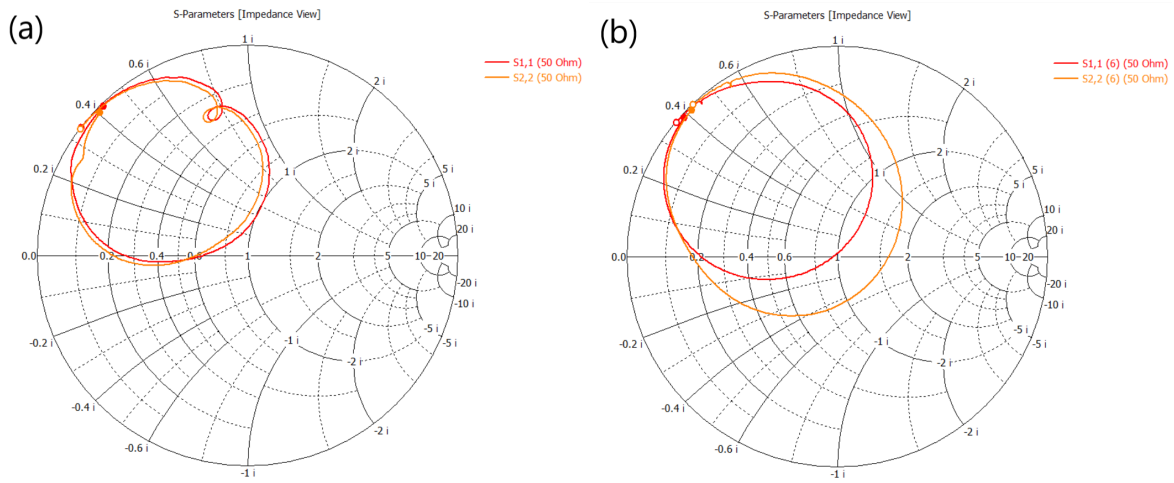


**Figure B.27:** The optimised double antennas smith chart behaviour. (a) shows the behaviour of the curved IFA. (b) shows the smith chart of the MIFA.

### B.4.6 Assumptions and sources of error

The PCB had a thickness of 1,5 mm meaning that they're almost twice the thickness of the original RTX8950 PCB. This will cause a difference. Another aspect is the port extension. The S21 is high for the Curved IFA double PCB, but it is expected for it to decrease as in reality. It is possible for the measurements of MIFA left antenna right year and right antenna left ear to have been affected by the RF pigtail. This is due to the emergence point of the pigtail, with the pigtail pointing upwards for these two specific measurements.